BEHAVIOR OF DUAL LAYERED ENCASED STONE COLUMNS IN LOOSE SAND UNDER SHEAR LOAD

Ph.D. THESIS

Submitted in partial fulfillment of the requirements for the award of the degree

of

DOCTOR OF PHILOSOPHY

in

CIVIL ENGINEERING

by

AKASH JAISWAL

(Scholar No.- 193111014)

MAULANA AZAD NATIONAL INSTITUTE OF TECHNOLOGY, BHOPAL – 462003 (INDIA)

July,2023

MAULANA AZAD NATIONAL INSTITUTE OF TECHNOLOGY, BHOPAL

CANDIDATE'S DECLARATION

I hereby certify that work which is being presented in this thesis entitled **"Behavior of Dual Layered Encased Stone Columns In Loose Sand Under Shear Load"** in partial fulfillment of the requirements for the award of the degree of Doctor of Philosophy and submitted in the Department of **Civil Engineering** of the Maulana Azad National Institute of Technology, Bhopal is an authentic record of my own work carried out during the period from **July 2019 to July 2023** under the supervision of Dr. Rakesh Kumar, Associate Professor, Department of Civil Engineering, Maulana Azad National Institute of Technology, Bhopal.

The matter presented in this thesis has not been submitted by me for the award of any other degree of this or any other institution.

Akash Jaiswal

(Name and Signature of the Candidate)

This is to certify that above the statement made by the candidate is correct to the best of our knowledge.

Dr. Rakesh Kumar

Date: (Name and Signature of Supervisor)

The Ph.D. Viva-Voce Examination of Mr. Akash Jaiswal, Research Scholar, has been held on _________ .

Signature of Supervisors Signature of External Examiner

ABSTRACT

Rapid urbanization and civilization have led to a higher demand for land, requiring effective ground improvement techniques to enhance the load-bearing capacity and stability of weak soils. This thesis specifically examines stone columns as a commonly employed ground improvement method. Stone columns involve the placement of crushed stones into weak soils to enhance their engineering characteristics.

The focus was on bulging failure to improve the vertical load-bearing capacity of stone columns. Additionally, there were other failure modes identified that are associated with column groups and underlying issues. One of the observed failures in the stone column is shear failure, which has been observed beneath the embankments at the corner line of the column or might be found where the stone columns are susceptible to the lateral load. Additionally, the use of encasement has become one of the most popular concepts to enhance the efficiency of the stone columns. This study explores the possibility of enhancing the shear resistance of stone columns by implementing a new concept of dual-layered encasement. The use of two layers of geosynthetics to encase the stone columns is anticipated to enhance the overall stiffness of the soi-stone column combined body, resulting in enhanced shear strength and overall performance. The study aims to examine the behavior of dual-layered encased (DLE) stone columns under different normal pressures (50, 100, 150, and 200 kPa).

Various experimental tests were conducted using a large shear box apparatus to simulate different shear loading conditions. The tests examine variations in the dimensions of stone columns and encasement conditions installed in a loose sand bed, both for individual columns and groups of columns. The study compares the performance of dual-layered encased stone columns with conventional single-layer encased (SLE) and ordinary stone columns (OSC) under shear loading conditions. This comparison offers valuable insights into the effectiveness of the proposed approach.

Numerical modeling using the advanced Plaxis-3D software was conducted to enhance the understanding of the behavior of dual-layered encased stone columns, in addition to experimental investigations. The numerical models undergo validation through comparison with experimental results and previous studies to ensure their

accuracy and reliability. Numerical simulations aid in interpreting experimental results and offer further insights into the behavior of stone columns.

The research findings make a significant contribution to the field of geotechnical engineering by providing important insights into the shear resistance of stone columns with dual-layered encasement and comparisons with other encasement conditions of stone columns. This study also investigates the shear strength parameters of the soil-stone column system by using Mohor envelopes, as well as the concept of secant modulus for 10% and 20% deformation by comparing the secant modulus (E_{10} and E_{20}). The findings of this study can be utilized in practical civil engineering projects to enhance ground improvement methods for unstable soil conditions.

The findings suggest that the inclusion of stone columns in loose sand enhances their capacity to bear lateral loads. The preliminary observation suggested that the soil-stone column system demonstrates greater rigidity in comparison to the loose sand bed, and unencased stone columns rupture along the predetermined shear plane, whereas encased columns undergo bending without rupture. Encasement enhances the lateral load capacity of the stone column by mobilizing tensile forces. This results in significantly higher lateral resistance forces, up to 2.5 times greater. Dual-layered encased (DLE) stone columns exhibit a significant increase in strength mobilization when compared to other stone columns. This enhancement is particularly noticeable for smaller column diameters, while it becomes less prominent for higher area replacement ratios. Additionally, it has been observed that stone columns enhance the shear strength characteristics of the underlying soil bed. The largest increase in apparent friction angle is observed with the use of larger-diameter stone columns. Moreover, the most significant change in apparent cohesiveness is observed at lower levels of area replacement. Also, both the second moduli of elasticity, i.e., E_{10} and $E_{20,}$ were higher for the dual-layered-encased stone column than the single-layered-encased stone column, indicating the enhanced stiffness of the combined soil-stone column body.

The study demonstrates that the dual-layer encasement concept is superior to the conventional stone column. The dual-layered stone column approach can be recommended for areas where the foundation's underlying column is at high risk of failure due to lateral loads, as well as at the corner line of stone columns beneath structures such as embankments.

ACKNOWLEDGEMENT

First and foremost, I humbly thank the almighty God Shree Ganesha for bestowing upon me the ability to complete this monumental task.

I would like to express my heartfelt gratitude to Dr. Rakesh Kumar, Associate Professor in the Department of Civil Engineering at MANIT Bhopal, for his invaluable guidance throughout my research. His optimistic approach, insightful suggestions, instructions, fruitful discussions, expert opinions, motivation, and generous support were essential to the completion of this task. He contributed significantly to the provision of superior research facilities and the establishment of a conducive environment. I am extremely indebted to him for generously devoting his valuable time, and I express my deepest gratitude to him.

I am grateful to the members of the SRPC committee, namely Dr. Nitin Dindorkar, Professor in the Department of Civil Engineering at MANIT Bhopal, and Dr. Vilas warulkar, Associate Professor in the Department of Mechanical Engineering at MANIT Bhopal, for their insightful suggestions and contributions during the SRPC meetings. For his blessings, inspiration, and support, I sincerely thank Dr. H.L. Tiwari, the DPRC Coordinator of the Civil Engineering Department at MANIT Bhopal.

I am grateful to the faculty members of the Geotechnical Engineering Specialization, Dr. P.K Jain, Dr. Suneet Kour, and Dr. Kishan D, for their assistance in clarifying the fundamentals of geotechnical engineering, which aided me in achieving the goals of my research.

I am obligated to Dr. Karunesh Kumar Shukla, Director of MANIT Bhopal, and Dr. P.K. Agrawal Parashar, Head of the Department of Civil Engineering, for providing all of the necessary resources for the completion of my thesis. This research would not have been possible without their assistance.

I would like to thank my colleagues in the Geotechnical Engineering specialization, Mr. Aman Tiwari, Mr. Neeraj Kumar, Mr. Utkarsh, Miss. Vaishali Yede, and Mr. Abhijeet Shukla, who are also Research Scholars at MANIT Bhopal, for their invaluable assistance and encouragement throughout this research. I would like to express my heartfelt gratitude to all of my friends, specifically Mr. Hemant Choudhary, Mr. Abhishek Soni, Mr. Vinay Kumar, Mr. Satyam Mishra, Mr. Shrish Chandrawanshi, Mr. Ankur Sharma, Mr. Parth, Mr. Jitendra Namdeo, Mr. Oman Sayyed, Mr. Karan Moolchandani, Mr. Shashank Coudhary, Mr. Yash Rathore, Mr. Rahul Tanwar and Mr. V.Chiranjeevi for their moral support, which made my stay during the course enjoyable and memorable.

Special thanks go to the technical staff of the Department of Civil Engineering at MANIT Bhopal, particularly Mr. Amir Khan, Technical Assistant; Mr. Mahesh Kumar, AG-II; Mr. Nitish TIwari; Mr. Ahmad Khan; and Mr. Munna Kushwaha, Geotechnical Engineering Laboratory.

I am pleased to express my gratitude to my supportive father, Shri Shrihari Jaiswal; my beloved mother, Smt. Kiran Jaiswal; and my companion in life, Mrs. Anjali Jaiswal, as well as my dear siblings, Mr. Anurag Jaiswal and Miss. TejalRani Jaiswal, for their unwavering love, blessings, and tremendous support throughout my thesis work. I will be eternally grateful to them.

Finally, my heartfelt gratitude goes to everyone who helped out in some way, directly or indirectly, at every stage of this research project. Your contributions have been invaluable in realizing this project.

Akash Jaiswal

MANIT, Bhopal

July, 2023

TABLE OF CONTENTS

LIST OF FIGURES

LIST OF TABLES

1. INTRODUCTION

1.1 GENERAL

As a result of the rise of civilization and urbanization, the demand for land has expanded dramatically to improve living and transportation conditions. This tendency is expected to continue for the foreseeable future. Construction sites with suitable geotechnical characteristics are becoming scarcer, whereas sites that are unsuitable or less suitable are proliferating. Bearing failure, total and differential settlements, ground heave, instability (including sliding, flipping, and slope failure), seepage, erosion, and liquefaction have all been dealt with by engineers.

Depending on the type of project and the soil, there are already a variety of advanced ground improvement techniques that may be used. These techniques have proven to be highly efficient in improving strength, mitigating total and differential settlement, speeding up construction, cutting costs, and changing other factors that could affect how well they work for projects on soft ground. The applications of ground improvement techniques, such as using admixtures like fly ash, pond ash, and cement (Yadav et al., 2018), indicate an enhancement in the unconfined compressive strength of the soil as well as a reduction in the optimum moisture content of the soil system. Nonetheless, some researchers have also utilized waste materials, such as stone dust and industrial solid waste (Gautam et al. 2021), to resolve the issue of waste disposal as well. Scientific society is also concerned about waste plastic, which can be used to stabilize soil because its addition to subbase material considerably increases the dry density and CBR values (Paramkusam et al. 2013). The use of geosynthetic reinforcement (Sitharam et al., 2003, 2005) significantly increases the load-bearing capacity and decreases the surface heave when used beneath the foundation bed, whereas Geocells (Hegde A 2017; Roy et al., 2019), rubber reinforcement (Yadav et al., 2019) and fiber reinforcement (Tiwari and Sharma, 2013) also provide higher stiffness in the soil system. The different reinforcement type, micro piles, has been utilized successfully in various ground improvement applications, especially for strengthening existing foundations (Bhattacharjee et al., 2011). Additionally, soil and nails' composition increases the soil's apparent cohesion through its capacity to withstand tensile loads (Mittal et al. 2008;

Meenal et al. 2009). Expanded polystyrene (EPS), a polymeric material with a low density and a high strength-to-density ratio, is renowned for its use as a lightweight geosynthetic in embankments and retaining structures to improve slope stability and reduce lateral earth pressure (Khajeh, A. et al., 2020; Khajeh, A. et al., 2021; Patil et al., 2022; Gade and Dasaka, 2022).

In dynamic compaction, a heavy weight is dropped repeatedly on the surface of the soil. This makes the weaker upper layers of soil more compact and solid. This process is different at each site based on the soil's strength profile within the required depth of treatment and, to some extent, the type of deposit. For sediments without cohesiveness, blasting-based compaction is appropriate. The theory behind this method says that shock waves are sent through the medium when explosives go off, causing it to melt. This is followed by releasing water from the pores and rearranging the grains into a denser packing. Preloading is appropriate for peat, compressible silts, organic clays, and saturated clays. With this technique, a fill that is at least as heavy as the future structure is laid over the region that has to be improved. When the consolidation is finished, the fill is removed. A surcharge load may occasionally be used in conjunction with vertical drains to speed up improvements. Sand drains (Moran, 1926), rope drains (Mohan et al., 1977), cardboard drains, and geo-drains are just a few of the several drain types that are accessible depending on the scenario. In the lime pile technique (Broms, 1985), lime or cement columns with a maximum length of 15 mm and a maximum diameter of 0.5 m are created on site by combining soft clay with cement or quick lime using a specialized tool. When other, less expensive ground improvement techniques cannot be employed, the jet grouting method is used to address specific issues, such as the underpinning of structures. Through a pipe that is progressively withdrawn while being spun in the hole, jetting is accomplished. The high-pressure jet pierces the soft clay, and the hole is filled with cement slurry. After being jet grouted, the cement mortar or soil-cement column can be used as lateral support in deep excavation or as a foundation for construction. Other techniques include adding geosynthetics to the soil for reinforcement (Sharma & Phanikumar, 2005; Sitharam et al., 2003, 2005). significantly increases the load bearing capacity and decreases the surface heave when used beneath the foundation bed, whereas rubber reinforcement (Yadav et al., 2019) and fiber reinforcement (Tiwari and Sharma, 2013) also provide higher stiffness in the soil system. Providing a sand cushion for consolidation and dewatering (Boominathan, 1987), applying adequate surcharge pressure (Chen, 1988), and laying a mat foundation (Williams & Pellissier, 1992). These methods work well for shallow soil deposits in a small area or when they can only be used in a limited way. However, when deep soil deposits cover a large area, like embankments that spread over many kilometers, it is important to find technically sound, cost-effective, and quick solutions. Stone columns and granular piles are extremely well known to engineers when a civil engineering project encounters weak soil and the need for deep soil stabilization (Tandel et al. 2012). In addition to the granular fill column, some researchers have proposed appropriate experimental and numerical methods to estimate the uplift capacity of granular anchor piles in weak soils as a ground improvement technique (Kranthikumar, A. 2016, 2017).

1.1.1 Stone Column

Stone columns are a widely used ground improvement technique that involves inserting columns of crushed stones into weak soils to improve their load-bearing capacity and reduce settlement. Stone columns are frequently engineered to sustain the vertical loads imposed by the building built on top of them. In recent years, researchers have focused on enhancing the performance of stone columns through various means, including the use of alternative materials, modifications to installation techniques, and the inclusion of geosynthetics. Either displacement or replacement methods can install on the stone column. The displacement method of installation has benefits over the replacement one because the surrounding soil also gets compacted, and the relative density increases, which considerably impacts the ultimate capacity (Samanta 2010).

The longitudinal load can be transmitted to the ground via the action of bulging in the diameter, improving the bearing capacity of the ground. In addition, the intervening soil could lack adequate resistance to bulging or horizontal confinement in extremely loose soils to prevent bulging and lateral movement. To determine the vertical bearing capacity of stone columns, a number of numerical (Hosseinpour et al. 2014, Saxena and Roy 2022 a) and analytical studies (Das & Dey, 2018), as well as physical modeling (Deb et al., 2011; Vekli et al., 2012; Ghazavi & Nazari, 2013; Bailappanavar et al., 2021; Saxena and Roy 2022 b), have been done. According to these studies, the area replacement ratio, the type of soil in which the column is installed, the angle of internal friction of the material, and the length of the stone column have the major impact on the vertical load-bearing capacity of stone columns.

The circumferential bulging resistance of the stone column must be reinforced to enhance the capacity of the ground even further. The bearing strains in a vertically loaded column were substantially reduced when it was encased in various geosynthetics. (Yoo and Kim, 2009; Murugesan and Rajagopal, 2010; Khabbazian et al., 2010; Lo et al., 2010; Pulko et al., 2011; Yoo and Lee, 2012; Dash and Bora, 2013; Ali et al., 2014; Rajesh and Jain, 2015; Miranda and Costa, 2016; Hasan and Samadhiya, 2017; Yang et al., 2017) Furthermore, the use of horizontal layers of geosynthetics enhances bearing capacity while minimizing lateral bulging due to the impact that horizontal layers of geosynthetics and stone column aggregates have on interlocking and creating friction. (Hasan and Samadhiya, 2016; Parasd and Satyanarayana, 2016). On the other hand, only a few studies have been conducted to estimate the shear strength of stone columns.

1.2 NEED OF THE STUDY

To increase the vertical load-bearing capacity of the column, attention was paid to the bulging failure. However, failures related to the group of columns and deep-seated failure were found. External and internal stabilities were emphasized as major failure patterns in the design approach by Kitazume and Maruyama (2006, 2007), who stated the probability of coupled stone column and surrounding soil slide failure in external stability without column rearrangement. In addition, Han et al. (2005) conducted numerical research to determine that this rotational failure for deep mixed columns may be the dominant one beneath the embankments. The plane of the slip circle across the stone column serves as the shear failure plan of the column body, which is the most typical form of failure for compacted sand or gravel (Abusharar and Han, 2011). Bending moment and shear force graphs from Chen et al. (2015) indicated that failure begins in the columns along the edge of the slope due to low lateral resistance. Khabbazian et al. (2015) discovered through numerical analysis that granular columns under the embankment edge had an elevated probability of failure. Many scholars went on to study and analyze the behavior of stone columns under lateral stress. Previous studies have shown that granular column shear failure is an important element to consider when building granular columns. Some of the work (Mohapatra et al. 2016, Cengiz et al. 2019, Nazariafshar and Aslani 2020) was done to understand the behavior of stone columns when they are subjected to a lateral load, and one of the important outcomes indicates that the encasing of the stone column enhances the shear resistance of the body. This study aims to conduct an experimental program followed by a series of finite element-based analyses of granular column material in loose sand under direct shear load.

1.3 SCOPE OF THE STUDY

The single layer encasement has been used in the stone column for better load-bearing conditions, and it has been discovered from the literature that encasing the stone column also increases the shear resistance. In the current study, a concept is proposed to introduce dual-layered encasement to improve the confinement effect; this might improve the shear resistance of the stone column. In the current study, a comparison has been made between the conventional, single-layer encased stone column and the dual-layer encased stone column for the shear resistance offered when subjected to lateral displacement.

1.4 OBJECTIVES OF THE STUDY

- To investigate the behavior of a Single Dual Layered Encased stone column under shear loading at varying normal pressure for different Diameters.
- To investigate the behavior of the Group of Dual Layered Encased stone columns under shear loading at varying normal pressure for different Diameters.
- To compare the DLESC with SLESC and OSC under shear loading conditions for different Diameters at varying normal pressures.
- To Check the Shear Strength parameters for Combined Soil-Stone Column System.
- To evaluate the Shear Strength of the Combined Soil-Stone Column System using the Modulus of Elasticity.

1.5 METHODOLOGY

To fulfil the specified objectives of this research, a series of experimental tests have been designed to be conducted on the extensive shear box apparatus while varying the normal pressure conditions. The assessment of numerous cases was conducted with consideration given to the dimensions of the stone column, as well as the encasement circumstances for both individual and grouped stone columns. Numerical modeling was conducted to simulate the large shear box test conditions using Plaxis-3D software. The models were validated against experimental results and previous studies. In addition, numerical simulations were conducted using the finite element-based software PLAXIS-3D to enhance comprehension and interpretation of the outcomes for all experimental cases.

1.6 ORGANIZATION OF THE THESIS

The thesis has been divided into Six main chapters, an introduction, and a concluding chapter.

- The introduction of the thesis is discussed in **Chapter 1.**
- **Chapter 2** presents a literature review pertaining to the behavior of stone columns, including the stone columns under lateral loads.
- Experimental investigation and methodologies are discussed in **Chapter 3.**
- **Chapter 4** discusses the numerical modeling involved in the study.
- **Chapter 5** addresses the interpretation of experimental tests and numerical study results.
- The study has been concluded in **Chapter 6,** which also identifies potential topics for further investigation.

2. LITERATURE REVIEW

2.1 GENERAL

This chapter presents background information on weak soil and methods for ground development. As discussed in the preceding chapter, the stone column technique offers an easy, quick, and cost-effective solution for ground improvement; it has been widely used for embankment construction, liquid storage tanks, and offshore structures, and it reduces the likelihood of liquefaction in soils; therefore, brief case studies of some of the success stories have been presented. The use of geosynthetics to encase the granular material has been suggested in the literature to increase their effectiveness in extremely soft soils, where the settlement of the composite ground may persist even after the building of conventional stone columns. Thus, the literature on the design, construction, and performance of conventional and encased stone columns has been reviewed.

2.2 WEAK SOILS

A soil with poor engineering properties, including low shear strength, low load-bearing capacity, and high compressibility, is called weak soil. In building and infrastructure projects, weak soils can cause a variety of complications, such as:

- Weak soils are susceptible to **settlement**, which can lead to foundation failure and structural damage. The weight of the building, the consolidation of the soil, or the erosion of soil strength through time can all cause settlement.

- Weak soils can result in **slope instability**, which can cause landslides and rockfalls. This can be especially troublesome in locations with steep slopes where soil stability is crucial for protecting structures and people.

- **Liquefaction:** During earthquakes, weak soils can liquefy, resulting in soil strength and stability loss. This can cause the collapse of structures and infrastructural damage.

- Weak soils are susceptible to **erosion**, which can lead to the loss of soil material and the instability of slopes. This can cause the collapse of retaining walls, embankments, and other structures that rely on the soil's stability.

The poor engineering features of weak soils include low shear strength, low load-bearing capacity, and significant compressibility. These soils can present various complications in building and infrastructure projects, including settlement, slope instability, liquefaction, and erosion. Several soil development techniques may be employed to increase the strength, stability, and load-bearing capability of weak soils to offset these issues.

2.3 GROUND IMPROVEMENT

Ground improvement is altering the soil or rock mass to improve its strength, stability, and other geotechnical features to make it acceptable for construction. When the native soil or rock mass at a construction site does not fulfill the geotechnical requirements of the project, measures for ground improvement are implemented. It involves modifying soil properties to increase its load-bearing capacity, shear strength, and resistance to erosion. Various methods are available for soil stabilization, including mechanical, chemical, electrokinetic, and thermal stabilization.

2.3.1 Factors Affecting Choice of Improvement Method (Hausmann M. R., 1990)

(1) Soil types: **-** The type of soil is a major factor because it significantly affects how to approach the project and what materials will work best. Mitchell (1981) presented a well-known figure indicating that ground improvement techniques only apply to particular soil varieties and/or grain sizes. This figure illustrates the fundamental relationship between soil type, grain size, and the feasibility of soil enhancement. A revised version of this figure can be found in Figure 2.1

(2) Area, depth, and location of treatment required:- When selecting a ground improvement method for a geotechnical project, the required treatment area, depth, and location are important factors to consider. Certain methods may not be viable for treating deeper soil horizons due to their depth limitations. In addition, the extent of the project area and the available financial and equipment resources may influence the selection of a particular method. The location of the project is also an important consideration, particularly if there are nearby structures or noise and vibration concerns. Temperature and the availability of water are two examples of additional location-related factors.

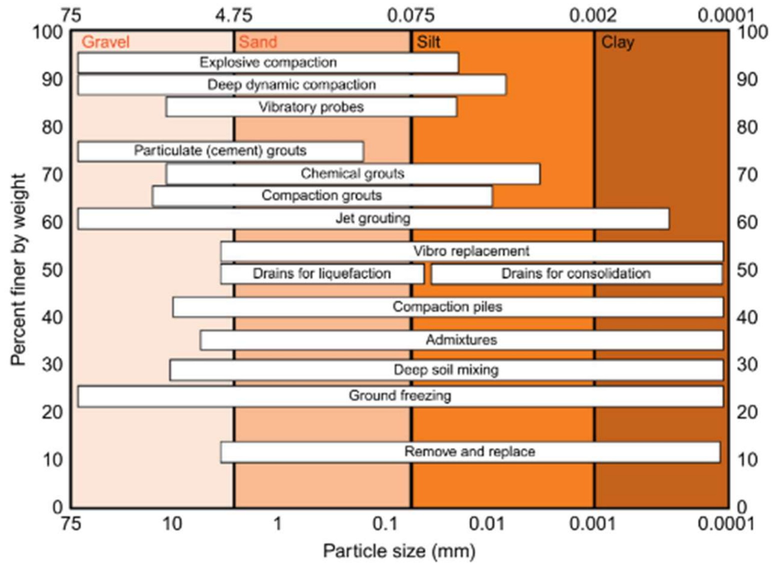

Fig 2.1: Soil Improvement methods applicable to different ranges of soil particle size.

Desired/required soil properties:- Evidently, different engineering properties are attained through various techniques, and various techniques will result in varying degrees of site development and uniformity.

Material accessibility:- Depending on the location of the project and the materials required for each practical ground improvement strategy, certain materials may not be accessible, or the cost and logistics of transportation may preclude the use of a specific technique.

Availability of skills, local experience, and local preferences:- The engineer may be familiar with and comprehend a preferred technique, but some localities and project owners may be unwilling to attempt something "unproven" in their region—the availability of talents, regional experience, and regional preferences. Even though this is predominantly a social issue, it should not be ignored, particularly in rural and underdeveloped areas.

Environmental concerns: - As environmental consciousness has increased, there has been a greater emphasis on minimizing the environmental impact of construction initiatives. This increased concern has resulted in substantial modifications to the methods, apparatus, and materials used for ground improvement. Recognizing the importance of sustainability and the preservation of natural habitats, engineers now pursue solutions with a smaller environmental footprint. These modifications are indicative of a larger shift in the construction industry toward more environmentally responsible practices.

Economics:- After evaluating all relevant factors, the ultimate decision regarding the ground improvement method is frequently based on the associated expense. The price may be the deciding factor when selecting between two or more viable options. In some instances, time constraints may necessitate the selection of a more expensive method if it will expedite the project's completion and allow for earlier use. These factors are essential for determining the most effective enhancement method(s) to be proposed. The decision should be made on a case-by-case basis.

2.3.2 Conventional Methods of Ground Improvements

In geotechnical engineering, several **conventional techniques for ground improvement** have been employed for decades. The following are some of the most prevalent traditional methods:

- Mechanical Stabilisation: - Mechanical soil stabilization is a method of ground improvement that entails modifying the physical qualities of the soil to increase its strength and stability. Typically, this is accomplished by adding materials to the soil, such as cement, lime, or fly ash, to improve its bearing capacity and decrease its compressibility. The additive material is blended with the soil on-site during mechanical soil stabilization using specialized equipment such as pug mills or soil mixers. The resultant mixture is then compacted and allowed to cure, resulting in soil that is more stable and less compressible. Mechanical mixing provides a more homogeneous soil, with the added ingredients serving as a binder to fill spaces and fortify the soil. The choice of additional material and its quantity is contingent upon the soil type, site circumstances, and planned application of the soil. Typically, lime is used to stabilize clay soils, whereas cement is used to stabilize sandy or silty soils. In addition to elements such as curing time and compaction technique, the success of the mechanical soil stabilization approach is also dependent on these variables.

- Compaction: This approach includes using mechanical energy to lower soil volume by compressing it. The reduction in volume causes the soil's density to rise, which increases its strength and stability.

- Vibro-compaction: Vibro-compaction is a technique that utilizes a vibrating probe to compact loose or fragile soils. Inserting the probe into the soil and vibrating it at a high frequency causes the soil particles to reorganize and compress.

- Stone columns: This technique includes the insertion of vertical stone columns into the earth. The columns serve as a reinforcement and raise the soil's carrying capacity, therefore decreasing settlement and boosting stability.

- Dynamic compaction: This technique includes using heavy equipment to dump weights onto the soil's surface, creating shock waves to propagate and compact the soil.

- Deep soil mixing: This approach requires the use of specialist equipment to mix and homogenize the soil with a binder, such as cement or lime. The combination enhances the strength and stability of the soil.

- Sand compaction piles: This technique includes installing sand columns into the soil. The columns serve as a reinforcement and raise the soil's carrying capacity, therefore decreasing settlement and boosting stability.

- Grouting: This procedure involves the injection of a cement or chemical grout into the soil to increase its strength and stability.

2.3.3 Unconventional Methods of Ground Improvements

Unconventional ground improvement techniques are newer or less commonly used methods of modifying soil or rock geotechnical properties. Here are some examples of unconventional ground improvement methods:

- Geosynthetics: These techniques involve the use of synthetic materials to strengthen or stabilize the soil, such as geotextiles, geogrids, and geocells. Geosynthetics are intended to disperse loads and minimize soil deformations.

- Electrokinetic: This technique changes the physicochemical characteristics of the soil by applying an electric field to it. The electric field can mobilize charged particles and modify the structure of the soil, resulting in greater strength and stability.

- Vacuum consolidation: This technique includes applying negative pressure to the soil in order to extract water and consolidate the soil. Reduce settlement and boost the soil's strength and stiffness via vacuum consolidation.

- Shockwave consolidation: This technique utilizes explosive charges to generate shockwaves that compact the earth. The soil particles can be compacted, and the shockwaves increase their density and strength.

- Thermal stabilization: This procedure stabilizes the soil by the use of heat. The soil's structure and qualities may be altered by heat, resulting in increased strength and stability.

2.4 STONE COLUMNS

Stone columns are a widely used ground improvement technique that involves inserting columns of crushed stones into weak soils to improve their load-bearing capacity and reduce settlement. In recent years, researchers have focused on enhancing the performance of stone columns through various means, including the use of alternative materials, modifications to installation techniques, and including geosynthetics.

During the installation process, a borehole is drilled into the soil to the desired depth, and the stone or granular material is then inserted into the borehole and compacted to form a column. The column may be formed using different methods, such as dry top-feed or wet bottom-feed methods, which may impact the performance of the column.

Granular piles may have been employed around 1830 in France (Hughes and Withers, 1974) to support huge iron works foundations at Atsenal in Bayonne (France). Wooden stakes were used to dig boreholes, which were subsequently filled with stone. This ground improvement technology was ignored until 1937 when Serzey Steuerman and Johann Keller found and used it in Germany. After that, Serzey Steuerman founded Vibro-flotation Foundation Corporation (V.F.C.) in Pittsburgh, Pennsylvania, and vibro-flotation technology developed. Cementation bought Steuerman's American technology from VFC in 1957 and used it at sites in Britain with finer and more cohesive soils. Cementation and Keller created a wet or dry process for backfilling stone material to meet site circumstances and costs. This laid the groundwork for today's wet and dry vibro displacement methods. Granular piles can be 0.5 m to 1.5 m in diameter and up to 20 m deep (Broms, 1979). (Hughes and Withers, 1974).

2.4.1 Application of stone columns

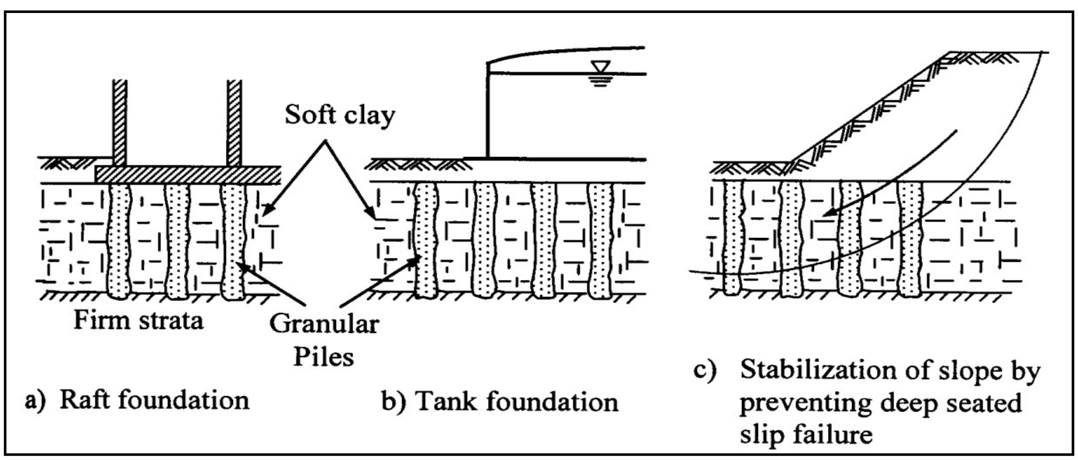

Figure 2.2: Typical applications of stone columns (Brauns, 1978)

Stone or granular columns are commonly used in a variety of geotechnical engineering applications, such as foundation support for warehouses, shipbuilding facilities, sewage treatment plants, parking garages, miscellaneous buildings, oil storage tanks, water storage tanks, reducing liquefaction potential in seismic zones (McKelvey and Sivakumar, 2000), and railroads, some of the examples are shown in figure 2.2. They are suited economically and technically for soft, cohesive soils (McCabe et al., 2009). According to several case studies, "stone column construction is employed for a broad variety of soils and projects, including landfills, embankments, roads, airports, railways, slope stability, and bridge abutments" (McKelvey and Sivakumar, 2000). Stone columns may be cautiously utilized in very soft coastal clays, thin layers of peaty clay, and mine tailings clays (Raju and Sondermann, 2005).

2.4.2 Method of Installation of stone columns

Two main methods for installing encased stone columns (ESC) are described by Tandel et al. (2012). These are (1) the Displacement Method and (2) the Replacement Method.

2.4.2.1 Displacement Method

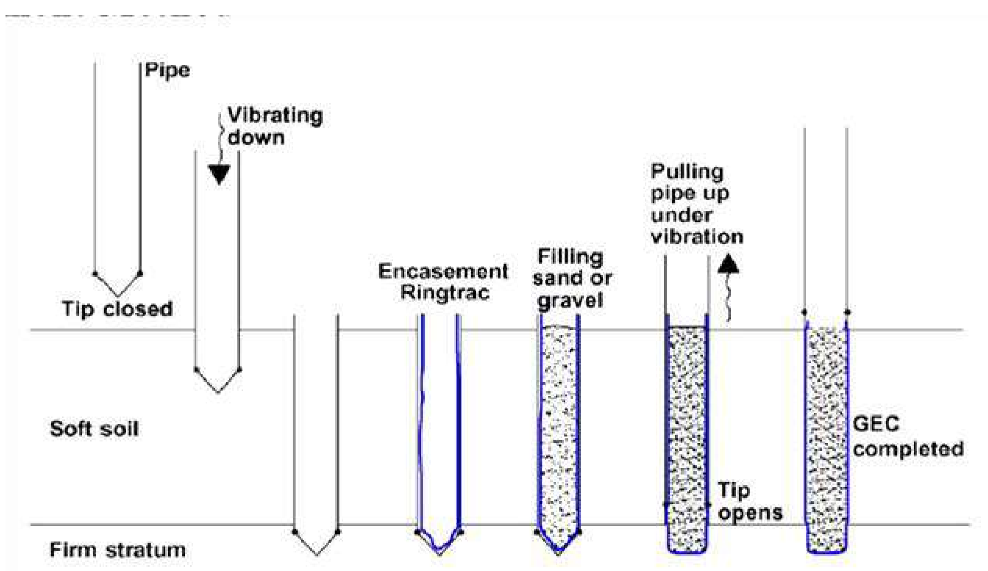

Figure 2.3: Displacement method (Alexiew et al., 2005)

As described by Alexiew et al. (2005), the displacement method is used to improve the ground in very soft soils, typically those with undrained shear strength (cu) values below 15 kPa. This technique involves inserting a steel tube with a closed tip into soft soil. The empty tube is then filled with a geotextile and fill material cylinder frame.

Subsequently, the tip of the tube is opened, and the vibration is applied to pull the tube upwards. This method is depicted in Figure 2.3.

2.4.2.2 Replacement Method

As demonstrated by Gniel and Bouazza (2010), the replacement method is utilized when there is concern regarding the impact of vibrations on nearby structures or when the soil presents substantial resistance to penetration. This method requires the installation of an open steel pipe into the soil until a hard layer is reached. Using auger boring, the soil within the pipe shaft is subsequently extracted. Figure 2.4 depicts the replacement method's procedure.

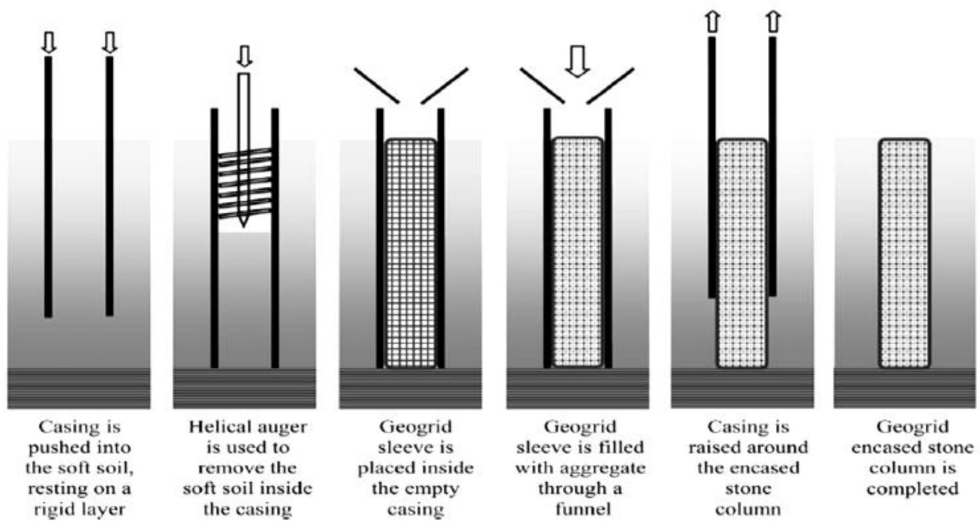

Figure 2.4: Replacement method (Gniel & Bouazza, 2010)

Lee et al. (2008) presented a new construction technique for partially encased stone columns. This method uses a polyester geogrid designed to match the intended column diameter (0.8m). The geogrid lengths are two or three times the column's diameter. Drilling with an auger is followed by the installation of a casing during construction. The soil is then removed, as depicted in Figure 2.5. Subsequently, 25mm diameter stones are layered and compacted inside the casing to create the shape of the stone column. The cylindrical geogrid is then inserted at the specified height into the stone column. The construction will continue until the stone column reaches a depth of 5.5 meters below the surface of the ground. Figures 2.6 and 2.7 are provided for your visual reference.

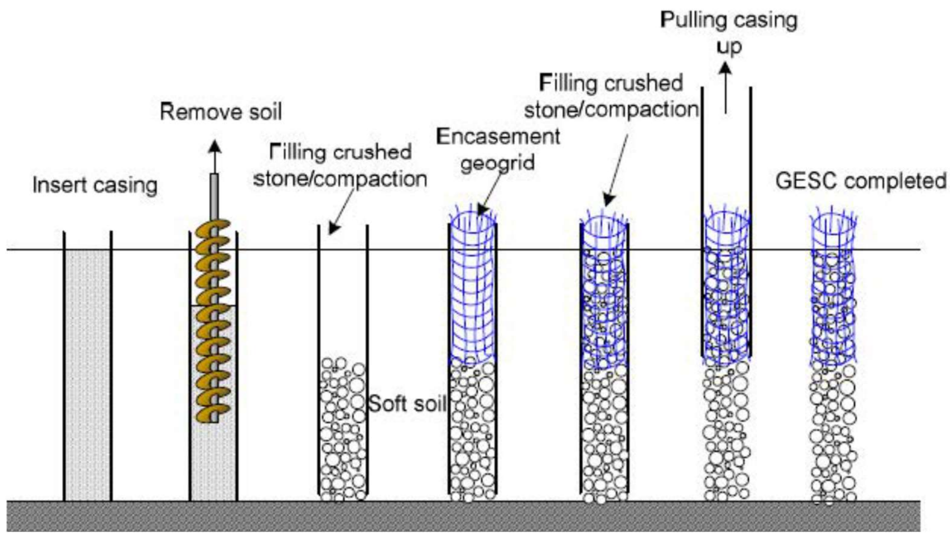

Figure 2.5: Installation of the partially encased stone column in the field (Lee et al., 2008)

Figure 2.6: Inserting a geogrid net into a pre-bored and partially constructed stone column (Lee et al., 2008)

Figure 2.7: Construction of a partially encased stone column in soil (Lee et al., 2008)

2.5 DESIGN APPROACHES OF STONE COLUMN

The interaction between the column and the surrounding soils is instrumental in determining the bearing response of the soil/column system. The properties and interactions of both materials influence this response. To theoretically address this complex problem, a level of idealization known as unit cell idealization is employed. Existing theories frequently disregard the imperfections of stone and clay by treating them as ideal elastic or elastic-plastic materials (Hughes and Withers, 1974; Barksdale and Bachus, 1983; Priebe, 1995). Therefore, essential parameters such as the used grid pattern, the area replacement ratio, and the stress concentration factor (Sections 2.6.1.1 to 2.6.1.3) must be considered when designing stone columns. The following is a summary of Watts's (2000) proposal for a commonly proposed design procedure:

- Consider the undrained shear strength of the soil and the internal angle of friction when calculating the maximum load-bearing capacity of an individual column.
- Determine the appropriate column diameter and spacing between columns using a formula.
- Assess and estimate the potential amount of settlement.

2.5.1 Basic Design Parameters

2.5.1.1 Unit Cell Idealization

According to Balaam et al. (1977), unit cell idealization is used to model the behavior of individual columns and the surrounding soil. It assumes the identical behavior of each unit cell within a group (Figure 2.8). This method assists in determining the area over which stresses are distributed vertically (Barksdale and Bachus, 1983). The three most common patterns for installing stone columns are triangular, square, and rectangular. The equilateral triangle pattern is the most practical and effective for achieving uniform densification rates over large areas. Typical patterns for isolated spread footings are square and rectangular (Watts, 2000; BSI, 2005).

Figure 2.9 depicts typical stone column layouts in various patterns. It is practical to associate each stone column with a nearby soil drainage area. A circle (unit cell) with an equivalent diameter (De) and a comparable total area can approximate this tributary area. The column spacing (S) is a crucial factor because it has a direct effect on the degree of improvement. Typically, the spacing is determined to provide a zone of overlap that treats a large area of soil. Greenwood (1970) suggests that a narrower spacing is preferable for isolated foundations compared to larger raft foundations.

Nevertheless, the spacing is typically between two and three times the column diameter (Hughes and Withers, 1974). The relationship between the distance between stone columns and their equivalent diameter is depicted in Table 2.1 and is dependent on the arrangement of the columns.

Table 2.1 Equivalent unit cell diameter (adopted from Balaam & Booker, (1981)

Arrangement	Equivalent unit cell diameter(D_e); (S) centre to centre spacing
Triangular	$({}^{12}/_{\pi})^{0.25}$ Deq =1.05S
Square	$({}^{16}/_{\pi})^{0.25}$ Deq =1.13S

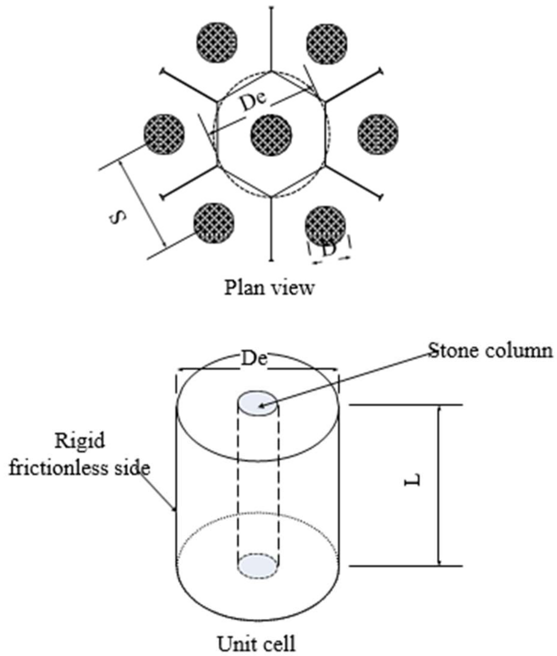

Figure 2.8 Unit cell concept (Barksdale and Bachus, 1983)

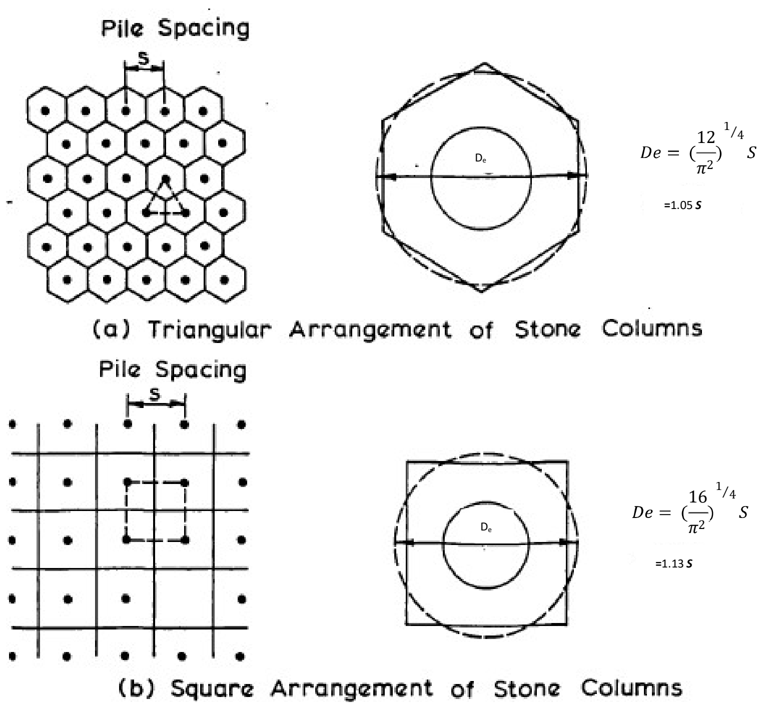

Figure 2.9 Stone Column arrangements in (a) Triangular (b) Square (Balaam & Booker, 1981)

2.5.1.2 Area Replacement Ratio

Using the unit cell concept, the geometry of a mesh composed of stone columns can be utilized to calculate the extent of soil replacement and determine the area replacement ratio, denoted as As. The definition of the area replacement ratio is the ratio of the area of each column, Ac, to the total soil area, A (Barksdale and Bachus, 1983).

$$As = {}^{Ac}/_{A} = [{}^{Dc}/_{De}]2$$

Where: D_c is the compacted stone column diameter, and D_e is the equivalent unit celldiameter. The area replacement ratio also can be presented in terms of the diameter and spacing of thestone column as follows: $As = Cg\left(\frac{Vc}{S}\right)^2$

Where: Dc is the diameter of the compacted stone column; S is center-to-center spacing; cg is a constant dependent upon the pattern of stone columns used.

Increasing the area replacement ratio positively affects the performance of the combined soil system, resulting in an increase in bearing capacity and a decrease in settlement. Wood et al. (2000) suggested that an area replacement ratio of at least 25 percent is required for bearing capacity improvements exceeding 30 percent

2.5.1.3 Stress Concentration Factor (n)

Significant stress concentration is transferred from the loaded foundation to the stone column. In contrast, the remaining stresses are transferred to the soil due to the soil's relative weakness in comparison to the column material. Within the unit cell, the vertical stress distribution, also known as the concentration factor, is the ratio of stress on the stone column to stress on the surrounding soil (Han & Ye, 1991). Aboshi et al. (1979) and Barksdale and Bachus (1983) reported that the concentration factor typically falls within the range of 2 to 6.

$$n = \frac{\sigma_s}{\sigma_c}$$

Where: σ_s is the stress in the stone column, and σ_c is the stress in the surrounding soil.

Several variables, including the type of foundation, column length, and consolidation time, can influence the magnitude of stress concentration. Juran and Guermazi (1988) observed that the concentration factor (n) increases as consolidation time increases and decreases as column length increases. In addition, using a rigid foundation to load the soil/column system typically results in a greater stress concentration than using a flexible foundation (Barksdale and Bachus, 1983).

According to Ambily and Gandhi (2007), the modular ratio also plays a significant role in stress concentration. They discovered a direct relationship between the modular ratio and the concentration factor, with an increase in the modular ratio resulting in a rise in the n factor. Additionally, it was discovered that an increase in the surrounding soil's strength decreased the concentration factor. The total vertical stresses σ in stone columns and the surrounding soil over the unit cell area and corresponding to a given area replacement ratio can be expressed as:

$$\sigma = \sigma_s . A_s + \sigma_c (1 - A_s) \quad \text{....2.4}$$

Where the terms have been previously defined.

Consequently, the stress concentration factor can be estimated (as follows) using the elastic theory as a function of the modular ratio between the column and the soil (Barksdale and Bachus, 1983; Babu et al., 2013).

$$\sigma c \leq \mu c \sigma = \mu_c (\sigma_s | \mu_s)^2$$

Where: μ_c *and* μ_s are the stress ratios in the clay and stone columns, respectively.

$$\mu_s = {}^{n}/[1 + (n - 1)^{A_s} A_s]$$

$$\mu_c = {}^{1}/[1 + (n - 1)^{A_s} A_s]$$

2.6 FAILURE MECHANISM OF STONE COLUMNS

Stone columns may fail due to different mechanisms under compressive loads. Stone column failure is influenced by parameters including diameter, length, and spacing (Wood et al., 2000).

Hughes and Withers (1974) identified three loading patterns for stone columns.

- Small Footing Loading: Single stone columns supported by small footings, where the lateral restraint is uniform around the column's periphery.
- Widespread Loading: Large footings apply loads to stone columns whose lateral restraint is uniform in all directions and increases as the soil settles.
- Strip Footing Loading: Stone columns arranged in a line to support loads applied by strip footings, with lateral restraint provided only in the strip footing direction.

Kirsch and Kirsch (2010) presented a diagram (Figure 2.10) to demonstrate the main loading scenarios of stone columns. The stress distribution between the stone column and the soil depends on their relative stiffness when subjected to the foundation's stresses on the granular mat or foundation. Greater stiffness of stone columns results in increased contact stresses. Kirsch and Kirsch (2010) identified the failure mechanism at one of the interfaces depicted in Figure 2.11.

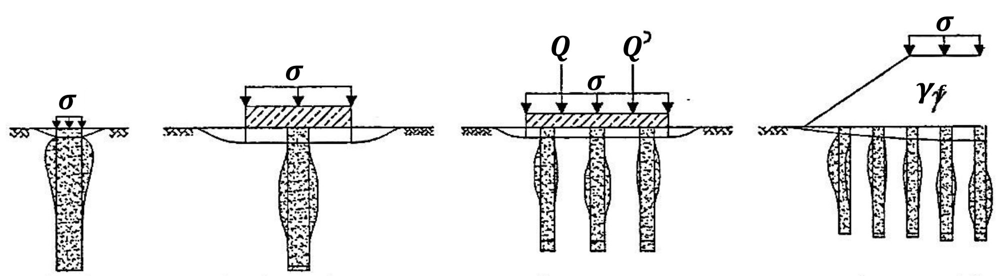

Single column	**The single column below the footing**	**Column group below the footing**	**Column grid below embankment**

Figure 2.10: Different loading scenarios for stone columns (Kirsch and Kirsch, 2010)

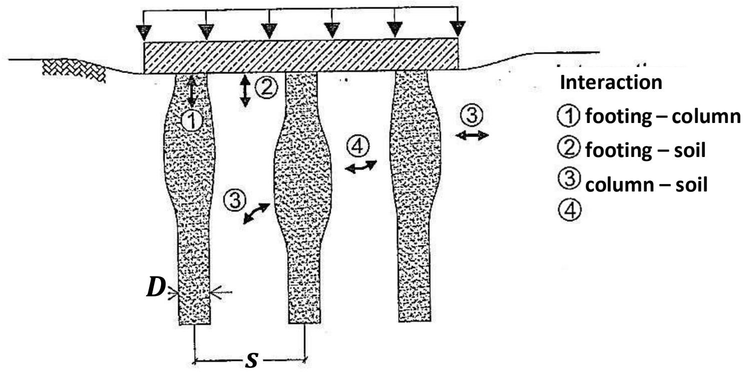

Figure 2.11: Interaction of load application with stone columns and soil (Kirsch and Kirsch, 2010)

2.6.1 Single Stone Columns

In contrast to pile foundations, where the load-bearing mechanism relies on tip and skin resistances, stone columns derive their strength from lateral confinement. This is accomplished by transferring the load from the soil to the column by stimulating lateral earth pressure (Kirsch and Kirsch, 2010). The stone column bulges under excessive lateral stress, causing soil deformation due to further increases in lateral stress. Kirsch and Kirsch (2010) identified the following causes for the failure of footings with single stone columns:

- bulging of long, end-bearing columns
- shearing of short, end-bearing columns
- punching failure by sinking short, floating columns
- bulging in deeper layers

The primary cause of failure is the bulging of the stone column when the surrounding soil can no longer withstand the added lateral stress (Figure 2.12(a)). The depth at which bulging occurs in homogeneous soils is approximately 4D. For short stone columns with a length shorter than 4D, stone column punching is possible (Figure 2.12(c)). Conversely, if a short column is bearing on a hard stratum, shear surfaces will develop near the ground level through the column head and the adjacent soil (Figure 2.12(b)). As shown in Figure 2.12(d), failure can also occur due to bulging at depths greater than 4D if there is a sufficiently thick layer of soft soil beneath the stone column (greater than 2D).

Van Impe et al. (1997) observed bulging and pile failure mechanisms in stone columns of varying lengths. Longer columns are prone to bulging failure, whereas shorter columns are more susceptible to pile-type failure. The capacity is determined by the limiting stress of the mutually exclusive mechanisms.

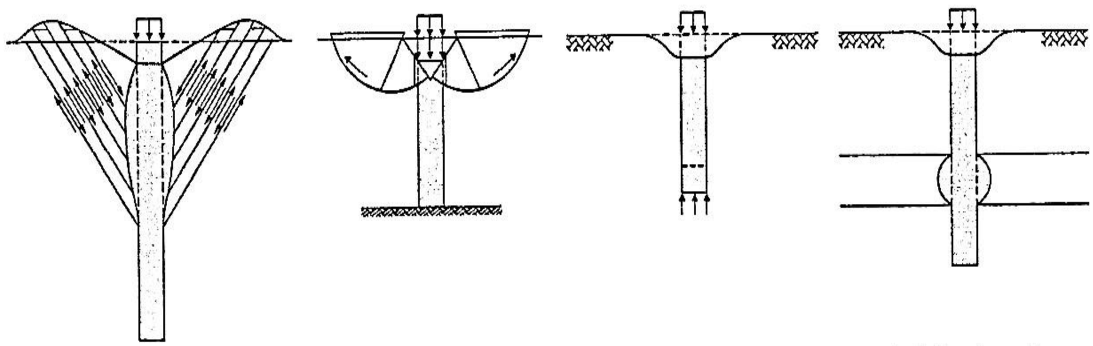

(a)Bulging **(b) Shearing** **(c) Sinking** **(d)Bulging in the soft deeper layer**

Figure 2.12: Failure mechanisms of isolated stone columns (Kirsch and Kirsch, 2010)

Madhav (1982) identified a critical length beyond which bearing capacity does not significantly increase, resulting in bulging failure. Columns shorter than the critical length undergo pile-type failure, as loads are transmitted throughout the entire depth of the stone columns. However, this is not applicable in lengthier columns. The determination of the critical length of a granular pile (Lcr) involves considering the internal friction angle of the column material (ϕc), undrained shear strength of the soil (cu), unit weight of the soil (γs), diameter of the granular pile (D), and diameter of the footing (Df), as depicted in Figure 2.13.

Ambily and Gandhi (2006) conducted laboratory model tests and two-dimensional axisymmetric FEM analyses on single stone columns in a unit cell. The study found that single stone columns experience failure from bulging, with the depth of bulging being around 0.5 times the diameter of the column. The results were corroborated by Finite Element Method (FEM) analyses.

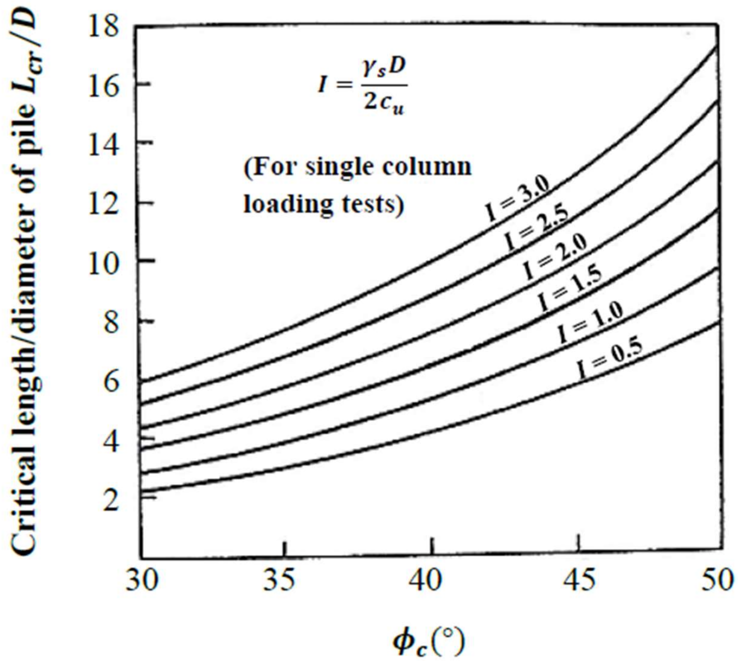

Figure 2.13: Relation between Lcr/D and ϕc (Madhav, 1982)

Murugesan and Rajagopal (2006) conducted Finite Element Method (FEM) analyses to study single end-bearing stone columns. Similar mobilized lateral stress was observed around stone columns with different diameters under identical loading conditions. The authors reported that the stone column bulges when loaded, typically at a depth between $1.5D$ and $2.0D$ from the ground surface. The shape of failure in single stone columns is influenced by the strength parameters of the column and soil, as well as the length and diameter of the column, as shown in various studies**.**

2.6.2 Group of Stone Columns

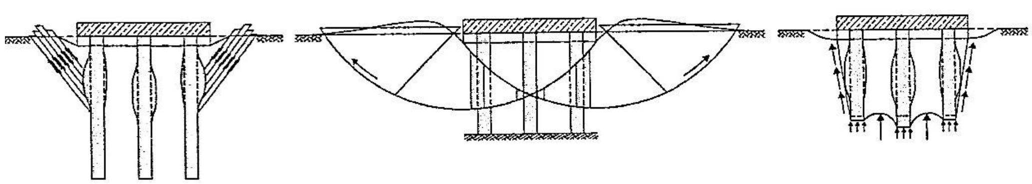

(a) **(b)** **(c)**

Figure 2.14: Failure mechanisms for column groups (Kirsch and Kirsch, 2010)

Kirsch and Kirsch (2010) stated that the failure mechanisms of groups of stone columns are more complex than those of single stone columns. Figure 2.14 depicts potential failure mechanisms in rigid foundations that a group of stone columns supports. Hughes and Withers (1974) noted that the bearing capacity issue only applies to stone columns located at the outer edges of a large group.

According to McKelvey et al. (2004), as the applied stress increases, both short columns (L/D = 6) and long columns (L/D = 10) with circular footings tend to bulge in unrestrained directions. In the case of short columns, complete bulging and punching into the soil by approximately 10 mm were observed, whereas, in the case of long columns, bulging was observed only a few stone diameters from the top of the stone column. In the case of long columns, this suggests that only a small portion of the load is transmitted to greater depths. The authors concluded, based on these findings, that an L/D ratio of 6 is too short, resulting in complete deformation and partial punching into the clay, whereas an LD ratio of 10 is too long, as the bottom portions of the column remain undeformed. Consequently, they suggested that the optimal L/D ratio for stone columns lies between 6 and 10. Moreover, for L/D ratios greater than 10, there is no significant increase in bearing capacity, but there is a notable improvement in settlement.

McKelvey et al. (2004) conducted experiments that revealed three distinct failure modes for stone columns:

- Bulging Bending
- Shearing

They observed that short columns typically fail as a result of punching and complete bulging into soft soil. In contrast, long stone columns display minimal punching, and bulging is typically restricted to the column's upper portion. Long stone columns typically feature shear planes. Regardless of the LD ratio, all columns bend in a direction that is not constrained.

Wood et al. (2000) conducted another investigation into the failure mechanisms of stone column groups. Similar to McKelvey et al. (2004), they estimated the failure modes and analyzed the stress distributions using the shapes of the stone columns after the tests (Figure 2.16). Wood et al. (2000) added punching to the list of failure mechanisms established by McKelvey et al. (2004). Consequently, they described four distinct failure modes (Figure 2.17), as observed in laboratory tests:

Mode 1: Bulging - This occurs when a loaded column can freely expand radially due to the presence of closely adjacent columns. The increase in mean stress causes the column to bulge (shown in Figure 2.16 as Mode A). This type of failure is frequently observed in columns located in or near the footing's center. Significantly, the depth of bulging increases as the area replacement ratio rises. This failure mode is most prevalent in columns supported by rigid footings, where the footing pushes a soil cone undergoing limited deformation downward.

Mode 2: Shear Plane - This mode occurs when a stone column is subjected to high stress ratios with limited lateral restraint, leading to a minimal increase in mean stress. The column fails due to shear along a diagonal plane (Mode B in Figure 2.16). Typically, this failure mode is observed in columns near the footing's edge.

The combination of modes 1 and 2, which involve a combination of bulging and shear planes at different locations, can be used to estimate the zone of influence beneath the group of stone columns. Near the edges, this zone assumes a roughly conical shape with an angle of (Figure 2.15(a)). The angle increases as the area replacement ratio increases (Figure 2.18(b)). In addition, it was discovered that the diameter of the footing has a more significant impact on the depth of influence than the diameter of the stone column. This mode occurs when the columns are relatively short and transmit a significant portion of the load to a soft clay layer beneath the column tip. The column, therefore, penetrates the soft clay (Figure 2.16 (b)). This effect is more pronounced in columns with shorter lengths and higher area replacement ratios. Long Column Absorbs Deformation Along Its Length - Mode 3(b) The load transmitted to the underlying soil decreases as the length of the column grows. If a column is sufficiently long, the footing penetration is absorbed along the column's length (Figure 2.17(c)). This effect is more pronounced in columns with longer lengths and lower area replacement ratios.

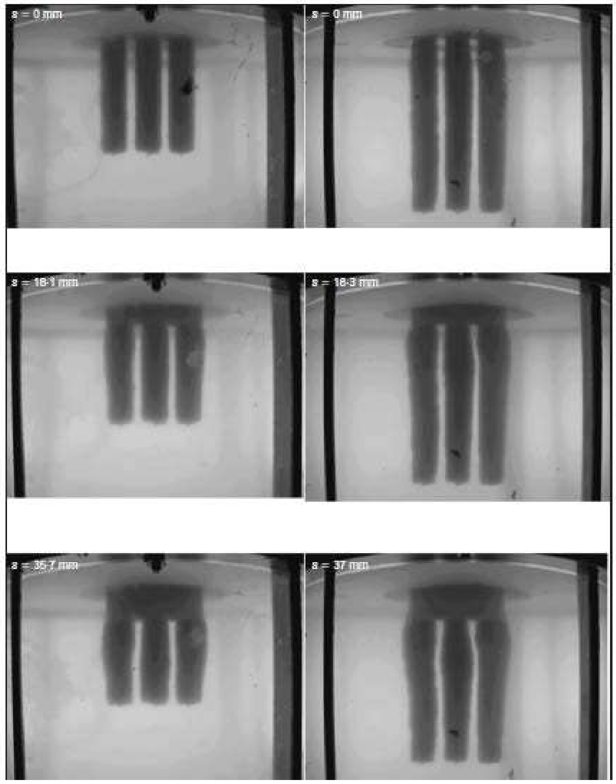

(a) (b)

Figure 2.15. Photographs of a group of sand columns (a) *L/D*= 6 and (b) *L/D*= 10 (McKelvey et al., 2004)

Mode 4: Bending (Buckling) - This mode occurs when axial loads are applied to a column with limited lateral strength. The columns behave similarly to laterally loaded piles, causing clay beneath the footing to move laterally. The columns resemble inclinometer models (Figure 2.16(d)). Typically, this failure mode affects columns located outside of the loading plate.

In contrast to the behavior observed in single stone columns, no bulging failure is observed in groups of stone columns, as noted by Ambily and Gandhi (2006). Their FEM analyses also supported this conclusion.

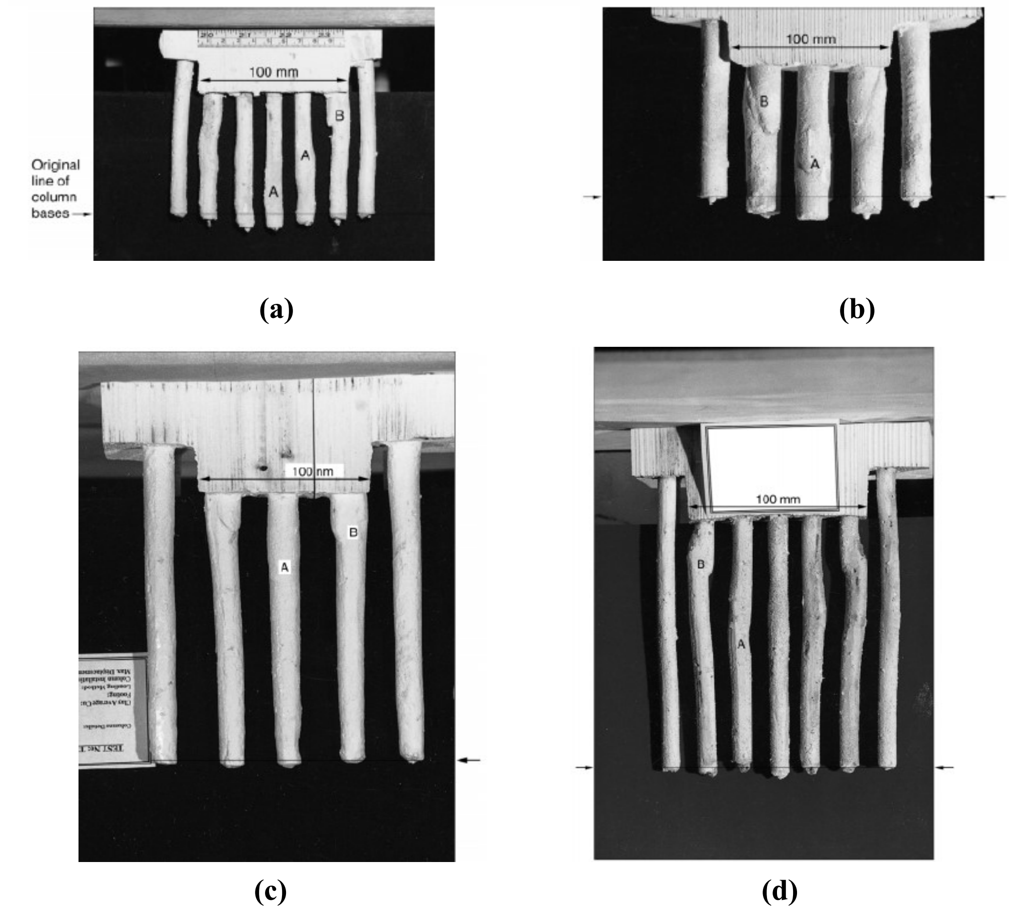

Figure 2.16: Photographs of deformed sand columns where the arrows indicate the original level (a) L/D = 9 and ar = 24% (b) L/D = 5.7 and ar = 30% (c) L/D = 9.7 and ar = 24% and (d) L/D = 14.5 and ar = 24% (Wood et al., 2000)

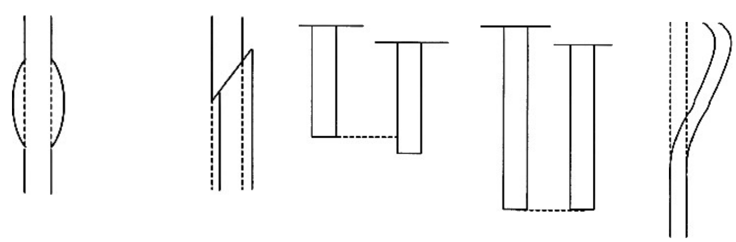

(a) (b) (c) (d)

Figure 2.17: Modes of failure mechanisms develop in a group of stone columns

(a) bulging (b) shear failure (c) punching (d) bending (buckling) (Wood et al., 2000)

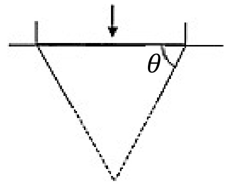

(a)

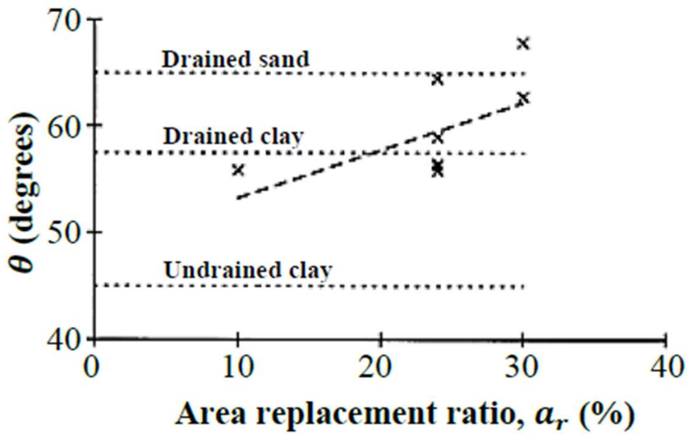

(b)

Figure 2.18: (a) 'Rigid' cone beneath the footing and (b) relation between θ and ar (Wood et al., 2000)

2.7 STUDIES ON STONE COLUMN

2.7.1 Experimental Studies

Sivakumar et al. (2004) investigate the behavior of small laboratory specimens of porous clay (undrained shear strength of 30 kPa) reinforced with sand columns when tested under known boundary stress conditions. Two sets of experiments were performed on kaolin samples in a triaxial cell (diameter 100 mm, height 200 mm). The first set of specimens was reinforced with a 32 mm diameter, 80, 120, 160, or 200 mm long column of sand. Either compacting moist sand into a prebored cavity or freezing a moist sand column before inserting it into a prebored opening was used to install columns. Before installation, geogrids were used to reinforce the second set of columns. Either uniform loading, which applied the weight to the entire surface area of the specimen, or foundation-type loading, which loaded only a small area in the center of the specimen, was applied to the specimens. Under uniform loading, specimens with full-depth columns were substantially stronger than specimens without columns. Les specimens of wet compaction with single, partially penetrating columns were weaker than those without columns. When frozen columns were positioned, their strength increased progressively. Bearing capacities increased with increasing column length when subjected to foundation-type loading. Geogrid reinforcement substantially increased load-bearing capacity.

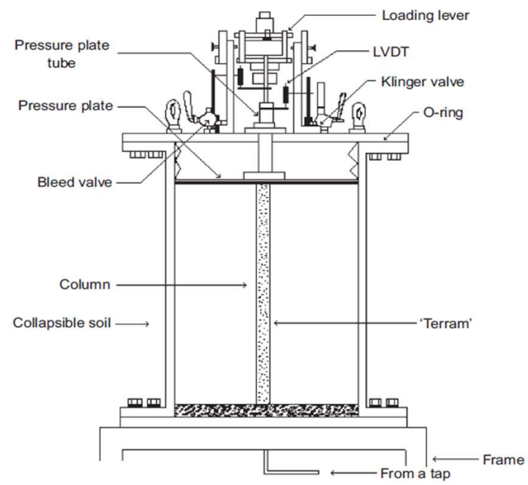

Figure 2.19: Cross-section of testing apparatus (Hanna and Ayadat, 2005)

Hanna and Ayadat (2005) present the results of an experimental investigation on the performance of stone columns encased in geofabric and installed in a layer of collapsible soil subjected to flooding (Figure 2.19). The bearing capacity and settlement characteristics of the columns were evaluated. Different sand column lengths, degrees of saturation, and four non-woven geofabrics were tested in this investigation (Terram 700, 1000, 1500 and 2000). According to the results of the present experimental investigation, unreinforced sand columns in collapsible soil did not significantly improve the performance of the soil. Additionally, the column collapsed prematurely. The bearing capacity of encapsulated sand columns increases as the strength and/or column length of the geofabric material increases, as shown in Figure 2.20, As column rigidity and/or column length increase, the head of the column settles less due to external loading and flooding (up to a maximum value equal to the collapsible soil layer thickness). Theoretical models were developed to forecast the carrying capacity and settlement of these columns.

Comparing the findings predicted by the proposed theory and the experimental results of the current study with those reported in the literature revealed a high level of concordance.

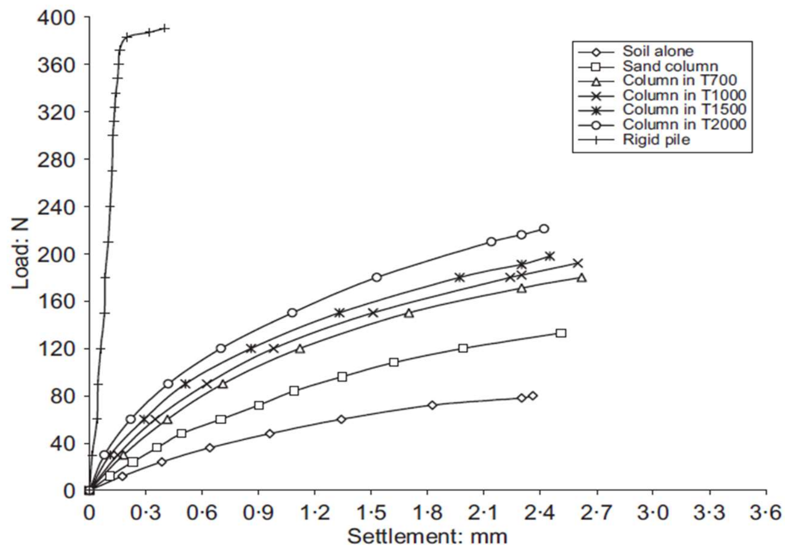

Figure 2.20: Load–settlement curves for various foundation supports (L =410 mm) (Hanna and Ayadat, 2005)

Black et al. (2006) describe an innovative test arrangement for evaluating the performance of footings made of soft clay reinforced with granular columns. This sophisticated testing method evaluates the settlement of granular column-supported footings. The axial loading system allows samples to be consolidated under Ko conditions while the load is applied to a small foundation area of the sample, and the relatively large sample size of 300 mm in diameter and 400 mm in height are two of the equipment's most significant features.

In addition, the system includes pressure cells beneath the footing and top cover to detect pressure distribution in relation to foundation displacement and a lateral strain gage to monitor boundary effects, the test setup is shown in the Fig. 2.24. This paper discusses some of the preliminary test results obtained using this equipment. Testing samples were produced by consolidating kaolin slurry in a large one-dimensional consolidation container. Using the replacement technique, the granular columns were fitted by compacting pulverized basalt uniformly graded with 90% between 1.5-2 mm particle sizes into a preformed hole. The preliminary tests yielded encouraging outcomes, validating the functionality of the equipment and indicating the possibility of expanding knowledge regarding settlement response and the design of a substructure supported by granular columns.

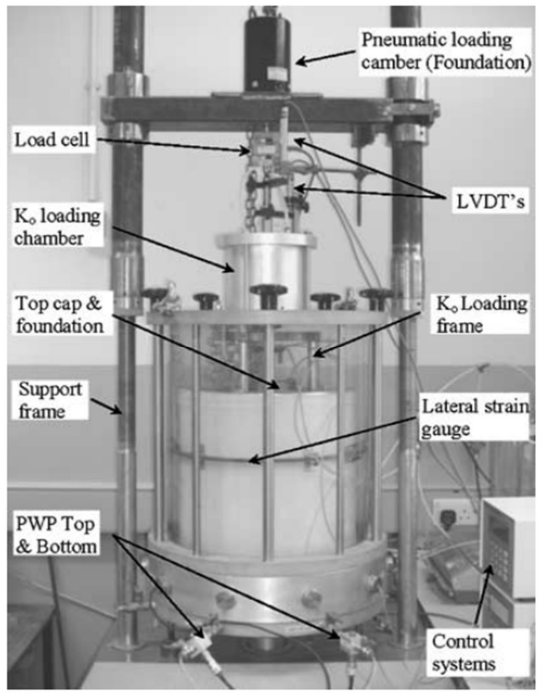

Figure 2.21: Triaxial cell apparatus. (Black et al. 2006)

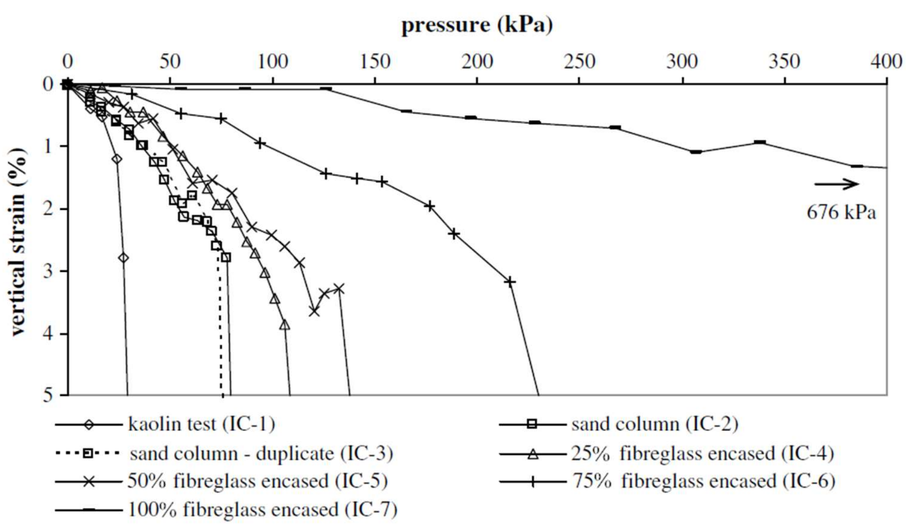

Figure 2.22: Vertical stress–strain behavior of isolated column tests (Gniel and Bouazza 2009)

Table 2.2: Sample properties for isolated column tests. (Gniel and Bouazza 2009)

Test number	Test description	Consolidated kaolin clay			Sand column
		Moisture content (%)	Undrained cohesion (kPa)	Sample height (mm)	Relative density (%)
IC-1	Kaolin clay	67	5	322	
IC-2	Non-encased	63	5.1	311	90
IC-3	Non-encased (duplicate)	65	4.5	311	94
IC-4	25% Encased (fibreglass)	64	4.5	308	92
IC-5	50% Encased (fibreglass)	67	4.1	315	93
IC-6	75% Encased (fibreglass)	63	4.6	311	93
IC-7	100% Encased (fibreglass)	65	3.7	317	92

Gniel and Bouazza (2009) present the results of several small-scale model column experiments conducted to investigate the behavior of geogrid-encased columns. The primary objective of the tests was to determine how varying the length of encasement affected the column's behavior and whether a partially encased column would conduct similarly to a fully encased column. Additionally, the behavior of group columns and isolated columns were compared. The results of experiments on partially encased columns for isolated columns are shown in Fig. 2.22, which revealed a gradual decrease in vertical strain with increasing encasement length. The Legends used as IC are defined in Table 2.2. Just beneath the base of the encasing, a protrusion of the spine was observed. Fully encased columns exhibited an increase in column rigidity as well as a reduction in column strain in the range of 80%. This range of performance may make partial and complete geogrid encasing techniques applicable to various site applications.

Samadhiya et al. (2009) analyzed the behavior of a single pile embedded in flexible clay and reinforced with geogrid layers. Researchers have examined in the laboratory the response of a geogrid-reinforced granular pile to a solid circular footing. The effect of geogrid layer separation and reinforced pile depth (depth of the bottommost geogrid layer) on reinforced pile performance has been investigated. In addition, a finite element numerical analysis was conducted using rocscience, Phase 2, version 6, and the results were compared to those of the experimental investigation.

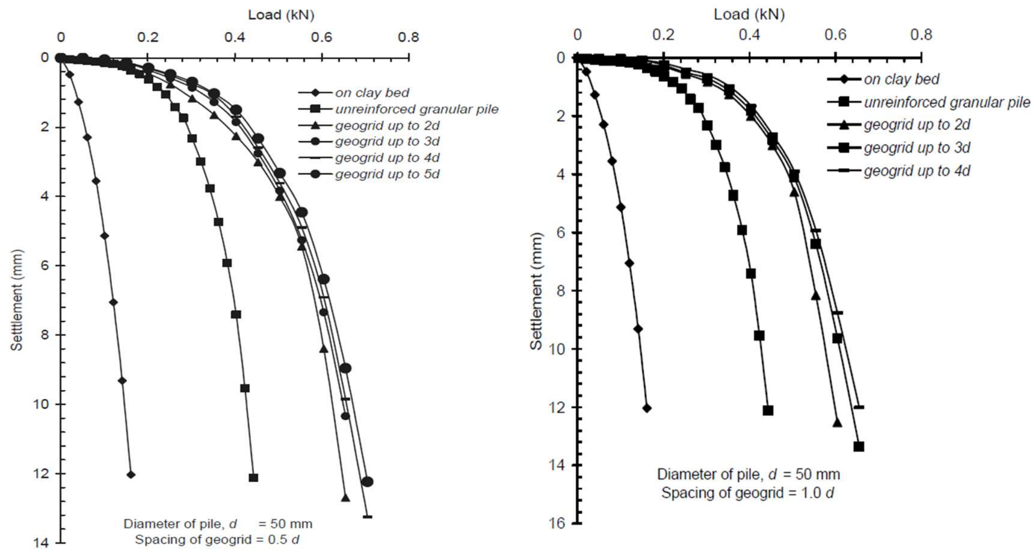

(a) with geogrid spacing 0.5 d **(b) with geogrid spacing 1.0 d**

Figure 2.23: Load-settlement curve

It has been demonstrated that granular foundations with geogrid reinforcement significantly increase load carrying capacity, the variation of geogrid spacing is demonstrated in Fig 2.23. Using geogrid layers as reinforcement has been found to reduce pile protrusion width.

Murugesan and Rajagopal (2010) investigate the qualitative and quantitative improvement of individual load capacity of stone columns by encasing them in a large-scale testing tank using laboratory model experiments on stone columns installed in clay beds prepared under controlled conditions. Load tests were conducted on solitary stone columns and groups of stone columns with and without encasing. Various geosynthetics were evaluated for the encasing of a stone column. The results of the load experiments revealed that encasing significantly increased the load capacity of the stone column. The encasement modulus and the diameter of the stone column significantly influence increased axial weight capacity. The experiments assessed the increase in stress concentration caused by the encasing of the stone columns. The test results developed design guidelines for geosynthetic encasement design for the prescribed load and settlement.

Das and Bora (2013) investigate the effect of geosynthetic wrapping on stone structures floating in soft clay. When 60% of a column's length is embedded in geogrid, the column's bearing capacity increases fivefold. There is only about a twofold increase with full-length encasing (i.e., 100 percent). Therefore, the performance distinction between partially and entirely encased floating columns is evident. In the case of end-bearing stone columns, full-length encasing is believed to improve performance more than partial encasing. In the latter case (end-bearing columns), the stiffening effect of the encasement allows the column to transmit the surcharge pressure to the competent strata below, whereas in the former case (floating columns), the formation of a protrusion at a greater depth increases bearing capacity.

Ali et al. (2014) conducted model experiments on long floating and end-bearing single and groups of columns with and without reinforcement to determine the relative improvement in the failure stress of the composite ground due to various types of reinforcement. The failure process of various reinforcement types and configurations was analyzed using the exhumed deformed column morphologies. Geotextile and geogrid performed similarly well for horizontal circular discs and encasing arrangements for floating columns.

Chen et al. (2015) simulated the behavior of geosynthetic-encased stone columns (GECs) in porous soils under embankment loading using an indoor physical model test, numerical models, and two- and three-dimensional finite element methods. According to experimental and three-dimensional computer modeling findings, the failure of the GECs was caused by column deformation rather than shear.In contrast to a triangle or uniform distribution, a three-dimensional finite element analysis reveals that the distribution of unbalanced lateral loading operating on the supports is symmetric about a "hinge point" above the plastic hinge. Based on the distribution of unbalanced lateral pressures on the wall, a comparable shear resistance model for GECs is proposed. The stability of the embankment was investigated using the two-dimensional finite element method, which involved converting the columns into comparable soil walls and employing equivalent bending and shear resistance techniques. The equivalent bending resistance technique results were found to be more in accordance with estimates from three-dimensional analysis, which supports the bending failure process of GECs. It is recommended to add a second layer of these poles to increase lateral resistance in the soils in front of the toe, thereby enhancing the stability of the embankment.

Hong et al. (2016) use model experiments to investigate the effects of encasement stiffness and strength on the behavior of individual geotextile-encased granular columns embedded in soft soil. In order to ensure that the prototype-scale and model-scale geotextile-encased granular columns perform similarly, the appropriate properties of the constituents used in the model tests were first determined via a similarity analysis. The experimental results demonstrate that encasement increases the bearing capacity of all modeled sand columns, even when encasement rupture occurs; a significant improvement is attained for sand columns encased with geotextiles of medium to high stiffness. In addition, encasing significantly reduces the radial strain of the beams. Sand columns coated with geotextiles of low stiffness bulge most at the top 2.5D depth, whereas sand columns covered with relatively stiff geotextiles exhibit nearly uniform lateral deformation along their height. The bearing stresses of the clad columns modeled in this study are consistent with what would be predicted by an analytical solution based on cavity expansion theory.

Hasan and Samadhiya (2016) conducted laboratory model tests on combined vertical-horizontal floating granular piles installed in soft clay. The model tests utilized geotextile and geogrid as vertical encasement and horizontal strips along the entire length of the granular piles. Short-term loading was used to determine the vertical load-settlement relationship of untreated clay beds and unreinforced and reinforced granular piles. Due to the incorporation of geosynthetics, the laboratory tests revealed a significant increase in the load-bearing capacity of the granular piles. It was discovered that the ultimate load intensity of the reinforced granular piles increased compared to the untreated ground. The study also investigated the behavior of combined vertical encased-horizontally stripped granular piles, which demonstrated an improvement in the ultimate load intensity compared to granular piles with either vertical encasement or horizontal strips alone. Fig 2.24 indicates the variation in load settlement behavior for cay bed, unreinforced granular piles (URGP), Vertical encased granular piles (VEGP), and Granular piles with horizontal strips (GPHS) in soft clay.

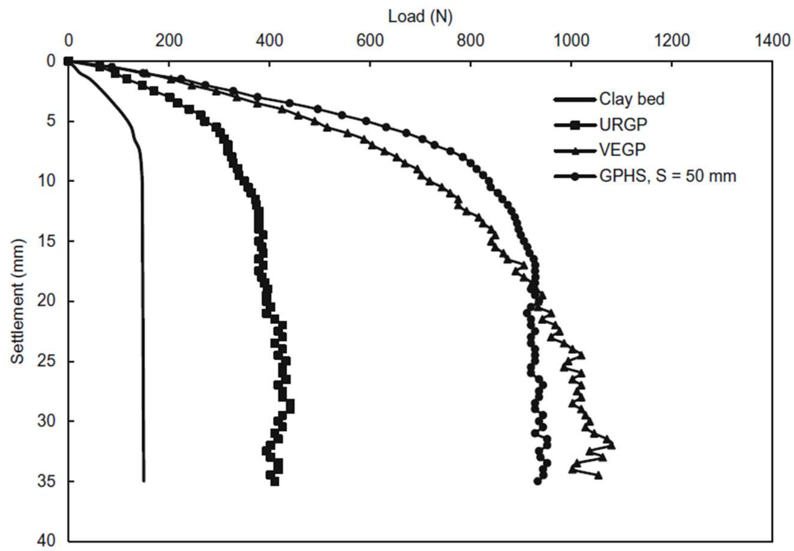

Figure 2.24: Vertical load-settlement behavior of granular piles

The ultimate load intensity of the combined reinforced piles was not significantly affected by the geogrid strips' center-to-center spacing. This study's findings contribute to the comprehension of the behavior of geosynthetic reinforced granular piles and provide valuable insights for designing and applying ground improvement techniques in soft clay soils.

2.7.2 Numerical Studies

Murugesan and Rajgopal (2006) used finite element analysis to investigate the qualitative and quantitative enhancements to the load capacity of clad stone columns in their study. Compared to conventional stone columns, encased stone columns have significantly higher load-carrying capacities and experience less compression and lateral bulging, according to the study's findings. In addition, the study revealed that the lateral confining stresses developed in stone columns when encapsulated are greater. It was determined that encasing the top portion of the stone column up to twice its diameter was sufficient to increase its load-bearing capacity. Further, as the rigidity of the encasement increases, the lateral stresses transferred to the surrounding soil diminish, resulting in the load capacity of encased columns being less dependent on the strength of the surrounding soil than that of conventional stone columns.

Guetif et al. (2007) presented a method for determining the increase in Young's porous clay modulus caused by installing a vibro-compacted stone column. To simulate the vibro-compaction technique and the primary consolidation of the soft clay a numerical analysis was conducted using Plaxis software and a composite cell model to simulate the vibro-compaction technique and the primary consolidation of the soft clay. Mohr-Coulomb perfect plastic behavior was utilized in the numerical simulation for the enhanced soil constituents. The obtained numerical data made it possible to estimate the degree of increase in Young's modulus of the soft clay. In addition, the predicted influence zone of the enhanced soft clay was determined.

Yoo and Kim (2009) present a comparative analysis of various finite element modeling approaches for modeling geosynthetic-encased stone column-reinforced ground for rapid embankment construction. The research examines three distinct models: an axisymmetric unit cell, a three-dimensional (3D) column, and a complete 3D model. Comparing the results of the unit cell model to those of the 3D models is used to evaluate the model's validity. In addition, the study examines the applicability of continuum elements for modeling the geosynthetic encasement. The findings indicate that the 3D column model yields result that are practically identical to those of the full 3D model, whereas the two-dimensional axisymmetric unit cell model tends to yield vertical effective stress and lateral deformation of the stone column that is 10 to 20% greater. A layer(s) of continuum elements, rather than membrane elements, can be used to model the geosynthetic encasement, provided the axial stiffness of the geosynthetic encasement is considered. Based on the analysis results, the paper discusses the effect of geosynthetic encasement on the performance of stone columns installed in the porous ground under embankment loading. The use of geosynthetic encasement in installing stone columns in soft ground for embankment construction reduced excess pore water pressures induced by embankment load and vertical stresses in the ground, thereby reducing settlement. This positive trend can be attributed to the increased rigidity of the stone column, which results from the increased confinement provided by the encasing.

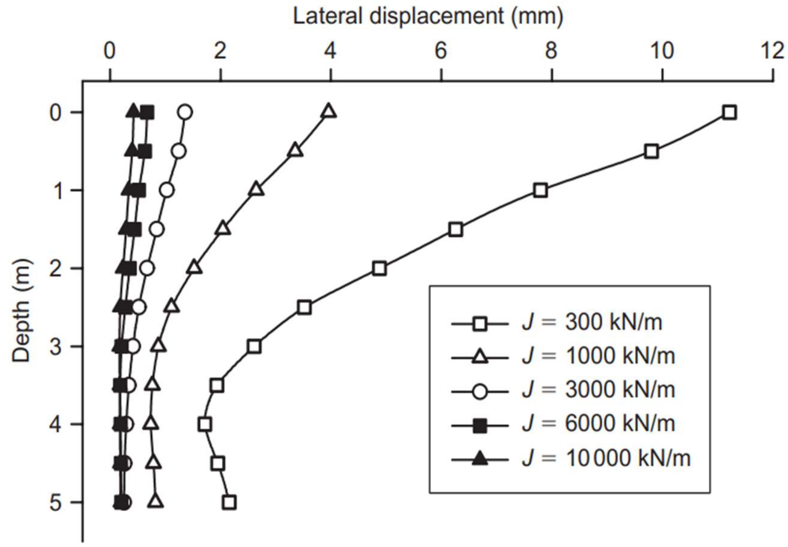

Figure 2.25: - Lateral displacement vs. depth at vertical stress of 100 kPa for a GEC with varying encasement stiffness

Using the computer program ABAQUS**, Khabbazian et al. (2010)** present a three-dimensional finite element analysis of the behavior of a single granular column with and without encasement in very porous clay. The analysis investigates the effect of various parameters, including geosynthetic rigidity, friction and dilation angle of the column material, length of geosynthetic encasement, column diameter and length, and coefficient of in situ lateral earth pressure. According to the findings, encoding granular columns significantly improves their stress-settlement behavior and load-carrying capacity. It was discovered that the stiffness of the encasing significantly impacted the stress-settlement response of the encased columns shown in Fig 2.25. The optimal length of encasing for partially encased columns was a function of the applied stress.

Kaliakin et al. (2012) conducted studies on using a high-strength geosynthetic to encase granular columns in soft clay. The study utilized three-dimensional finite-element analyses to simulate the behavior of a single column encapsulated in geosynthetics and investigated the results' sensitivity to the constitutive model used to simulate the behavior of the encased granular soil. The use of high-strength geosynthetics to encase granular columns increased column strength and enhanced stress-displacement response, according to the research. The study also emphasized the significance of selecting a constitutive model that effectively depicts the shear-induced volume-change behavior of encased granular soil. Researchers interested in modeling the behavior of geosynthetic-encased columns and practitioners seeking a better understanding of the performance of various constitutive models when simulating similar foundation elements can benefit from the findings of this study.

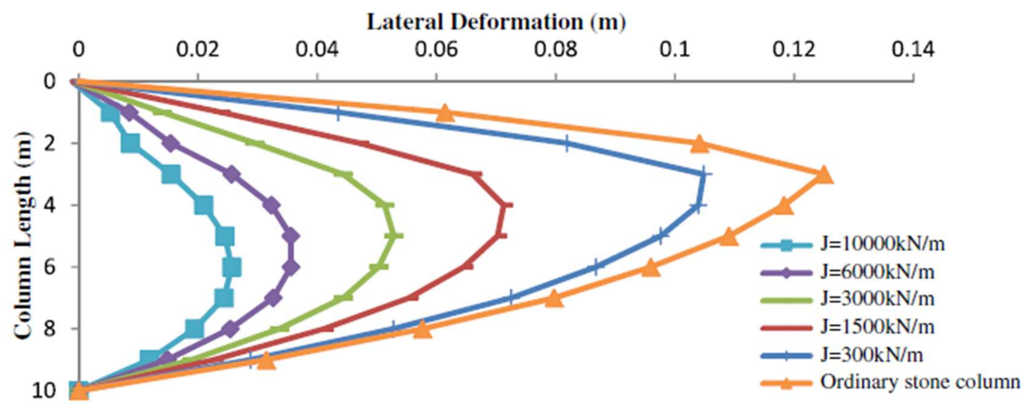

Figure 2.26: - Lateral deformations of stone column 25 obtained from models with various encasement stiffnesses.

Using a 3D numerical approach, **Keykhosropur (2012)** investigated the effect of various encasement lengths on the overall behavior of a group of Geosynthetic Encased Columns. The investigation compared the settlements and lateral deformations of the columns to those of completely encased columns. The analysis was calibrated utilizing GECs from a ground reclamation project in Hamburg, Germany. In addition, parametric studies were conducted to determine how geosynthetic encasement rigidity, column diameter, modulus of elasticity, and friction angle of the column material influence the GEC group's behavior. The research revealed that encasing only the stone column group's outermost columns is sufficient for optimal design. In addition, increasing the encasement stiffness enhances the general behavior of the GEC group by increasing the overall stiffness of the stone columns, the effect of encasement on lateral deformation can be seen in Fig.2.26 The research also revealed that the internal friction angle of the column material has a negligible effect on GEC performance and that the column material's modulus of elasticity has a negligible effect on group behavior in general.

Elsawy (2013) concentrated on the behavior of unreinforced and reinforced Bremerhaven clay under embankment loads. The study used consolidation analysis to investigate the long-term behavior of clay and found that using stone supports encased in geogrid increased the bearing capacity of the foundation and accelerated the reduction of surplus pore water pressure. In addition, the research revealed that encasing the stone columns enhanced their performance in porous soil and that tension concentration within the stone columns accelerated soil consolidation. Engineers and researchers interested in enhancing the stability and performance of foundations under embankment loads may find this information beneficial.

The study by **Ghazavi and Afshar (2013)** aimed to investigate the load-bearing properties of stone column footings, specifically looking at the effect of reinforcement on their performance. Large-scale laboratory tests were conducted on stone columns of varying diameters (60, 80, and 100 mm) and length-to-diameter ratios (five, six, and seven) with and without geotextile reinforcement. The results of the study showed that vertical reinforcing material increased the bearing capacity of stone columns, as did increasing the length and strength of the reinforcement. However, the column stress concentration ratio also increased. The use of geotextiles was found to decrease horizontal deformation. The study also investigated the influence of neighboring columns on the reference-loaded column by conducting experiments on groups of 60 mm-diameter stone columns. Finally, a numerical analysis using the finite element method (FEM) was conducted to investigate scale effects on small stone columns and to extend the reinforcement efficacy to large reinforced stone columns. Overall, the study provides valuable insights into the load-bearing properties of stone column footings and the effectiveness of reinforcement in enhancing their performance.

Using unit cell finite element analyses, **Hosseinpour (2014)** compared two types of reinforcement. The numerical results were first validated using field and experimental data, followed by parametric studies that varied the geosynthetic interval, geosynthetic tensile stiffness of laminated disks, and reinforced column length. According to the findings, both geosynthetic encasement and laminated disks increased the mobilized vertical stress on the reinforced column and decreased settlement on soft soil. However, the optimum interval between laminated disks to obtain the same performance as an encased column depends on the stiffness of the geosynthetics and the length of the reinforced column.

Rajesh and Jain (2015) utilized numerical analyses to investigate the behavior of conventional stone columns (OSC) and geosynthetic-encased stone columns (GESC) under embankment loading, focusing on the permeability of soft clay. The results revealed that both OSC and GESC generated comparable excess pore pressure during embankment construction in the adjacent soft clay. However, once the soft soil had settled, the presence of the stone column increased its load-bearing capacity. GESC outperformed OSC, especially when encased in a geosynthetic layer. The ultimate settlement of GESC-treated soil was 61% less than that of loose clay, compared to 43% for OSC. In addition, the consolidation time for GESC-treated ground was considerably lower than that for OSC-treated ground. The effective stress concentration ratio (ESCR) for GESC-treated ground gradually increased during the consolidation phase, indicating that the stone column effectively transferred additional load. Without geosynthetic encasement, ESCR increased to a certain point before decreasing, indicating that the stone column could not support the additional burden. These findings demonstrate the superior performance of GESC compared to OSC. The research highlights the significance of soft soil permeability in generating and dissipating excess pore water pressure, which affects post-construction settlement.

Chen et al. (2015) conducted an indoor physical model test and utilized numerical models with two- and three-dimensional finite element methods to investigate the response of geosynthetic-encased stone columns (GECs) to embankment loading in soft soils. The experimental and three-dimensional numerical modeling results indicated that the failure of the GECs is caused by the bending of the columns rather than shear failure. The authors proposed a model of the GECs' equivalent shear resistance based on the distribution of unbalanced lateral loads on the wall. In addition, the three-dimensional finite element analysis revealed that the distribution of unbalanced lateral loading operating on the columns is symmetric around a 'hinge point' above the plastic hinge instead of being triangular or uniform. To analyze the stability of the berm, the authors converted the columns into equivalent soil walls using both equivalent bending resistance and equivalent shear resistance methodologies within a two-dimensional finite element analysis. Results from the equivalent bending resistance method were closer to the estimations from the three-dimensional analysis, which agrees with the bending failure mechanism of the GECs. Based on their findings, an additional row of such columns may be necessary to provide greater lateral resistance in the soils in front of the toe to improve the embankment's stability.

Yoo (2015) describes a study in which a three-dimensional finite element model was utilized to investigate the settlement behaviour of embankments constructed with geosynthetic-encased stone columns on soft ground. The study investigated several factors influencing settlement, including soft ground thickness and consistency, geosynthetic encasement length and rigidity, embankment fill height, and area replacement ratio. The study determined that full encasement of the stone column is required to minimize settlement under embankment loading conditions and that increasing encasement stiffness is most effective when stress intensity in the soft ground is greatest. In addition, the study provides design charts for estimating the maximum settlement and stress concentration ratio during preliminary design.

This study by **Hasan and Smadhiya (2017)** investigated the effects of different reinforcement techniques, shear strength of the clay, encasement stiffness, and pile length on reinforced granular piles installed in soft clay. Using PLAXIS 3D software, laboratory model tests and numerical analyses were conducted. The results demonstrated that the incorporation of geosynthetic materials significantly enhanced the ultimate load intensity and stiffness of the treated soil. End bearing piles that are not reinforced could be effectively replaced with reinforced floating piles. The shear strength of the clay increased the ultimate load intensity of encased piles. For floating piles, the ultimate load intensity increased to a certain geotextile stiffness and remained constant, whereas it increased linearly with geotextile stiffness for end bearing piles. In laboratory tests and PLAXIS 3D simulations, the deformed forms of granular piles were observed in Fig 2.27. The primary failure mode of both unreinforced and encased piles was bulging, with encasement reducing bulging due to increased lateral confinement. The depth of bulging ranged from 1 to 1.6 times the diameter of the pile, while the length of bulging was approximately 1.5 to 2.5 times the diameter. End-bearing piles deformed without exhibiting significant bulging when the entire area was loaded. Using a comparison chart, they compared their study with existing theories and field studies. The relationship between the shear strength of the clay, the internal friction angle of the granular material, and the ultimate load intensity of the granular pile are depicted in Figure 2.28. Existing theories typically predict the load capacity of a single granular pile installed in an infinite soil mass without considering spacing.

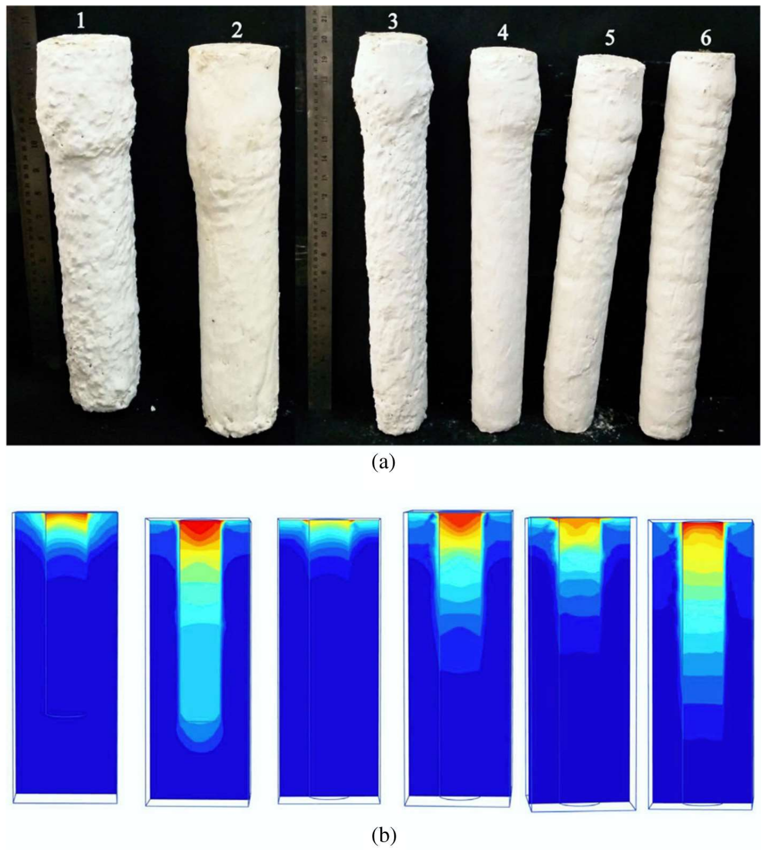

Figure 2.27: Deformed shapes of some granular piles; (a) laboratory model tests, (b) FEM. (Hasan and Samadhiya, 2017)

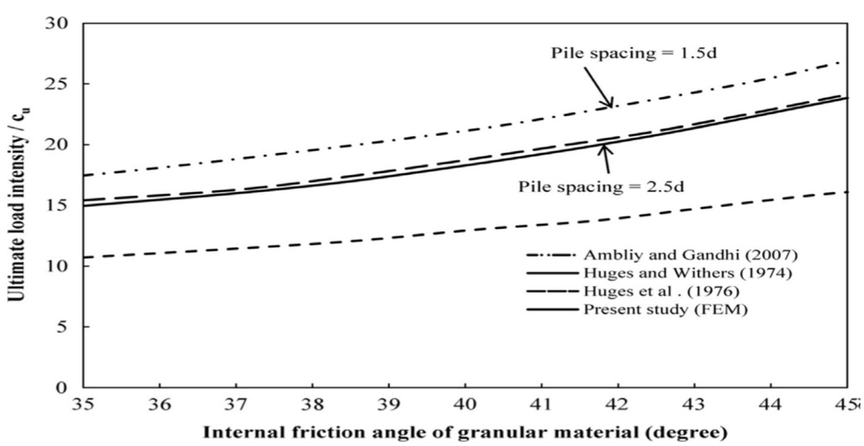

Fig. 2.28. Comparison of ultimate load intensity with existing theory and field studies.

2.8 LITERATURE SUMMARY

Insertion of stone columns in the soft ground deals with the Excessive settlement and bearing capacity problems of the soft/poor soil, hence came out as an effective tool for Soft Ground Improvement, which is in extensive application by Geotechnical Engineers nowadays for many structures like Embankments, oil storage tanks and buildings on the soft clays (Gniel and Bouazza, 2010; Ali et al. 2011; Shahu and Reddy, 2011).

It was observed that the bulging resistance or lateral confinement from the intervening soil may not be adequate for very loose soils. The stone column will not develop the required load-bearing capacity at the limiting settlement (Shahu et al. 2000). Afterwards, the circumferential bulging resistance must be increased for the increased capacity required of stone columns with ameliorated grounds. A vertically loaded column with the encasement of various geosynthetics found much efficiency in increasing the bearing stresses. (Murugesan and Rajagopal, 2006, 2007, 2010, 2011; Yoo and Kim, 2009; Lo et al., 2010; Pulko et al., 2011; Ali et al., 2012, 2014; Dash and Bora, 2013); Further enhancement of bearing capacity and reduction in lateral bulging can be observed by the use of horizontal layers of geosynthetics, which is due to the interlocking and frictional effects of horizontal layers with stone column aggregates (Ayadat et al., 2008; Prasad and Satyanarayana, 2016; Ghazavi, 2018). Lateral loading that caused Shear failure of the stone column was not well recognized; the behavior under lateral loading for a confined stone column was studied, and a shear strength increment was reported because of the encasing of granular material (Murugesan and Rajagopal 2007). Stiffness is the cause for the enhancement in shear strength for the smaller displacements, while on further increments in the displacements (larger displacements), the mobilization of tensile force is the cause for additive shear strength to an encased stone column, which will be present or persist till the rupture of the encasement (Mohapatra et al., 2016). Enhancement of shear strength for static as well as for cyclic lateral loading due to the encasement is also reported for the stone column near the toe of the embankment. (Cengiz et al., 2019).

When exposed to horizontal stresses, the shear collapse of granular columns has received little attention in the literature. Murugesan and Rajagopal (2009) investigated the behavior of granular columns under horizontal loads, which was done through-plane strain experimental tests for encased columns. It was discovered that the encasing of granular material improved the shear capacity of the columns, which the authors reported. Abusharar and Han (2011) discussed that shear failure was the most common failure mechanism for sand compaction and granular columns. Khabbazian *et al.* (2015) concluded that the granular columns located beneath the embankment's edge are more prone to failure than the other granular columns. Mohapatra *et al.* (2016) performed large shear box tests on granular columns at various normal pressures. Variations in strength were noted for three plan configurations with various column diameters and encasements. Shear strength increased as the area replacement ratio increased. The stiffness of the encased granular column along the shear plane increases shear strength, whereas, at larger displacements, the mobilization of tensile force increases shear strength. They have identified two sub-types of shear failure according to the behavior of the encasement. Aslani *et al.* (2019) also found that the soil-granular column system is stiffer than the soft clay layer and that this stiffness changes with area replacement ratios.

Cengiz *et al.* (2019) used a 1-G physical model to investigate the behavior of the unit cell while it was subjected to static and cyclic horizontal stresses. For this purpose, the Unit Cell Shear Device (UCSD), a novel multi-sectional shear box apparatus, has been developed specifically for this purpose, allowing for the modeling of the unit cell portion that is close to the slip circle. Because of the encasement, the granular column at the toe of the embankment has increased shear strength for both static and cyclic lateral loading. Nazariafshar and Aslani (2020) also performed experimental tests in a large shear box test setup for clay as the bed material, strengthened by the granular columns, to determine the values of stress concentration ratios at different arrangements of granular columns. The results indicated that as the diameter of the granular column increased, the stress concentration ratio decreased, and a square arrangement of granular columns had the largest stress concentration ratio and the lowest when a single granular column was used. Recently, Aghili *et al.* (2021) conducted an experimental study using a large-scale cyclic direct shear test to investigate the impact of the granular column on the cyclic shear parameters of clay strengthened by granular columns. The granular column enhanced the cyclic shear resistance of the treated clay model compared to untreated clay, and the maximum shear stress of the treated clay model improved as the granular column diameter and relative density increased.

2.9 PROBLEM FORMULATION

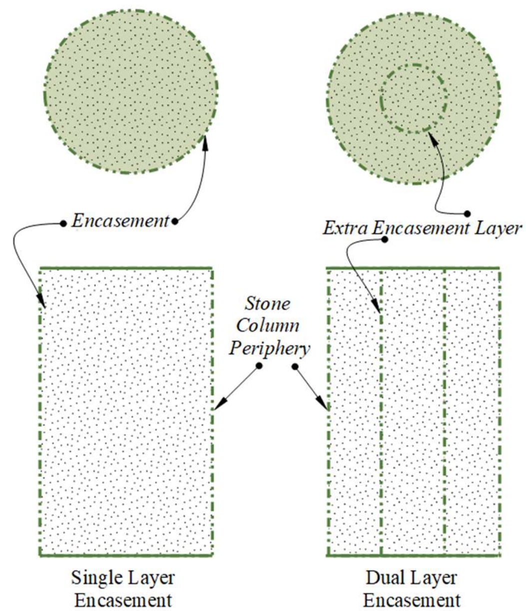

Fig 2.29: - Different encasement Conditions Insert in text

Literature review encouraged work with vertical reinforcement/encasement as these show good results in enhancing the vertical capacity of a column by confinement. The encasement also increases the resistance against lateral movement (i.e., against shear load). This gave the idea to provide more than one layer of encasement, one at the periphery and a second within the body of the stone column. An idea is made to Introduce **Dual layered Encasement** to enhance the confinement effect. It may increase the bearing capacity of the stone column offered by the bulging resistance of the column as well as the shear resistance. This may enhance the bulging resistance as well as the shear resistance. The proposed dual-layered encasement is shown in Fig-2.29, with the spacing between encasements being 0.5D (D=Diameter of column).

2.9 APPLICATION OF THE PROPOSED CONCEPT

- Places where the stone column is necessary and the tendency to fail under the lateral load is high.
- The corner line of the stone columns below any structure (Embankment) is susceptible to failure under lateral load. For such cases, the dual-layer encased stone columns might be used to resist the shear failure.

- The Dual Layered Encasement can be used for the Stone column installed by the Replacement Method.
- The plate holding both the layers of Encasement can be lowered in the borehole, followed by the material filling.

3. EXPERIMENTAL INVESTIGATION

3.1 GENERAL

To meet the stated objectives of this study, experimental tests have been planned to be performed on the large shear box setup under various conditions of normal pressure ranging from 100 kPa to 200 kPa. In the available large shear box test setup, the minimum normal pressure that can be applied is 100 kPa. Due to this limitation, in this study, numerical modeling and simulations were also performed on the PLAXIS-3D software to meet the limitations of the experimental setup.

The assessment of multiple cases involved the examination of both the diameter of the stone column and the encasement conditions for both single and grouped stone columns. The study used stone columns with a minimum diameter of 50 mm and a maximum diameter of 150 mm. The experimental trials conducted on singular stone columns involved varying diameters of 50, 100, and 150 mm. In contrast, only 50 mm and 75 mm-diameter stone columns were used for grouped stone columns. The maximum diameters of 75 mm in grouped stone column tests and 150 mm in single column tests were determined because, above these diameters, the arrangements could not be installed as the width of a large shear box setup is only 305 mm, limiting the use of diameter. The stone columns were created using only 50- and 75-mm diameters with square and triangular patterns.

The numerical modeling aimed to simulate the large shear box test conditions using Plaxis-3D software, and the models were validated against the experimental results of the current study and previous studies. In addition, numerical modeling was performed on the finite element-based software Plaxis 3D for all cases in which experiments were conducted to comprehend better and interpret the results. In addition, cases with a lower pressure range of 50 kPa and 75 kPa were considered in the numerical modeling, as these were not performed due to the limitations of the test setup.

The dual-layered stone column was not possible when the 50-mm stone column was considered, as there was insufficient space to install the two encasement layers. In the case of numerical modeling, however, there were no such restrictions, so the dual-layered encasement was simulated, and numerical modeling was conducted for both the 50 mm and 75 mm diameters of the stone column.

To compare the various types of stone column conditions and all the cases considered for the group of stone columns in the current study are shown in Table 3.2; all the specific cases considered for the single column case are listed in Table 3.1. For each diameter size, there are three types of encasement modes being considered: Uncased Stone Column (USC), Single Layer Encasement (SLE), and Double Layer Encasement (DLE). The "Y" indicates that these modes will be considered for the respective diameter sizes.

Additionally, numerical modeling and experimental setups are planned for specific diameter sizes. The "Y" indicates that numerical modeling and/or experimental setups will be performed.

In the case of the group of stone columns, for each case of encasement, two diameter options are considered: 50 mm and 75 mm. The normal pressure applied during the tests varies across three levels: 100 kPa, 150 kPa, and 200 kPa. The arrangement of the ordinary stone columns is tested in both triangular and square configurations. The dual-layer encased stone columns have a fixed diameter of 50 mm for the Numerical Modelling (N) and 75 mm for the Experimental analysis (E) and Numerical Modelling (N).

Table 3.1: Tests Planned: -Shear Loading Test (Group of Columns)

	OSC	**SLE**	**DLE**
Diameter(mm)	50,75	50,75	50 (N),75 (E, N)
Normal Pressure(kPa)	100,150,200	100,150,200	100,150,200
Arrangement	Triangular, Square	Triangular, Square	Triangular, Square

Table 3.2: Tests Planned: -Shear Loading Test (Single Column)

Sr No.	Dia (mm)	Normal Pressure(kpa)	Encasement Mode	Numerical Modelling	Experimental Setup
1	50	50	USC	Y	-
			SLE	Y	-
			DLE	Y	-
		75	USC	Y	-
			SLE	Y	-
			DLE	Y	-
		100	USC	Y	Y
			SLE	Y	Y
			DLE	Y	-
		150	USC	Y	Y
			SLE	Y	Y
			DLE	Y	-
		200	USC	Y	Y
			SLE	Y	Y
			DLE	Y	-
2	100,150	50	USC	Y	-
			SLE	Y	-
			DLE	Y	-
		75	USC	Y	-
			SLE	Y	-
			DLE	Y	-
		100	USC	Y	Y
			SLE	Y	Y
			DLE	Y	Y
		150	USC	Y	Y
			SLE	Y	Y
			DLE	Y	Y
		200	USC	Y	Y
			SLE	Y	Y
			DLE	Y	Y

3.2 DETAILS OF EXPERIMENTAL INVESTIGATION

3.2.1 Material Properties

3.2.1.1 Sand

The fine sand is used for the current study collected from a local site in the MANIT, Bhopal campus, which was obtained by the contractor from the locations near Hoshangabad (M.P). The sand was tested to determine its index properties which are shown in Table 3.3. The classification for the bed soil is poorly graded clayey sand (**SP),** The obtained minimum density of the sand was 15.1 kN/m^2 for the sand bed. Fig. 3.1 represents the gradation curve for the sand and also represents the characteristics used for the classification.

Using a pouring device, the process of creating the sand bed replicated the method used to achieve the minimum density on the relative density test apparatus." The specific quantity of sand required for the fixed volume was calculated prior to filling the test setup to a height of 150mm, ensuring an accurate measurement for the desired sample height.

3.2.1.2 Stone Aggregates

According to the soil classification system, the coarse-grained soil that was used as the infill material for the stone column was designated as GP. Various aggregate classes were used for the creation of different sizes of the stone column to maintain the column to an aggregate ratio near 6-7, as suggested by (Fox 2011 and Stoeber,2012). The average size (D_{50}) for the aggregate particles used in the stone column of size 50mm was 5.2mm, named Aggregate-1, whereas, in the case of the 75mm diameter stone column, this was maintained at 7.9 mm, named Aggregate-2. Aggregate-3 and Aggregate-4 are used for the 100mm and 150mm diameters, respectively, as the properties are shown in Table 3.3.

The obtained aggregate density results indicate that there is a decrease in density as the size of aggregates increases. Larger aggregates possess more significant interstitial gaps, leading to reduced overall density. This phenomenon occurs due to larger soil aggregates, resulting in reduced particle contact and increased pore spaces or voids. The voids in the soil are occupied by air or water, resulting in a decrease in the soil's total mass and subsequent reduction in density.

The maximum particle size recommendations made by Nayak (1983), according to which the size of the particle utilized within the stone column body should be smaller than 1/5 of the diameter of the stone column, are also satisfied. The prepared sample of stone column infill is shown in Fig-3.2 and Fig-3.3 for various stone column diameters. In the case of encased stone column, the column material was wrapped using Geonets, and the secant modulus of the geonets used was 150kN/m.

Table-3.3. Properties of sand and column material (aggregate) used in the Experimental Programme (IS: 2720 (Part-4): 1985)

Parameters	**Sand**	**A-1**	**A-2**	**A-3**	**A-4**
Working Density (kN/m^2)	15.1	17.4	17.1	16.7	15.8
C_c	1.30	0.973	0.966	0.902	0.91
C_u	1.77	1.18	1.27	1.164	1.46
D_{10}	0.21	4.90	6.60	7.9	12.4
D_{30}	0.31	5.20	7.31	8.1	14.4
D_{50}	0.35	5.57	8.04	8.8	16.3
D_{60}	0.37	5.75	8.40	9.2	18.2
Cohesion (kN/m^2)	4	1	0.8	0.9	1
Friction Angle (°)	27	41	40.5	37.2	39

(D_{50} :- Avg. Size of Particle)

(A_i= Aggregate Type for various stone column diameter, i=1,2,3 and 4)

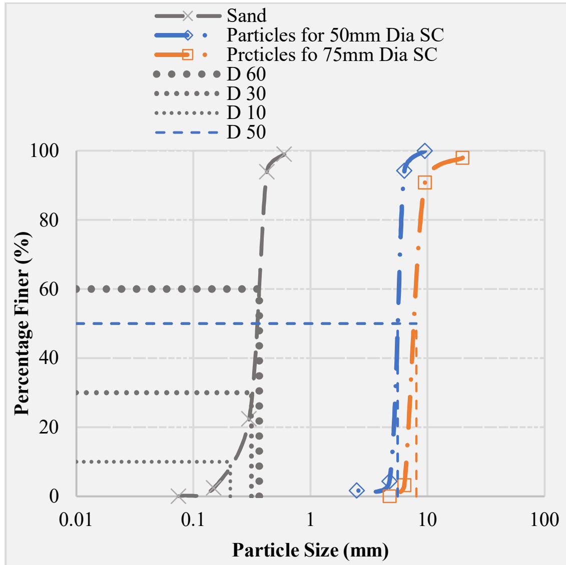

Figure 3.1: Particle size distribution for sand and aggregate samples

Figure 3.2: Prepared samples aggregates as infill material for various stone column diameters

Fig 3.3: Aggregate samples prepared for infill material of (a) 50 mm, (b) 75 mm diameter, (c)100 mm, (d) 150 mm

3.2.1.3 Geogrid

The geogrid sheet used to encase the stone column is acquired from the loacl market. It is commercially known as the Nova curtain and is manufactured by Tuflex India Pvt. Ltd. from geogrid sheets. The geogrid is cut and pleated to form an open-ended cylinder for wrapping the stone column (as mentioned in Figure 3.4, manufacturer's data in Table 3.4).

Table 3.4 Properties of geogrid used

Property	Value
Opening size, mm	2 x 2
Tensile strength(stiffness), kN/m	15
Thickness, mm	1
Weight, gm/m^2	260

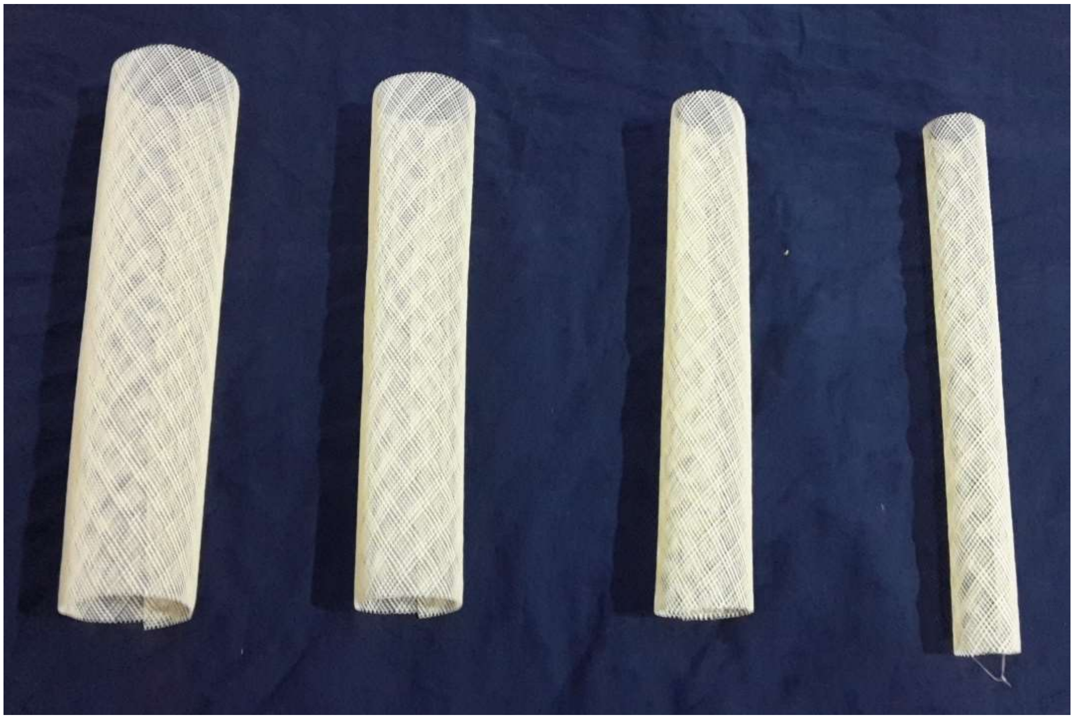

Figure 3.4: Geogrid used for encased stone columns

3.2.2 Test Setup

The large direct shear box setup consisting of the upper and lower units was used for the experimental program. The apparatus plan measures 305 x 305 mm (93,025 mm^2), with a 150 mm effective height accessible for soil specimens, Fig 3.5 shows the shear box setup used in the current study. A horizontal plane of failure has been predetermined for the apparatus, which is positioned in the vertical center of the specimen. This horizontal plane stays in place thanks to the two pieces that comprise the shear box mechanism. The bottom portion of the box is the component that travels along the roller in a horizontal direction, while the top half of the box stays stationary. As a consequence of this configuration, the mass of soil contained within the box tends to split along the horizontal plane that has been assigned. The strain in the lower box of the setup can be measured with the help of the Strain Gauge. The loading yoke, attached to the load transducer and measures the resistance to horizontal stress, supports the top part of the shear box. A motorised device applies the loading to the specimen, which enables the maintenance of a steady loading rate during the test. A loading cap was utilized to keep the normal load in place over the soil specimen, which was accomplished by manually adjusting calibrated dead weights at varying normal pressures.

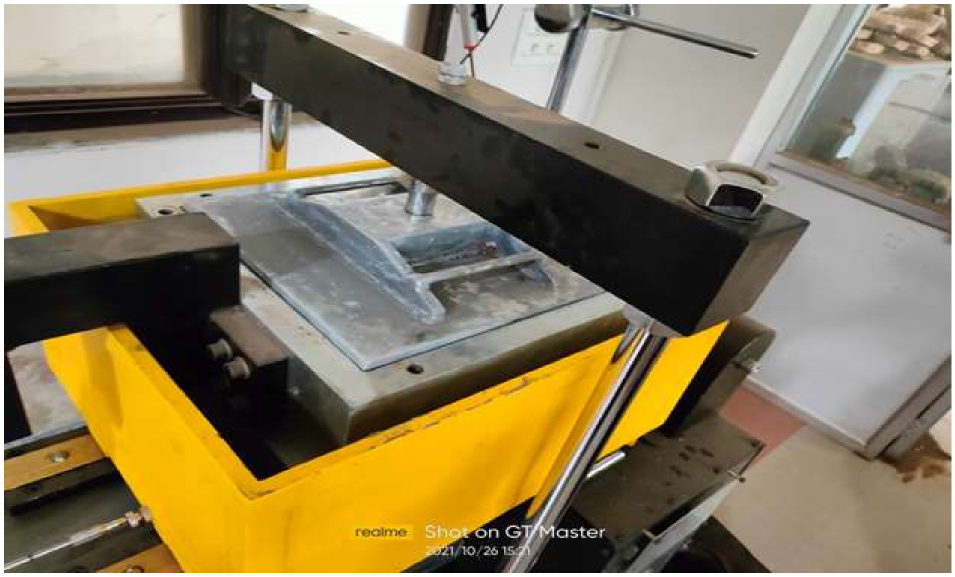

Figure 3.5: The Large shear Box setup used for the experimental study

3.2.3 Construction of Stone Column

An unencased stone column, a single-layered encased (SLE) stone column, and a dual-layered encased (DLE) stone column were prepared as samples for the experimental program. Figure 3.6 illustrates the difference between the SLE and DLE cases in the current study.

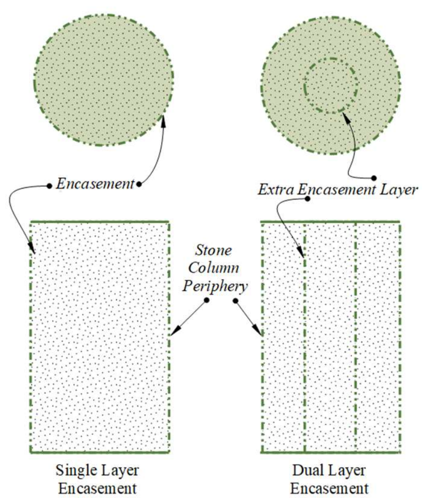

Figure 3.6: Different Encasement Conditions

(a) Placement of steel Pipe at the center

(b) Sand filling without compaction

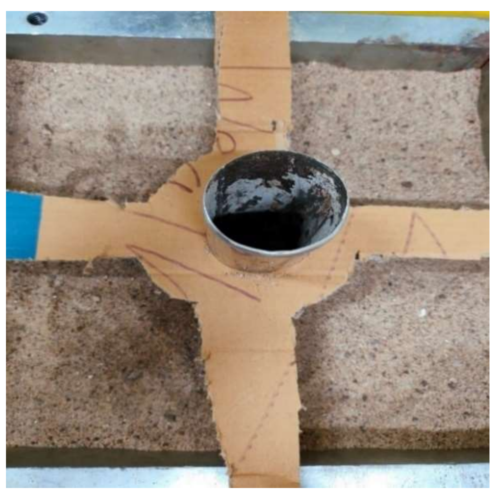

(c) Setup prepared for stone filling

Figure 3.7: Procedure of creating the sand bed with the stone column

To evaluate the unencased stone column, open-ended steel tubes with required inner diameters (50,75,100, and 150 mm) were positioned at the desired location at the base of the lower half of the large shear box. This arrangement was used to construct a triangle or square arrangement of the stone column as well as a single stone column. Figure 3.7 indicates the steps in creating the sand bed with the stone column at the center.

For each experiment, a known quantity of dry sand was placed in the shear box around the steel tubes. Ensuring that the sand bed had the lowest possible density, the box was filled to a height of 150 mm without compaction (Figure 3.8). Using the diameter of the stone column to determine particle size for a particular column dimension, a sieved sample of aggregate was collected. The measured quantity was then compacted in three equal layers inside the steel cylinders using an 8 mm diameter steel tamping rod to densify the aggregates in five layers. Each layer was tamped with a predetermined amount of material by lowering the tamper from a predetermined height.

After the aggregate had been poured and packed to the maximum height of the shear box, the steel tubes were slowly withdrawn from the sand bed. Reduced granular column and surrounding sand disturbance were achieved using steel tubes with smooth inner and exterior surfaces, Figure 3.9 shows the created ordinary stone column.

The construction process of the encased stone column involved attaching a temporary geonet to the steel tube. Once the material filling was completed, the steel tube was removed, leaving the geonet layer in its position (Figure 3.11). In the case of dual-layered stone columns, two steel cylinders were used, and the geonet layer was positioned in a way that allowed both layers to be created, as depicted in Figure 3.12.

The experimental program included investigations of single stone columns with diameters of 50 mm and 75 mm, as well as grouped columns arranged in triangular and square configurations for both unencased columns and single-layer encasement. It was not feasible to construct double-layered stone columns with a diameter of 50 mm; therefore, tests were only conducted with a diameter of 75 mm. In all cases where a group of stone columns was installed, the distance between each column was twice the diameter.

Figure 3.13 (b, c) illustrates a single-layered stone column with a square pattern for 75 mm diameter columns and a triangular pattern for 50 mm diameter columns, whereas Figure 3.13 (a) shows a dual-layered stone column of diameter 75 mm.

Fig 3.8: - Plan view of Created sand Bed

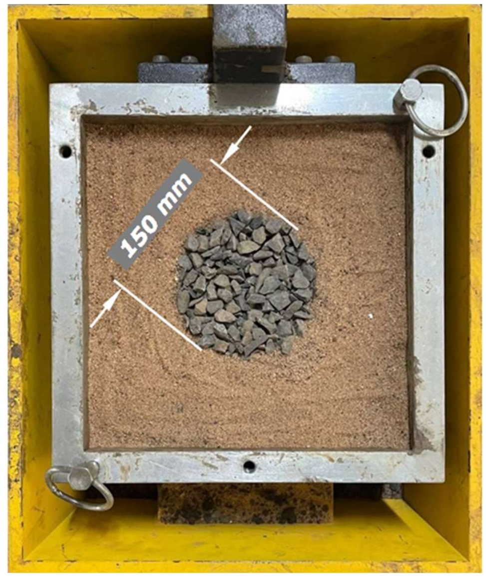

Fig 3.9: - Ordinary Stone Column installed in the sand bed

Fig 3.10: - Single Layer Encased Stone Column installed in the sand bed

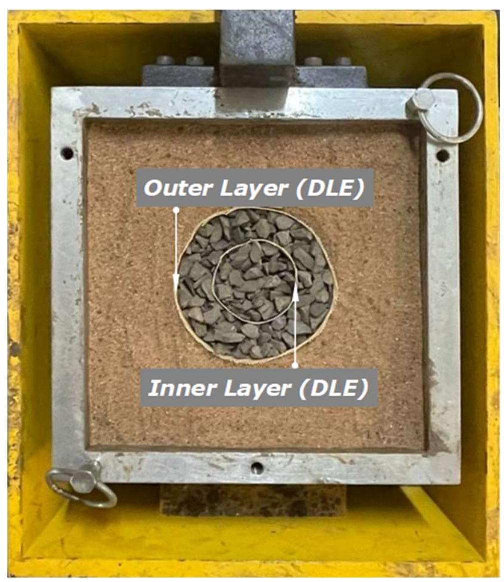

Fig 3.11: - Dual Layer Encased Stone Column Installed in sand bed

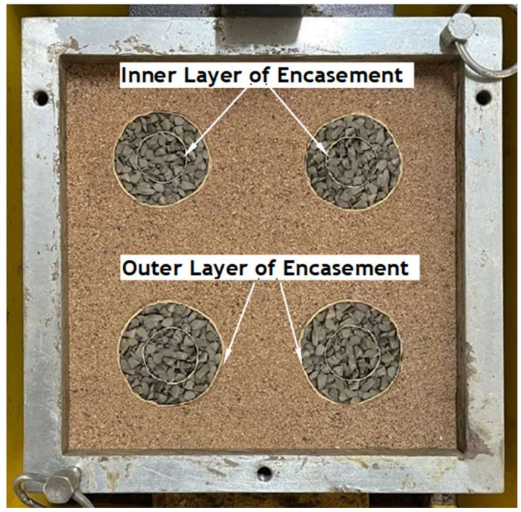

(a) 75GS DL

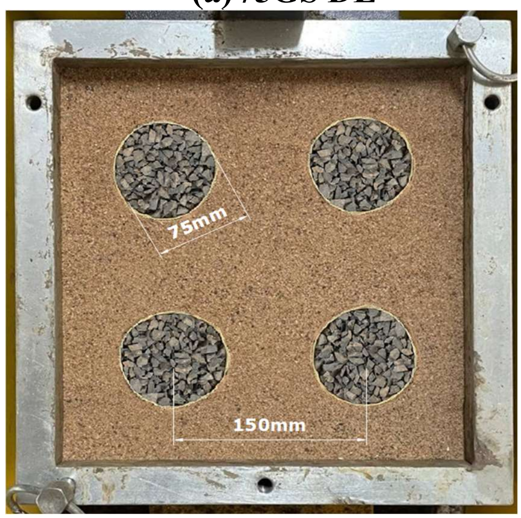

(b) 75 GS SL

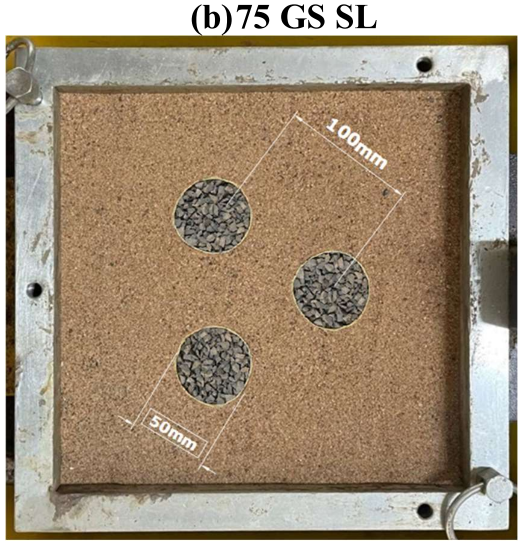

(c) 50 GT SL

Fig 3.12: - Installed Stone columns for experimental Study

3.2.4 Test Procedure

The experiments aimed to investigate the behavior of stone columns with a diameter of 150 mm under different conditions, specifically with and without encasings, on a sand bed. A normal pressure of 100 kPa was applied to the stone columns using the accessible top cover of the shear box. The shear box setup allowed for measuring the normal load on the stone columns.

To assess the resistance to horizontal displacement, the lower half of the shear box was subjected to a horizontal force with a constant displacement rate of 1.2 mm/min after the normal pressure was applied. At the end of each minute, readings from the load transducer were recorded to determine the level of resistance encountered during the displacement.

It is important to note that the large shear box configuration introduced boundary conditions that affected the experiments. Consequently, the experiments were terminated once a total horizontal displacement of 50 mm was reached. This displacement value provided sufficient data for analyzing the behavior of the stone columns under the given conditions.

4. NUMERICAL ANALYSIS

4.1 NUMERICAL SIMULATION/ FEM MODELLING: -

4.1.1 Introduction to PLAXIS-3D

PLAXIS-3D is a widely utilized and robust numerical modeling software that is specifically tailored for geotechnical analysis and engineering in three-dimensional (3D) settings. The platform offers engineers and geotechnical professionals an advanced tool for simulating and analyzing the intricate behavior of soil, rock, and other materials in diverse geotechnical projects. PLAXIS-3D is a versatile software that accurately models soil-structure interaction problems. It is widely used for various engineering tasks, including foundation design, tunneling, excavation, slope stability analysis, and retaining wall design.

The software enables users to create detailed 3D geotechnical models accurately representing the site's geometry and material characteristics. These models include various soil layers, rock formations, retaining structures, piles, and other relevant components, allowing for a thorough analysis of intricate engineering problems. PLAXIS-3D offers a range of material models, such as linear elastic, Mohr-Coulomb, Hardening Soil, Soft Soil, and user-defined models, to accurately depict the mechanical behavior of diverse soil and rock materials. PLAXIS-3D provides engineers with a wide array of features that allow flexibility in defining boundary conditions and loading scenarios during analyses. Users can specify fixed displacements, loads, and support conditions to replicate real-world simulation conditions accurately. The software accommodates diverse loading options, including surface loads, point loads, line loads, and prescribed displacements, rendering it applicable to a broad spectrum of geotechnical projects.

PLAXIS-3D offers advanced features for conducting complex analyses, surpassing the scope of basic static analysis. Engineers employ various analytical techniques to study different aspects of construction processes. These techniques include staged construction analysis for simulating progressive construction, time-dependent analysis for capturing soil consolidation and creep behavior, dynamic analysis for assessing response to dynamic loads, and thermal analysis for studying heat transfer effects. PLAXIS-3D provides robust visualization and post-processing tools to enhance the interpretation of simulation results. Users can create deformation plots, stress contours, settlement analysis, and other visual representations to gain insights into the behavior of analyzed geotechnical systems.

In summary, PLAXIS-3D is a powerful numerical modeling software that enables engineers and geotechnical professionals to analyze and resolve intricate geotechnical issues within a three-dimensional framework. PLAXIS-3D is widely recognized and utilized in geotechnical engineering projects globally due to its comprehensive features, precise material models, and advanced analysis capabilities.

4.1.2 Features of PLAXIS-3D

PLAXIS-3D is a highly versatile and powerful numerical modeling software for geotechnical analysis, offering a comprehensive range of features. Notable features of the subject include:

- PLAXIS-3D facilitates the development of intricate 3D models, enabling engineers to depict intricate geotechnical systems accurately and analyze their behavior in three dimensions.
- The software offers various material models for simulating soil and rock behaviors, such as linear elastic, Mohr-Coulomb, Hardening Soil, Soft Soil, and user-defined models. This practice guarantees the precise depiction of material characteristics and the attainment of realistic outcomes in the analysis process.
- PLAXIS-3D allows users to specify boundary conditions, including fixed displacements, applied loads, and support conditions. The software provides a range of loading options, such as surface loads, point loads, line loads, and prescribed displacements, facilitating realistic and comprehensive analysis.
- Staged construction analysis allows engineers to simulate progressive construction processes. This feature allows for modeling construction sequences and evaluating the impacts of construction stages on the geotechnical system.
- PLAXIS-3D enables time-dependent analysis, facilitating the simulation of soil consolidation, creep, and other time-dependent phenomena. This method is

particularly advantageous for analyzing long-term settlement and deformation patterns.

- Dynamic analysis is facilitated by the software, allowing for the evaluation of geotechnical systems' reactions to dynamic loads, including earthquakes, vibrations, and machine-induced vibrations. Structural dynamics analysis aids in assessing the stability and integrity of structures subjected to dynamic conditions.
- PLAXIS-3D incorporates thermal analysis features for investigating the impact of heat transfer on geotechnical systems. This feature is beneficial for projects related to geothermal energy, underground cables, or thermal barriers.
- PLAXIS-3D offers robust visualization tools for facilitating the interpretation of analysis outcomes. Users can generate various visual representations, such as deformation plots, stress contours, and settlement analysis, to gain insights into the behavior of the geotechnical systems being analyzed.
- The software enables parametric modeling, facilitating engineers in efficiently examining various scenarios by manipulating input parameters and automating the generation of models. This feature enhances the efficiency of the analysis process and enables the conduction of sensitivity studies.
- PLAXIS-3D incorporates a comprehensive material database containing predefined material properties designed for frequently utilized soils and rocks. Using predefined material properties saves time and guarantees consistency in the analysis process.

These features, among others, make PLAXIS-3D a robust and versatile software tool for geotechnical engineers, allowing them to conduct precise and detailed analyses of complex geotechnical systems.

4.1.3 Modelling Process

PLAXIS-3D is a robust software application utilized for the purpose of geotechnical analysis and modeling. This software enables engineers to simulate intricate geotechnical problems and analyze the response of soil and structures to various loading conditions. The following section comprehensively explains the steps involved in PLAXIS-3D modeling.

Problem Definition: During the problem definition phase, it is essential to precisely establish the purpose and objectives of the analysis. The soil types, geometry of the problem, and boundary conditions need to be identified. Select the desired analysis type, such as static, dynamic, staged construction, etc. This step is crucial for establishing the basis of the subsequent modeling process.

Geometry Creation: The 3D geometry of your problem can be created using the modeling tools available in PLAXIS-3D. This entails the delineation of soil strata and introducing structural components such as piles, retaining walls, or foundations. Ensuring an accurate representation of the physical system's geometry is crucial for obtaining precise results in analysis.

Material Definition: Material Definition involves specifying the geotechnical properties of the soil and other materials used in the analysis. PLAXIS-3D offers a range of constitutive models, including Mohr-Coulomb and Hardening Soil models, for the characterization of soil behavior. Material parameters such as unit weight, shear strength parameters, Young's modulus, Poisson's ratio, etc., should be inputted based on laboratory tests or field data.

Boundary Conditions: Boundary conditions are essential for conducting realistic analysis. In PLAXIS-3D, the user specifies the constraints, loads, and displacements that are to be imposed on the model. It is important to incorporate boundary conditions that accurately represent the field conditions or laboratory tests to simulate the problem precisely.

Mesh generation: Mesh generation is a crucial step in achieving accurate results in finite element analysis. PLAXIS-3D provides meshing tools that effectively represent the geometry and capture significant problem features. It is essential to appropriately modify the mesh density in accordance with the problem's complexity and the desired level of accuracy to obtain dependable outcomes.

Analysis Setup involves configuring the analysis parameters and options within the PLAXIS-3D software. The user is requested to specify the specific type of analysis, such as linear or nonlinear, static or dynamic. Furthermore, it is necessary to establish exact time or step intervals for staged construction or time-dependent calculations. These settings ensure that the study is conducted in accordance with the problem's specific requirements.

Analysis Execution: After completing the setup for the analysis, the analysis is executed in PLAXIS-3D. The software computes the solutions to the governing equations of the system and determines the deformations, stresses, strains, and other pertinent outcomes for the model. This step entails a computationally intensive process that yields valuable insights into the problem.

Post-processing is conducted following the analysis phase. In this section, the obtained results are analyzed and interpreted. PLAXIS-3D offers post-processing capabilities for visualizing various effects, including deformations, settlements, pore pressures, safety factors, and more and using plots, graphs, and contour maps aids in enhancing comprehension of the analyzed system's behavior.

The complexity and requirements of the modeling process may vary depending on the geotechnical problem and desired level of detail. To ensure accurate and reliable analysis, it is crucial to consult the PLAXIS-3D user manual and seek guidance from experienced professionals.

4.1.4 Validation

To overcome the limitations of laboratory experiments and gain a thorough understanding of the mechanism inside the shear box, the FEM software PLAXIS-3D is utilized for all laboratory model tests. First, the FEM software PLAXIS-3D was validated based on experiments conducted by Javad and Majid (2020) and Mohapatra et al. (2016), indicated as Validation I and Validation II, respectively, in the present study.

4.1.4.1 Validation-I

Clay was used as the bed material by Nazariafshar and Aslani (2020), and pulverized pebbles and fine-grained sand were used as the granular column materials. To conduct physical modeling and experiments, they utilized a large direct shear machine and installed a granular column using the replacement method, holding it in position with open-ended steel pipelines. In the present investigation, all evaluations for a single column were numerically modeled, and FEM modeling results were compared. Each column material (sand and gravel) was tested separately for three diameters of 124.5mm, 145mm, and 169mm of granular column in the center of the large shear box test, known as Ordinary Granular Columns (OGC) since they are not encased. Nazariafshar and Aslani (2020) detail the material properties used for each combination. All combinations were assessed at standard pressures of 30kPa, 45kPa, 60kPa, and 75kPa.

The validation-I study simulated the behavior of clay as the bed material and stone aggregates as the column material using the linear elastic perfectly plastic Mohr-Coulomb failure criterion. This model has been extensively utilized in the analysis of embankments and shallow foundations, as well as in comparable studies by other researchers on granular columns (Pulko et al. 2011, Ghazavi and Nazari 2013, Hosseinpour et al. 2015, Hasan and Samadhiya 2017, Chenari et al. 2019). As shown in Table 4.1, input parameters for models (c and φ) were taken directly as given by Nazariafshar and Aslani (2020), whereas the modulus of elasticity and the poisons ratio was obtained from the empirical equations given by Janbu (1963). To simulate the large shear box test, plates were created, and boundary conditions were established so that the upper half of the shear box is immobile and constrained in all directions, while the lower half can only move horizontally and is constrained in the other two directions. The model consisted of a wide shear box containing a sand substrate and a granular column measuring 152.4 mm in length, as shown in Fig. 4.1, an interface with weaker strength properties than the material was created at the material's periphery. After designating the required properties, mesh generation was accomplished, and the resulting mesh is depicted in Figure 4.2.

Table 4.1 Model Properties for FEM Model (Validation -I)

Parameters	Column Material	Clay Bed
Young's modulus, E (kPa)	44000	4600
Undrained shear strength, cu(kPa)	11	21
Angle of internal friction, φ (°)	35	6
Poisson's ratio, μ	0.28	0.36
Dilation angle, ψ (°)	5	0

Note:- The equation used to determine the modulus of elasticity is

$$E_s = k \cdot P_a \left(\frac{\sigma}{P_a}\right)^n \text{.... Eq 4.1}$$

where σ is lateral confining pressure, and pa is atmospheric pressure. Parameters K and n are specific to the soil.

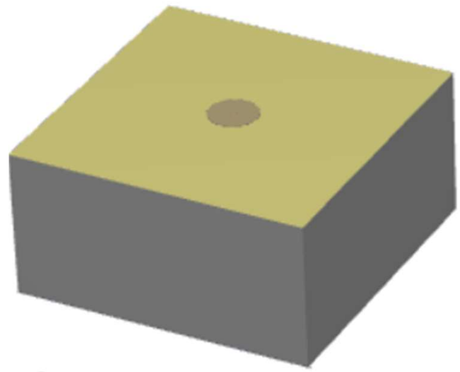

Figure 4.1: Schematic diagram of soil bed and single column modeled

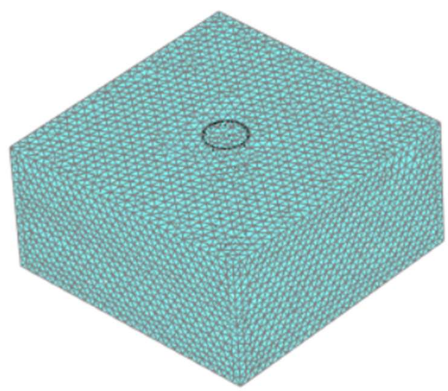

Figure 4.2: A generated mesh of the model with an ordinary granular column (OGC)

All possible scenarios with a maximum horizontal displacement of 30 mm were analyzed numerically. Figure 4.3 depicts the normal load applied to the soil bed's surface and the shear force imparted on the lower portion of the large shear box test. Figure 4.4 illustrates the variation of shear stress with horizontal displacement for a 145 mm diameter granular column installed in a clay substrate at varying normal pressures when pea gravel was used as the column material. The results of the numerical study were found to be consistent with those of the considered experimental study.

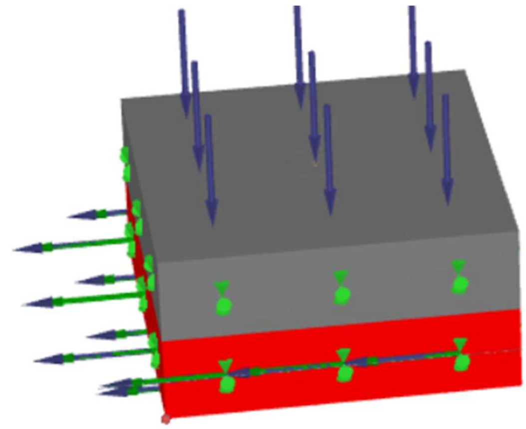

Figure 3: Model with applied normal and horizontal load

The results shown in Figure 4.4 indicate that the shear values derived from the numerical model are marginally greater than the experimental shear values at maximal displacement. However, at a 30 mm displacement, the difference between the two is no more than 5 kPa. The numerical analysis results indicate that the shear stress values are nearly constant for small horizontal displacements but increase as the displacement increases for all normal stress conditions. Fig. 4.5 illustrates the shear stress change with diameter at a constant normal pressure. The results of the present numerical study correspond to those of the previous experimental study.

4.1.4.2 Validation -II

In their 2016 study, Mohapatra et al. used sand as the bed material and aggregates as the granular column materials. They conducted physical experiments using a large direct shear apparatus. To validate their findings, a 100 mm diameter ordinary single column installed in a sand bed was modeled in PLAXIS 3D, with all conditions kept the same as in the original study. The FEM modeling was performed similarly as discussed earlier in validation-I, and the material properties used in the modeling are summarized in Table 4.2.

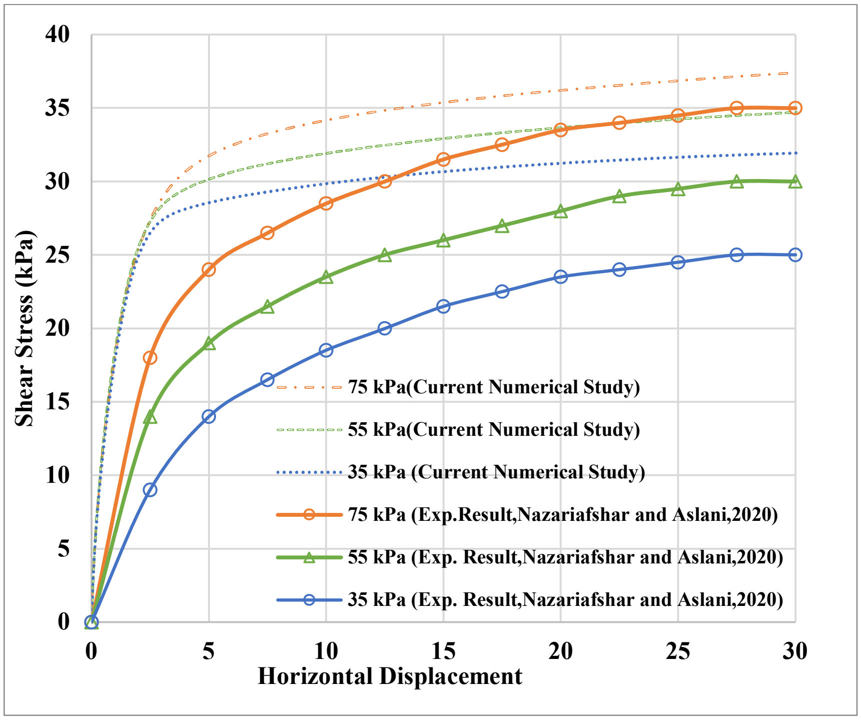

Figure 4.4: Shear stress vs. horizontal displacement at different normal pressure for 145 mm diameter granular colu

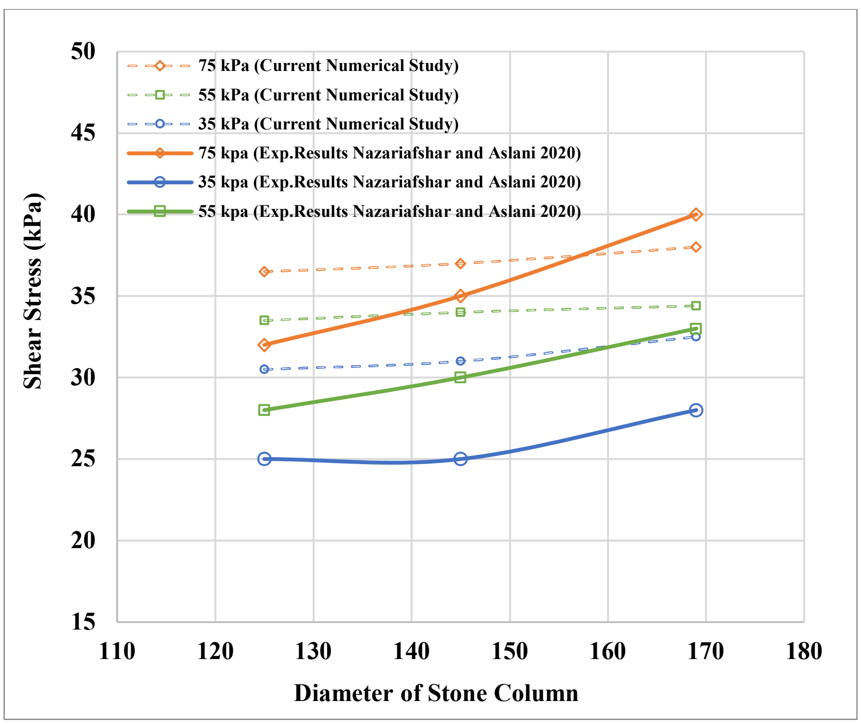

Figure 4.5: Variation of shear stress with diameter for granular pile

Figure 4.6 demonstrates that the numerical model shear values at smaller displacements of 20mm are nearly identical to the experimental shear values. The shear stress values obtained in the experimental investigation of Mohapatra et al. (2016) are in good agreement with the present numerical study under all normal pressure conditions of 15, 30, 45, and 75 (kPa). However, the current numerical study results are slightly higher than the experimental results because the FEM model exhibits linear elastic behavior at lower displacement values, and these shear stress levels are at a lower horizontal displacement of 20mm.

Table 4.2 Model Properties for FEM Model (Validation -II)

Parameters	Column Material	Sand Bed
Young's modulus, E (kPa)	50000	12000
Undrained shear strength, cu (kPa)	1	1
Angle of internal friction, φ (°)	41	31
Poisson's ratio, μ	0.28	0.30
Dilation angle, ψ (°)	11	1

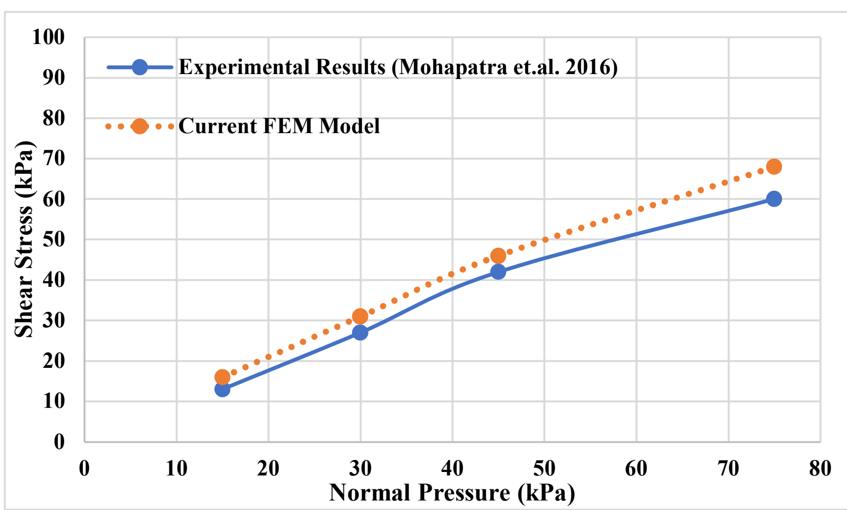

Figure 4.6: Comparision of shear stress value at 20mm horizontal displacement for various normal pressure

4.2 Numerical Modelling for cases considered

After the validation, the cases considered in the current study are simulated using PLAXIS-3D. Utilizing plate elements, the structure was divided into two halves. The upper half of the shear box was fixed and limited in all directions, whereas the lower half was limited in only two directions and could only move horizontally. The model structure consisted of a large shear box with a cross-sectional area of 305 mm by 305 mm and a height of 150 mm, filled with sand and a stone column in the box's center. The appropriate diameter was selected for the stone column, and the property R_{inter} was assigned to the circumference of the Ordinary Stone Column (OSC). At the intended location, geogrid with the necessary tensile strength was given to encased stone columns (ESC). Medium-coarseness meshing was conducted, Figure 4.7 depicts the OSC model, and Figure 4.8 shows the generated mesh for the model.

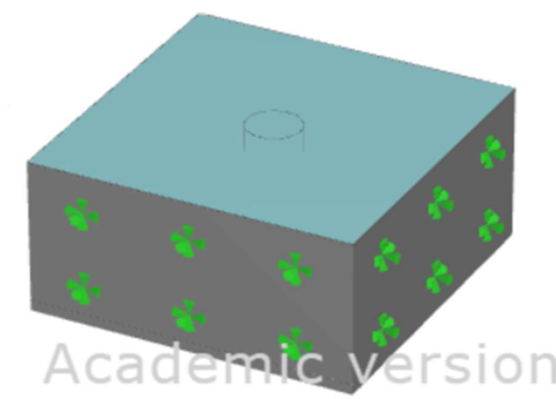

Figure 4.7: Schematic diagram of soil bed and single column modeled

The linearly elastic, fully plastic Mohr-Coulomb model was used to simulate sand and stone aggregates. Several researchers, such as Ghazavi and Nazari (2013), Hosseinpour et al. (2015), Hasan and Samadiya (2017), and Chenari et al. (2018), have utilized this paradigm in their experiments on stone columns (2019). Poisson's ratio was selected based on Bowles's suggested typical values (1997). The input parameters for the model, shown in Table 4.3, including c, φ, can be obtained from laboratory experiments, and the modulus of elasticity from equation 4.1, the Dilation angle, is considered as (φ-25)°.

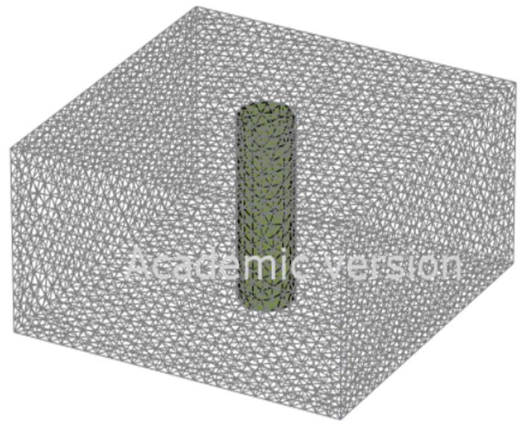

Figure 4.8: A generated mesh of the model with OSC

Table 4.3 Model Properties for FEM Model (Current Study)

Parameters	Column Material	Bed Material
Max. dry unit weight (kN/m^3)	17.8	16.96
Min. dry unit weight (kN/m^3)	14.9	15.2
Cohesion(kpa)	01	04
Friction angle (φ °)	42	29
Dilation angle, ψ (°)	17	4
Young's modulus, E (kPa)	48000	12000

Efforts were made to ensure that the majority of sand particles were smaller than 2 μm in diameter and between 2 μm and 50 mm during the development of PLAXIS material properties via a tab, as shown in Figure 4.9. To keep the material within the Vibro replacement range, approximately 5% of the material was allocated to particle diameters between 2 and 50 mm.

A constant normal load was applied to the sand bed, which is depicted in Figure 4.10. The lower half of the shear box underwent a predetermined displacement of 50 mm. Figure 4.11 represents the horizontal displacements, whereas Figure 4.12 represents the contour lines of displacement. The study examined various diameters of the stone column (50 mm, 75 mm, 100 mm, and 150 mm) for each case of OSC, ESC, and DLE under distinct normal pressure conditions of 50kPa, 75kPa, 100kPa, 150kPa, and 200kPa, as listed in Table 4.3.

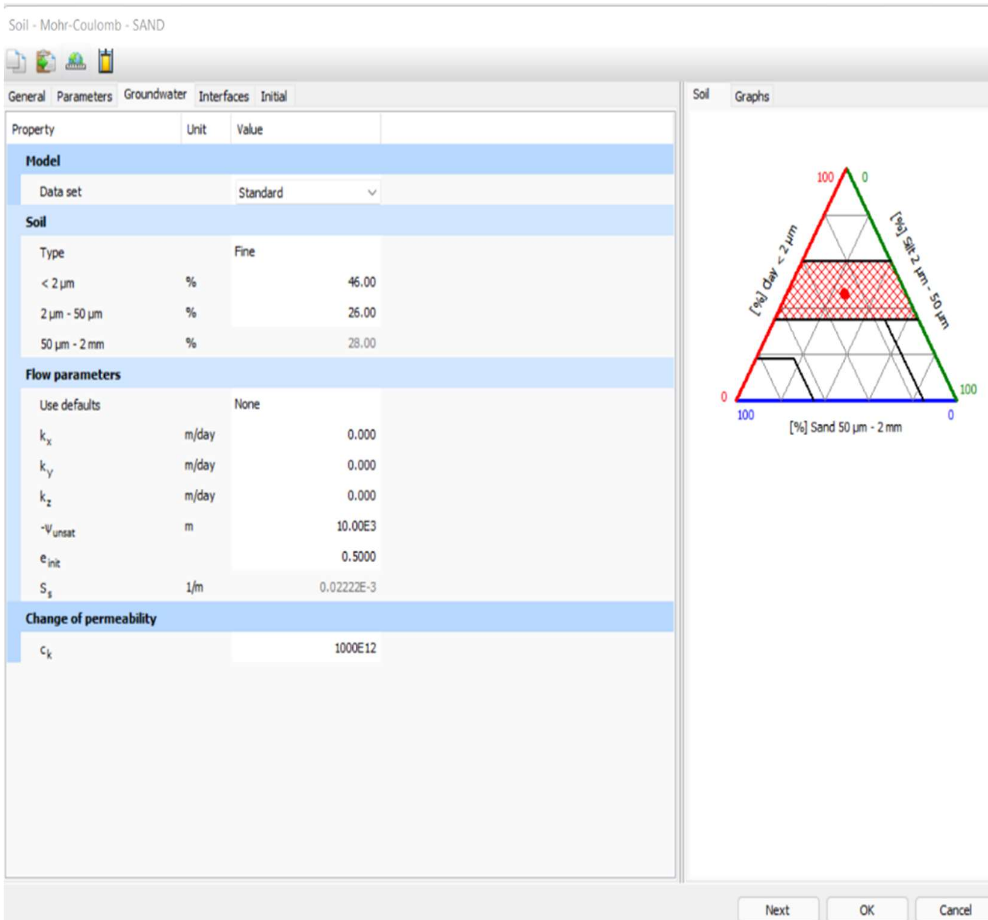

Figure 4.9: Tab showing the input required for the Material Data set

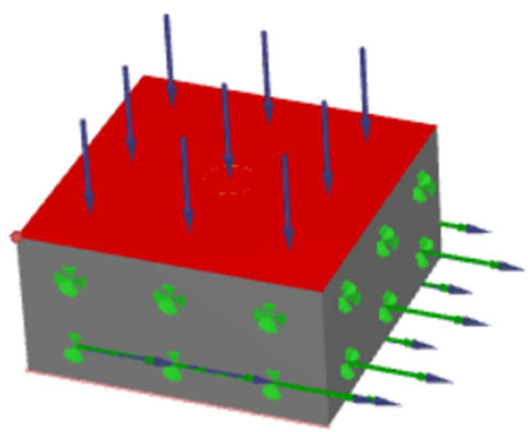

Figure 4.10: Model with applied normal and horizontal load

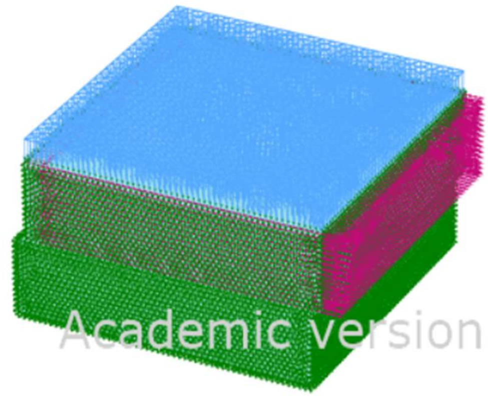

(a)

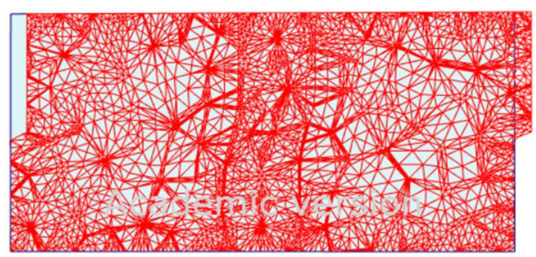

(b)

Figure 4.11: Provided total displacement in x-direction (u_x)

(a) Isometric view with load and displacement

(b) cross-sectional view on distribution plane A-A

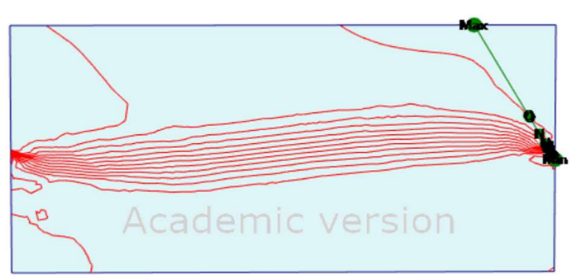

Figure 4.12: Contour line of displacement in x-direction (u_x)

Figures 4.13 and 4.14 are illustrative depictions of the Dual Layer Enclosure models. The images depict DLE stone column cases with square patterns of 50mm diameter and triangular patterns of 75mm diameter. These images effectively illustrate the activation and deactivation of various materials in the model, allowing for a better understanding of the placement of the dual-layer Encasement. In addition, Figure 4.15 provides details for a 100-mm-dia SLE stone column case for a better comparative view with Single Layer Encasing placement.

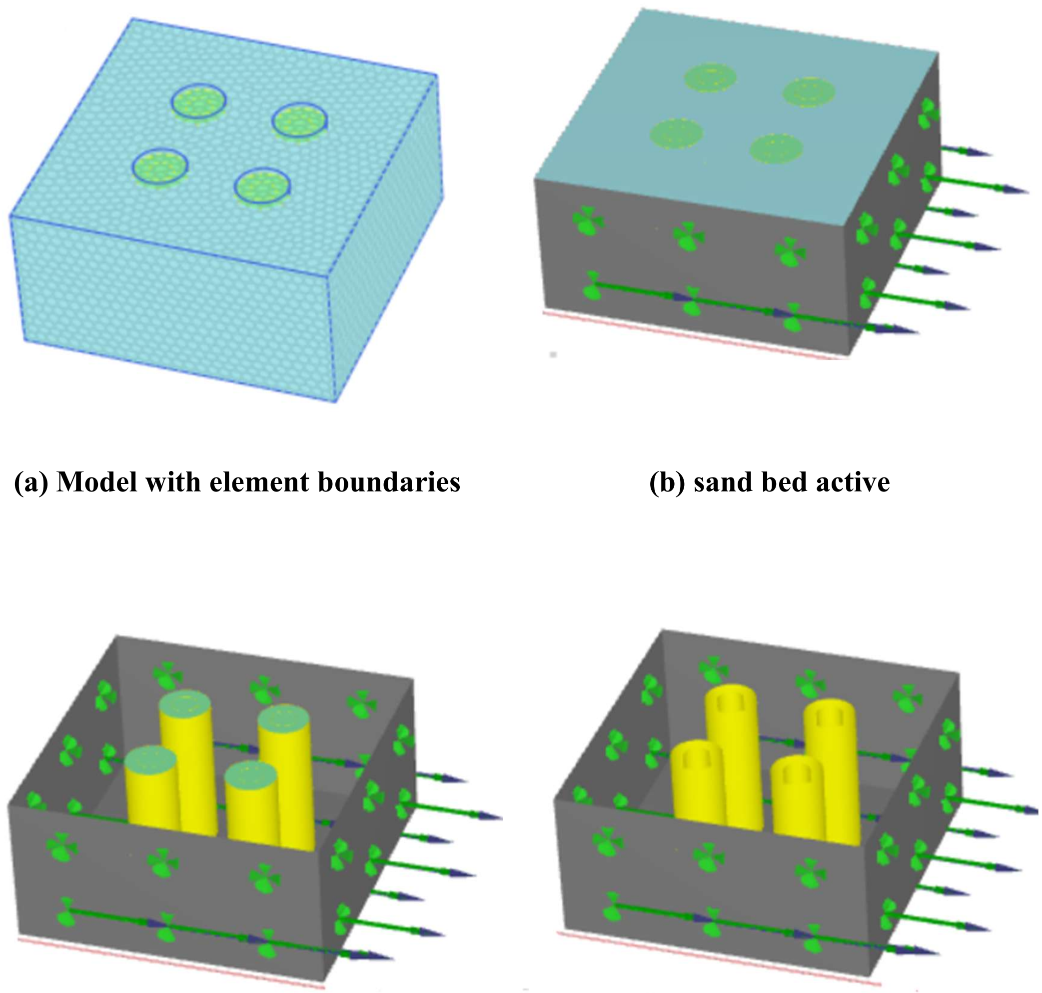

(a) Model with element boundaries **(b) sand bed active**

(c) sand bed deactivated **(d) Stone column material deactivated**

Figure 4.13: Model of 50 mm diameter DLE stone column arranged in a square pattern

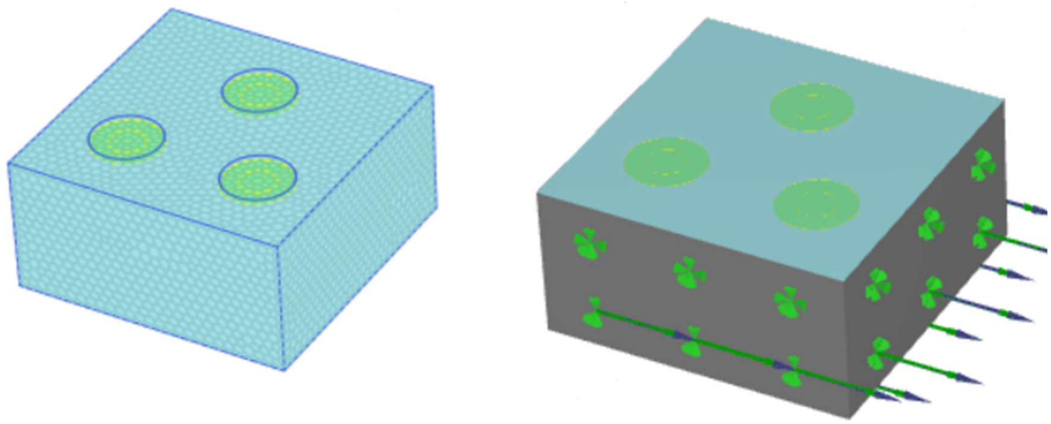

(a) Model with element boundaries **(b) sand bed active**

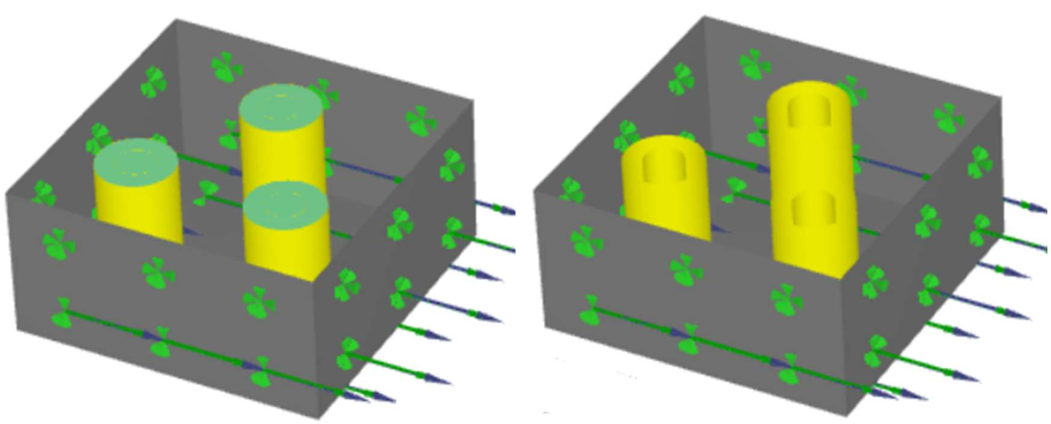

(c) sand bed deactivated **(d) Stone column material deactivated**

Figure 4.14: Model of 50 mm diameter DLE stone column arranged in a ttriangular pattern

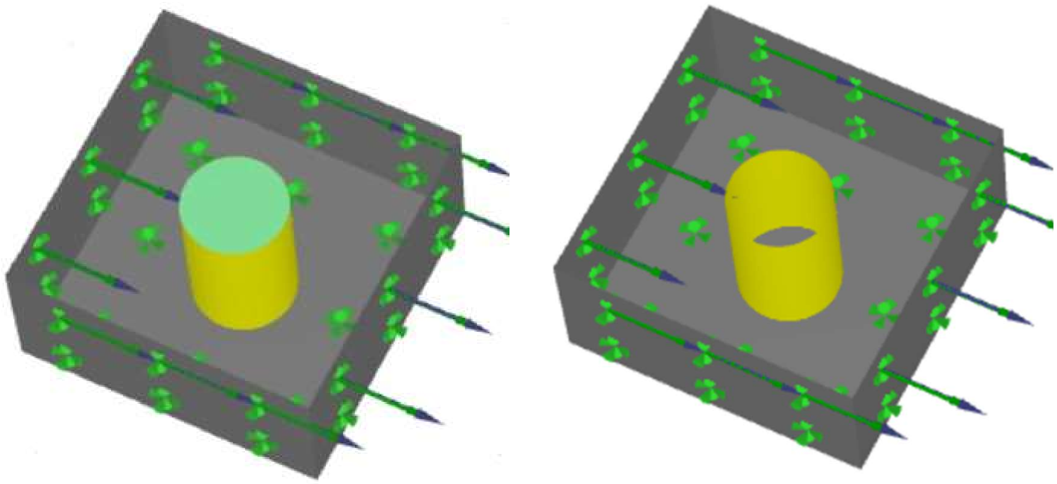

(a) sand bed deactivated **(b) Stone column material deactivated**

Figure 4.15: Model of 100 mm diameter SLE stone column

5. RESULT AND DISCUSSION

5.1 COMPARISON OF EXPERIMENTAL AND NUMERICAL RESULTS FOR THE CURRENT STUDY

Experimental and numerical analyses have been conducted for several types of stone columns to determine how they behave under lateral loads. Fig. 5.1 depicts the variation of shear stress with horizontal displacement for both types of studies on an ordinary stone column, a single-layered encased stone column, and a Dual Layered Encased stone column for a 150 mm diameter stone column subjected to 100 kPa of normal stress. It can be observed that the numerical analysis validates the findings of the experimental investigation done in the present study. The maximum shear stress value obtained at 50 mm horizontal displacement for OSC is 104kPa, whereas, for SLESC and DLESC, it is 120 kPa and 125 kPa, respectively. Because of the encasements, the combined soil-stone column system provides improved strength.

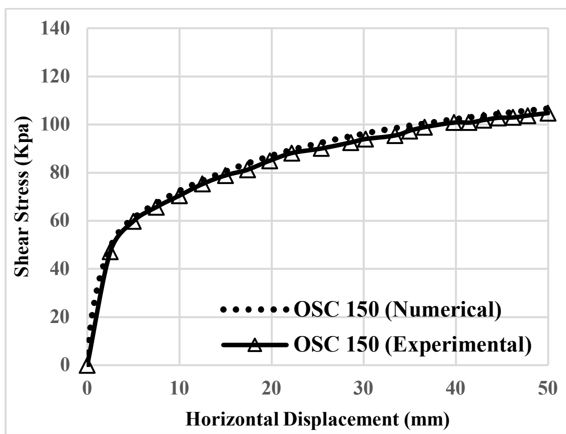

(a)

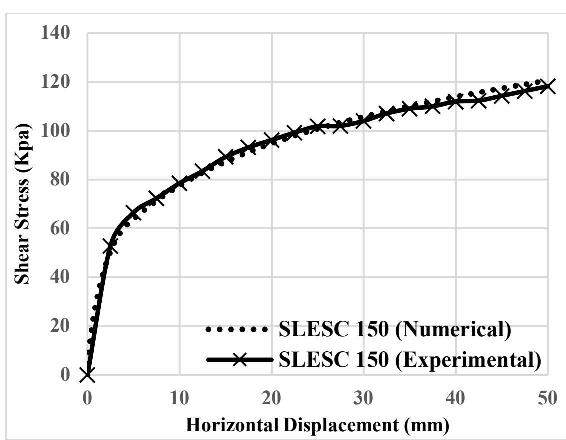

(b)

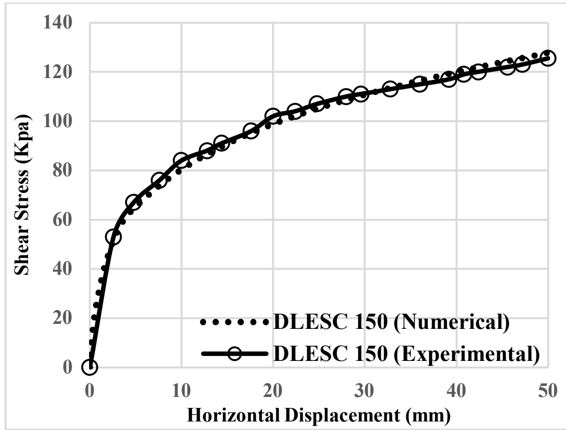

(c)

Figure: 5.1 Shear stress vs. horizontal displacement for 150 mm diameter (at 100 kPa normal)
(a) OSC (b) SLESC (c) DLESC

5.2 Results of the Experimental Programme

5.2.1 General

The soil bed and soil-stone column combined body were tested using the large shear box test apparatus to create the horizontal movement, and Graphs of shear stress vs. shear strain were produced. The values of shear stresses for the 25% strain, or 37.5 mm of horizontal displacement, may be seen from Figs. 5.2-5.25 to be larger in the case of USC than that in the case of the sand bed. Table 5.1 summarises the peak shear stress for all the cases considered. The inclusion of USC in the sand bed improves shear resistance, demonstrating that the stiffness of the combined soil-stone column system is increased when a material with a greater elastic modulus is employed to replace loose soil. Under various circumstances of normal pressure, it was shown that the shear stress in cases of USC was 6–10% greater in cases of single columns and up to 15% higher in groups of stone columns compared to sand bed alone. This demonstrates unequivocally that the stronger material in the shear path has enhanced resistance to the external lateral load at the failure plane. Shear stress values for the sand bed case at maximum displacement are 76,106 and 134 kPa under normal pressures of 100,150, and 200 kPa, respectively.

The shear stress values at equal levels of displacement were found to be 81, 113, and 134 kPa in the case of USC. This indicates that a roughly similar amount of shear resistance increases in USC and Sand bed when the normal pressure rises by the same amount. In the present investigation, it is observed that the amount of shear resistance achieved for a sand bed deformed by 25 % under lateral load is reached in the initial 10-15 % deformation stage when USC is utilized.

In situations where confinement is present, there is an enhanced improvement, whereby the resistance to shear stress is equivalent to a range of 5% to 10% of deformation. Previous studies conducted by Jaiswal and Kumar (2022) through numerical analysis, as well as by Mohapatra (2016) through experimental investigation, have also revealed that un-encased stone columns exhibit distinct shearing characteristics under lateral loads. Conversely, encased stone columns display solely a deformed shape at the junction, indicating a bending of the encased body. The confined column demonstrates comparable strength at a lower level of deformation when compared to the later-stage sand bed. This alteration in the combined system of soil-stone columns can significantly contribute to the design of foundations for structures, as it enables adherence to permissible deformation limits.

Table 5.1: Peak Shear Stress (at 37.5 mm Displacement)

Conditions of Sample			Shear stress (kPa) in different encasement conditions		
Diameter of Stone column	Normal Pressure (kPa)	Arrangement	USC	SLE	DLE
			134		
50	200	Single	143	154	-
		Triangular	144	174	-
		Square	147	168	-
75		Single	144	156	165
		Triangular	160	206	234
		Square	161	233	256
			105		
50	150	Single	113	121	-
		Triangular	114	142	-
		Square	117	140	-
75		Single	113	130	135
		Triangular	126	171	195
		Square	135	200	236
			75		
50	100	Single	80	88	-
		Triangular	81	106	-
		Square	82	109	-
75		Single	80	94	101
		Triangular	89	133	153
		Square	99	160	181

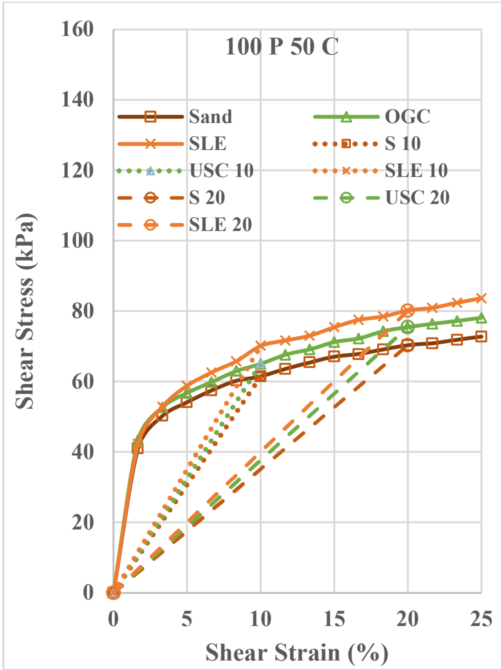

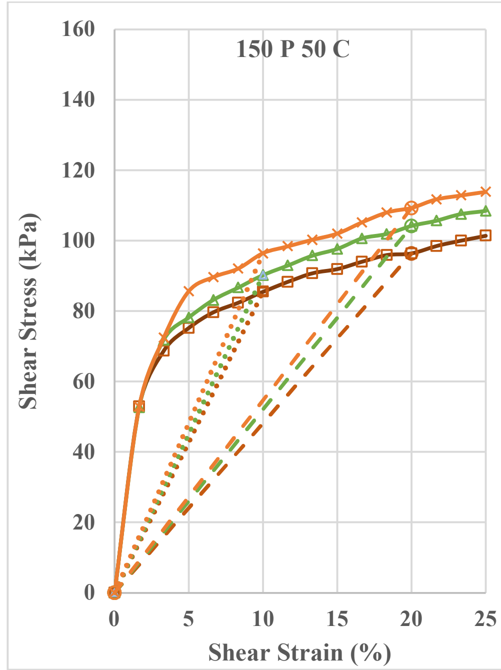

Fig 5.2:- Shear Stress-Strain curve for 50 mm Diameter single Stone column under 100kPa Normal Pressure

Fig 5.3:- Shear Stress-Strain curve for 50 mm Diameter single Stone column under 150kPa Normal Pressure

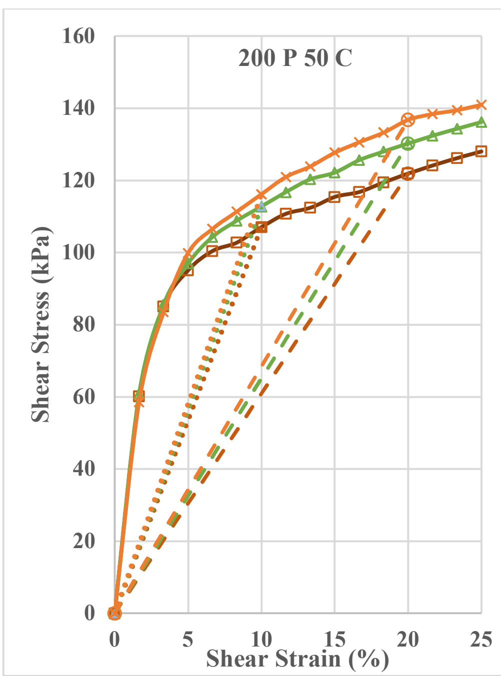

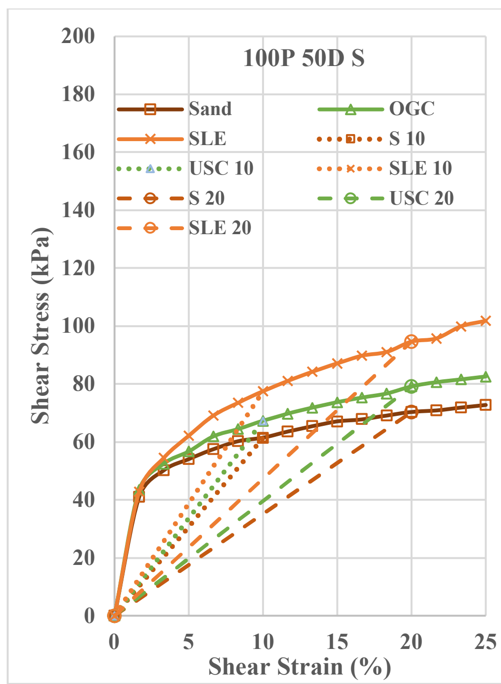

Fig 5.4:- Shear Stress-Strain curve for 50 mm Diameter single Stone column under 200kPa Normal Pressure

Fig 5.5:- Shear Stress-Strain curve for 50 mm Diameter, Square arrangement, 100kPa Normal Pressure

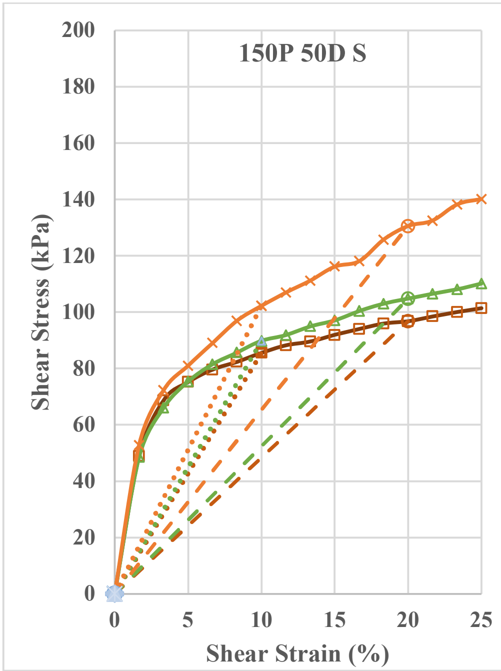

Fig 5.6: - Shear Stress-Strain curve for 50 mm Diameter, Square Arrangement, 150kPa Normal Pressure

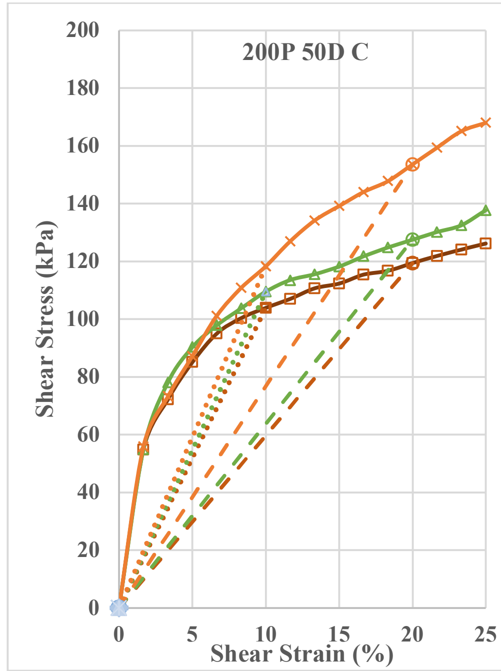

Fig 5.7:- Shear Stress-Strain curve for 50 mm Diameter, Square Arrangement, 200kPa Normal Pressure

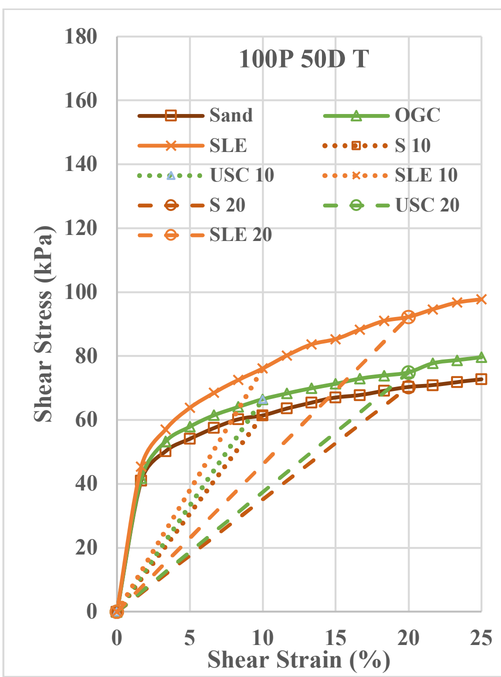

Fig 5.8:- Shear Stress-Strain curve for 50 mm Diameter, Triangular Arrangement, 100kPa Normal Pressure

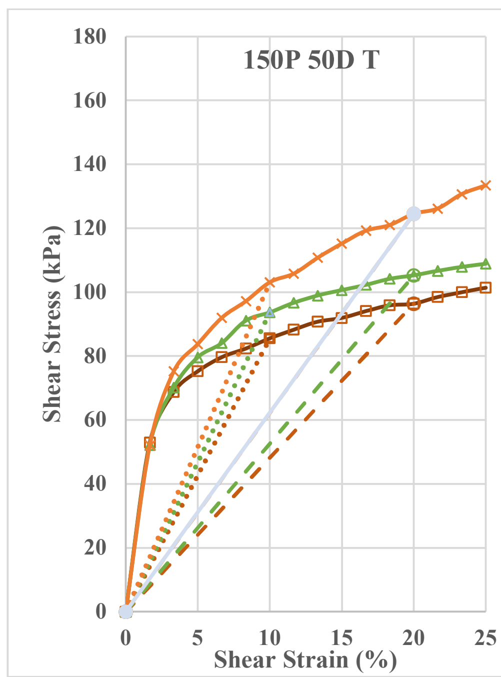

Fig 5.9:- Shear Stress-Strain curve for 50 mm Diameter, Triangular Arrangement, 150kPa Normal

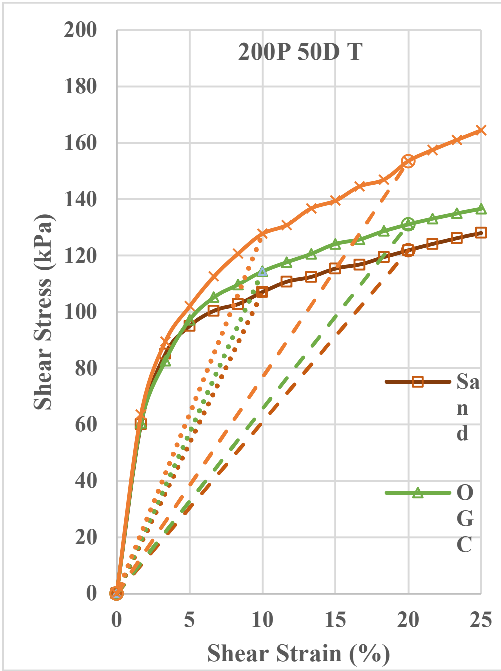

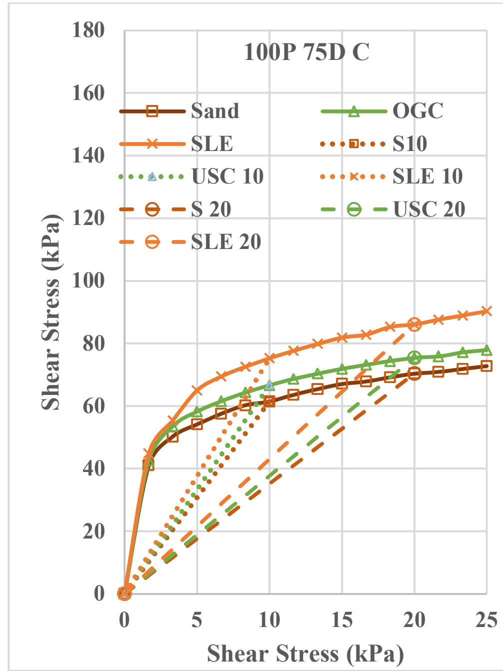

Fig 5.10:- Shear Stress-Strain curve for 50 mm Diameter, Triangular Arrangement, 200kPa Normal Pressure

Fig 5.11:- Shear Stress-Strain curve for 75 mm Diameter, Single Column, 100kPa Normal Pressure

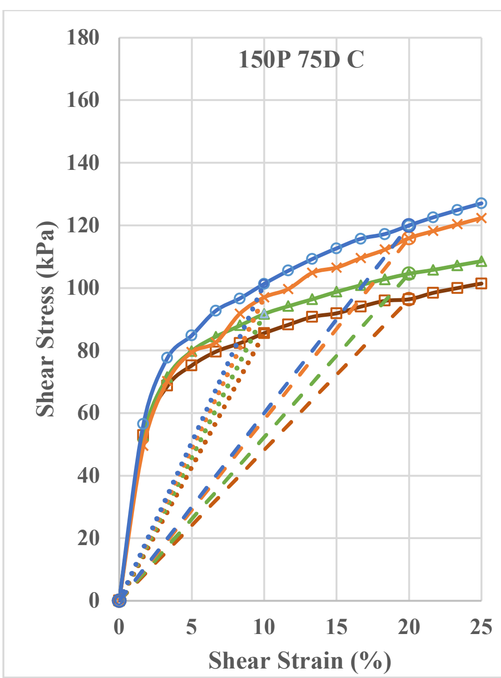

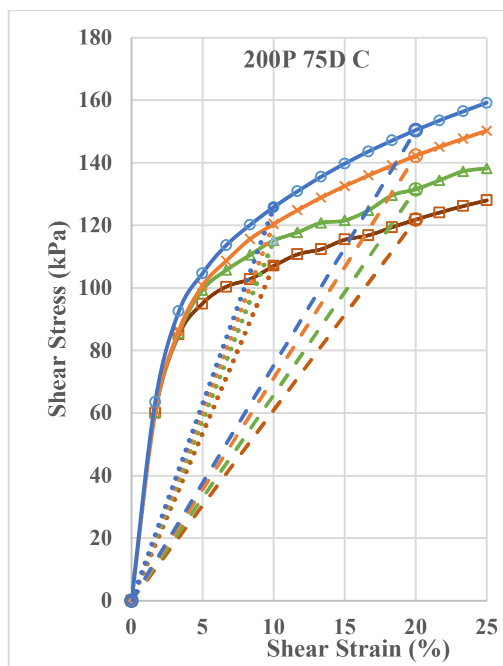

Fig 5.12:- Shear Stress-Strain curve for 75 mm Diameter, Single Column, 150kPa Normal Pressure

Fig 5.13:- Shear Stress-Strain curve for 75 mm Diameter, Single Column, 200kPa Normal Pressure

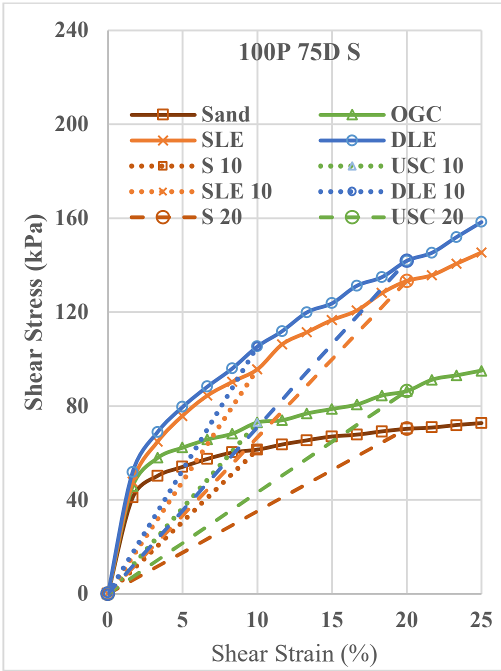

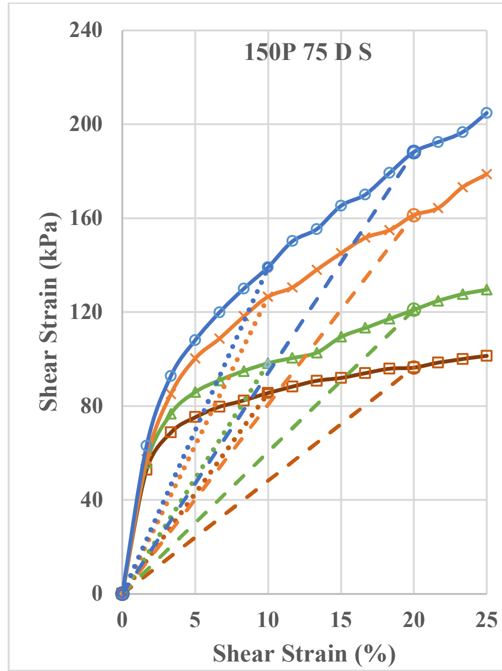

Fig 5.14:- Shear Stress-Strain curve for 75 mm Dia, Square Arrangement, 100kPa Normal Pressure

Fig 5.15:- Shear Stress-Strain curve for 75 mm Dia, Square Arrangement, 150kPa Normal Pressure

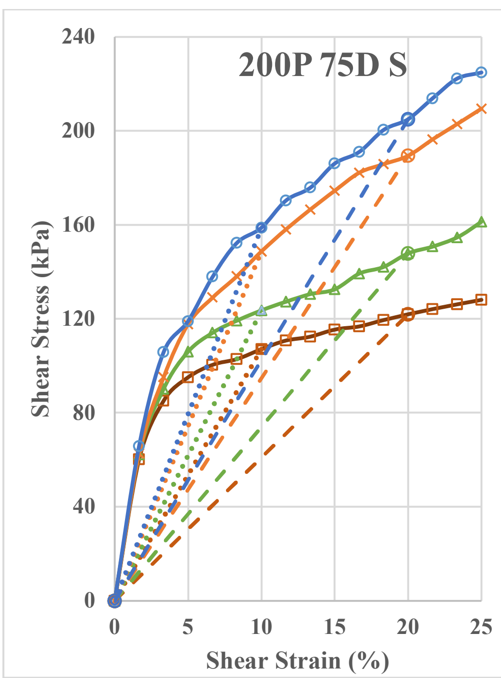

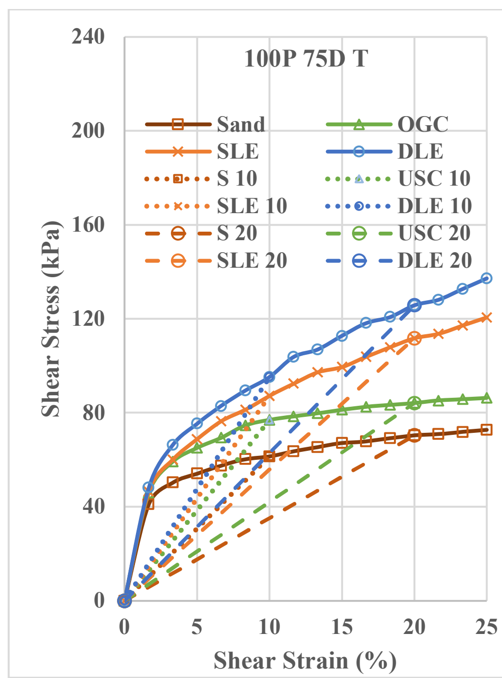

Fig 5.16:- Shear Stress-Strain curve for 75 mm Dia, Square Arrangement, 200kPa Normal Pressure

Fig 5.17:- Shear Stress-Strain curve for 75 mm Dia, Triangular Arrangement, 100kPa Normal Pressure

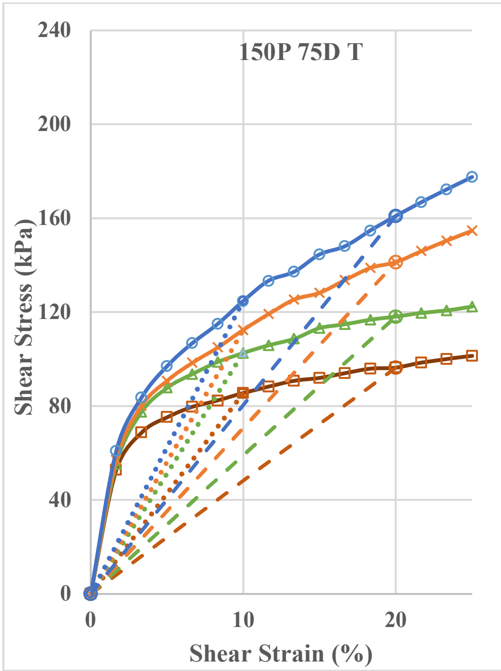

Fig 5.18:- Shear Stress-Strain curve for 75 mm Diameter, Triangular Arrangement, 150kPa Normal Pressure

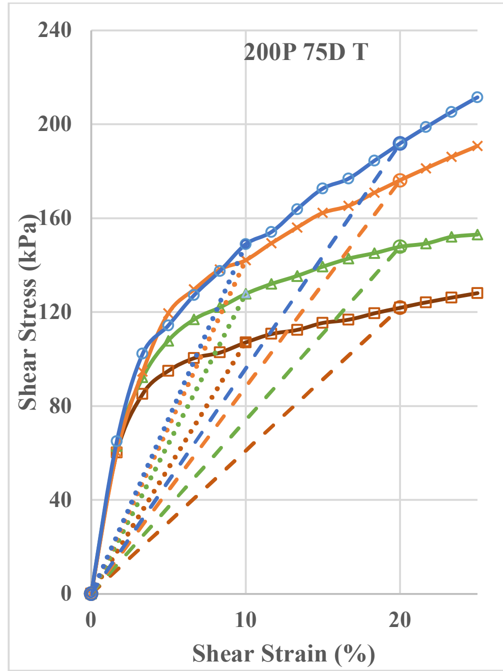

Fig 5.19: - Shear Stress-Strain curve for 75 mm Diameter, Triangular Arrangement, 200 kPa Normal Pressure

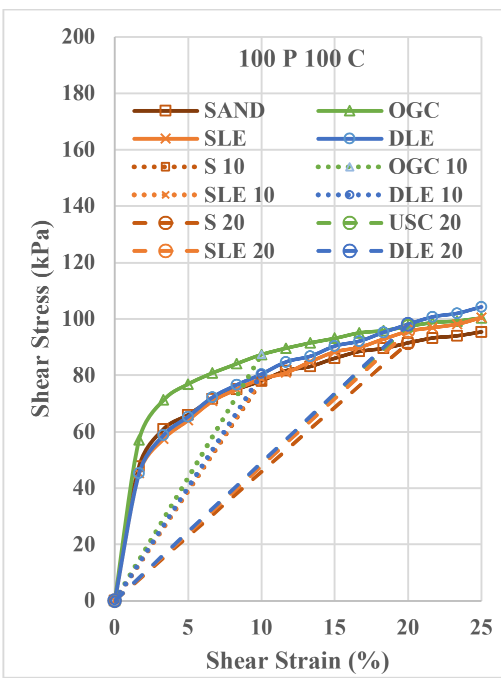

Fig 5.20:- Shear Stress-Strain curve for 100 mm Diameter, Single Column, 100kPa Normal Pressure

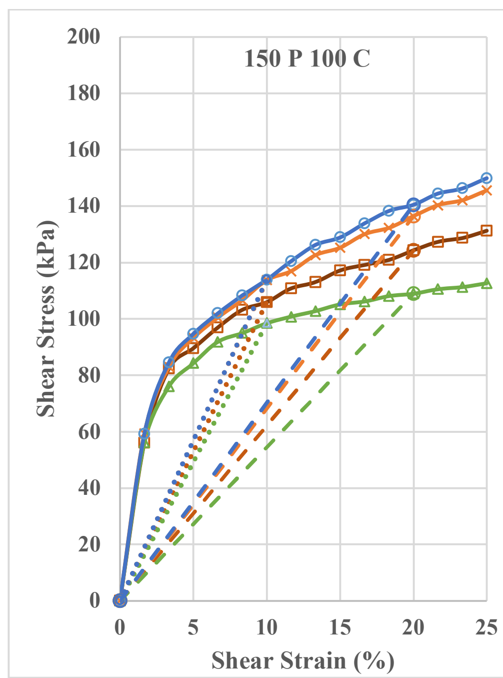

Fig 5.21:- Shear Stress-Strain curve for 100 mm Diameter, Single Column, 150kPa Normal Pressure

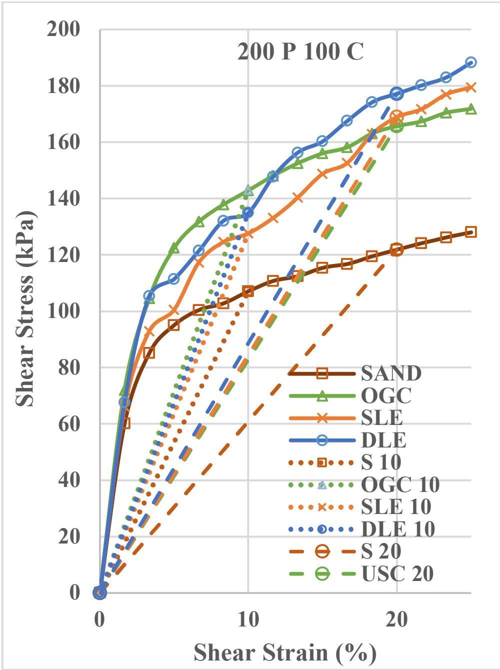

Fig 5.22:- Shear Stress-Strain curve for 100 mm Diameter, Single Column, 200kPa Normal Pressure

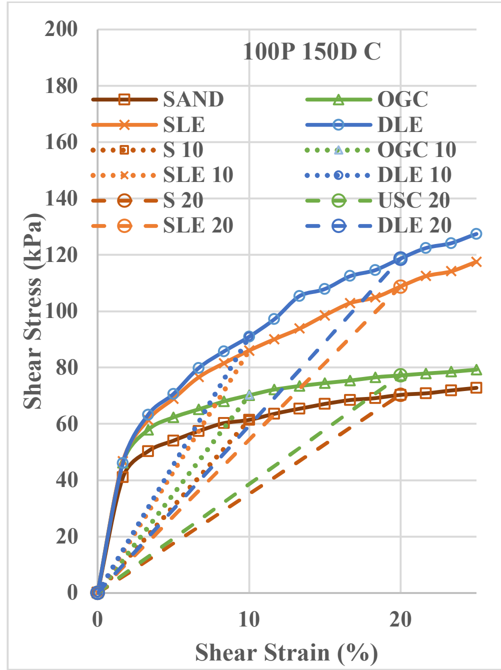

Fig 5.23:- Shear Stress-Strain curve for 150 mm Diameter, Single Column, 100kPa Normal Pressure

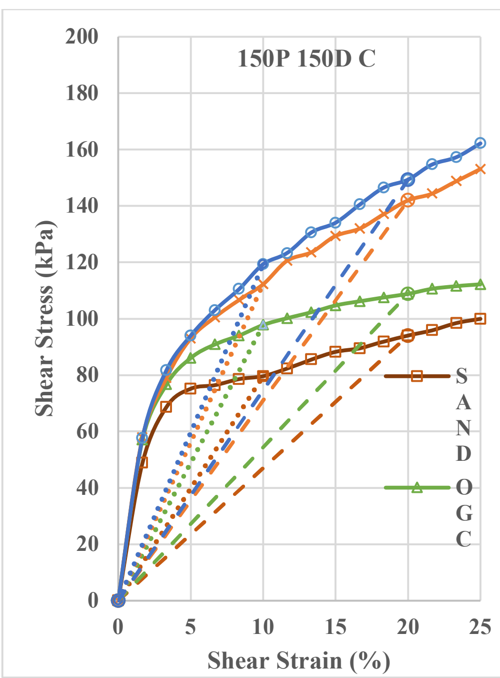

Fig 5.24: - Shear Stress-Strain curve for 150 mm Diameter, Single Column, 150 kPa Normal Pressure

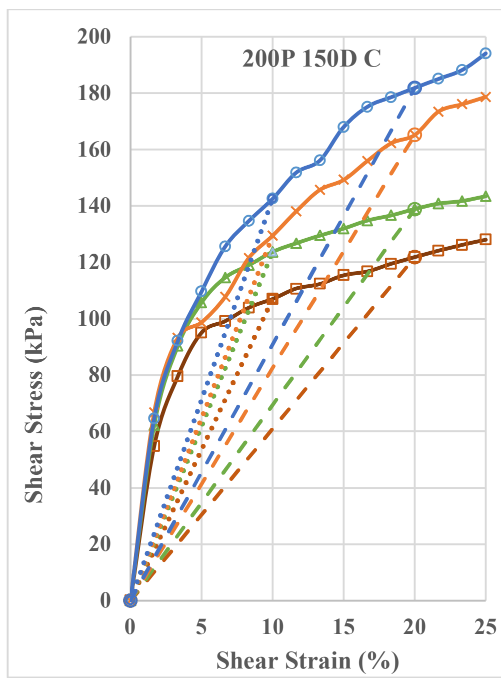

Fig 5.25: - Shear Stress-Strain curve for 150 mm Diameter, Single Column, 200kPa Normal Pressure

5.2.2 Shear Modulus/Stiffness

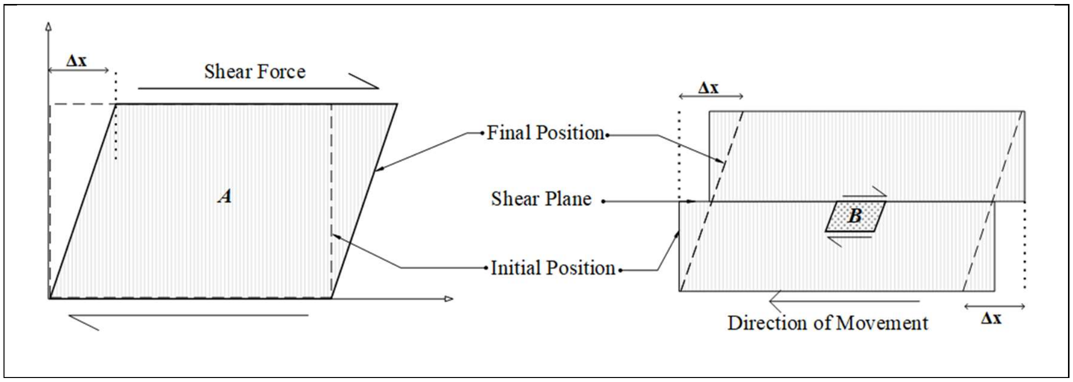

Fig 5.26: Consideration of soil element under the shear load

The shear modulus represents the soil's response to shear deformation, indicating its resistance to such deformations. It is determined by the ratio of shear stress to shear strain in the material, applicable to element A, depicted in Figure 5.26, where the element transforms shape. Shear strain can be defined as $\Delta x/X$, while shear stress is measured as the ratio of shear force to the area over which the shear occurs. In the case of a large shear box test setup, as the lower box reaches its final position, element B situated at the shear plane, behaves similarly to element A due to the shearing that occurs at the plane caused by the movement of the lower box. Therefore, element B can be considered equivalent to element A, enabling the use of shear modulus to compare different soil samples or the soil-stone column system within the large shear box setup.

The initial length of the area is taken as 150 mm, and a 25% (37.5 mm) deformation was induced in the sample for which shear stress-strain graphs were generated. This study plots the secant shear modulus for 10% and 20% deformation on shear stress-shear strain graphs for various cases involving normal pressure, stone column diameter, and arrangements. It is generally observed that the initial tangent modulus of elasticity for all cases of the sand bed, un-encased column, and encased column are nearly identical. However, as strain increases in the body, the secant modulus at different displacement percentages begins to exhibit variations among the different samples. To facilitate comparison, the secant modulus of shear for 10% and 20% deformation are plotted on all shear stress-strain curves using the slope equation of the line connecting the origin to the corresponding stress point denoted by E_{10} and E_{20}, respectively. Examining E_{10} values for stone columns of different diameters and normal load conditions yields significant insights into the behaviour of such foundations. Significant variations in E_{10} values among USC, SLE, and DLE patterns provide insights into the performance characteristics of the columns.

When The sand bed was subjected to a normal pressure of 100 kPa and yielded a secant modulus (E_{10}) of 6.144 kN/m², the unencased and single-layer encased stone column cases yielded values of 6.501 kN/m² and 7.014 kN/m², respectively, when a single column was installed at the center. The results indicate that under normal pressure conditions (as shown in Figures 5.27-5.28), the soil-stone column system exhibited higher E_{10} and E_{20} values than the sand bed alone.

The E_{10} values exhibit a percentage change ranging from 3.05% to 22.58% between USC and SLE for all diameter sizes (50, 75, 100, and 150 mm). The transition from USC to SLE leads to significant variations in the load-carrying capacity of the stone columns. The impact of pattern selection on column performance is substantial, especially for larger diameters, as the percentage change is more pronounced.When comparing USC to DLE, the percentage change in E10 values varies from 10.12% to 21.56%. This study examines the effect of transitioning from USC to DLE patterns on the load-bearing capacity of columns. The study shows that the selection of pattern has a notable impact on the behavior of the column, particularly in larger diameter columns where percentage changes are more pronounced.

The USC pattern shows E_{20} values ranging from 3.772 kN/m² to 6.512 kN/m² under varying normal load conditions. In the SLE pattern, E_{20} values increase from 4.008 kN/m² to 6.839 kN/m². The most significant rise is observed at a standard pressure of 200 kPa, where the E_{20} value reaches 6.839 kN/m².The DLE pattern exhibits an increase in E_{20} values ranging from 4.275 kN/m² to 7.261 kN/m². The E_{20} value experiences a significant increase of 7.261 kN/m² under the normal pressure condition of 200 kPa, similar to the USC to SLE comparison.A consistent increase in E_{20} values is observed when comparing USC to SLE and USC to DLE variations. The USC to SLE variation displays a percentage change ranging from 6.2% to 12.6%, with the highest increase occurring under the normal pressure condition of 200 kPa. The USC to DLE variation displays a percentage change between 13.8% and 19.4%, with the greatest increase observed at a normal pressure of 200 kPa.

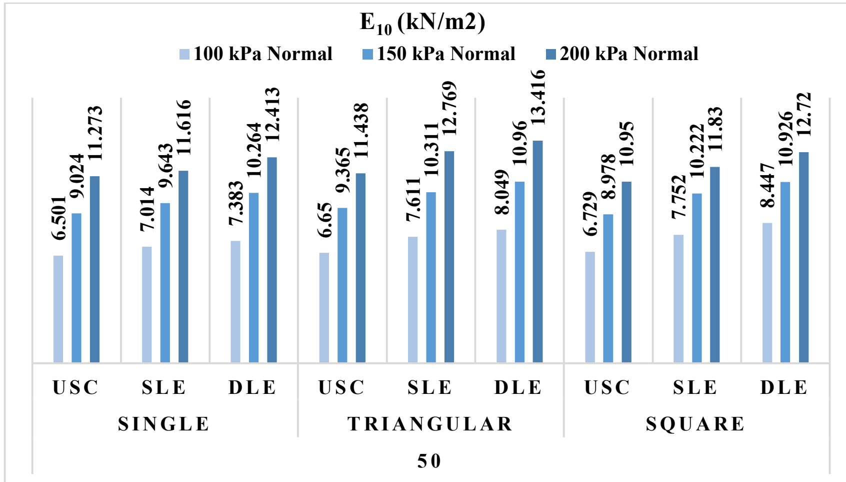

(a)

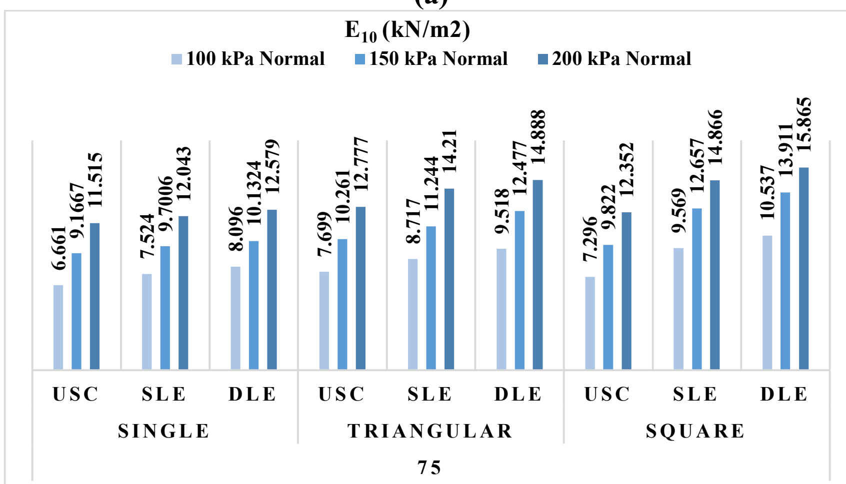

(b)

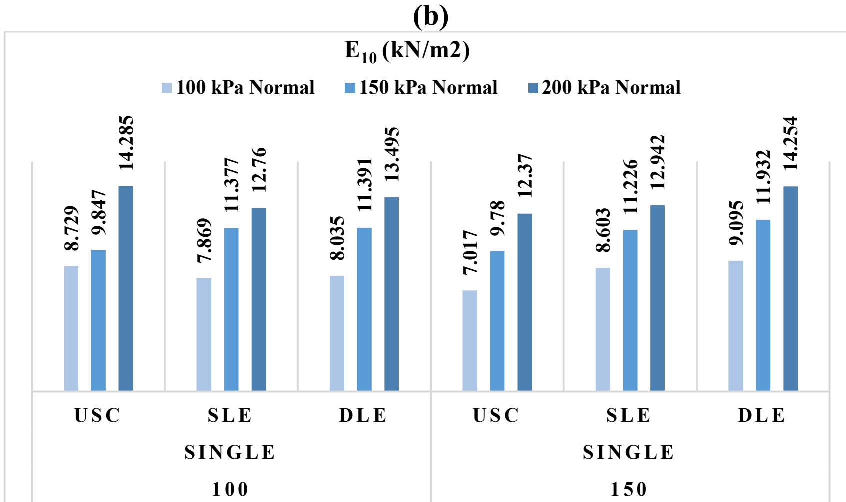

(c)

Fig 5.27: - Comparison of Secant Modulus E_{10} for Various patterns of arrangement
(a) 50 mm diameter (b) 75 mm diameter (c) 100 mm and 150 mm diameter

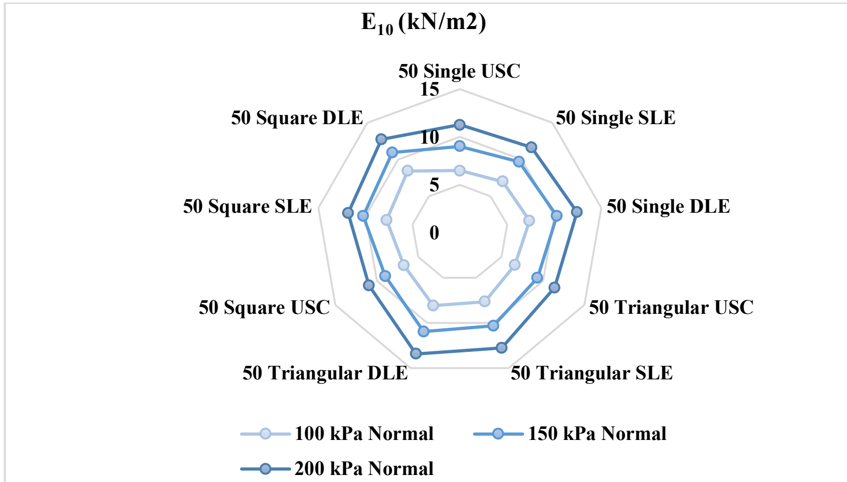

(a)

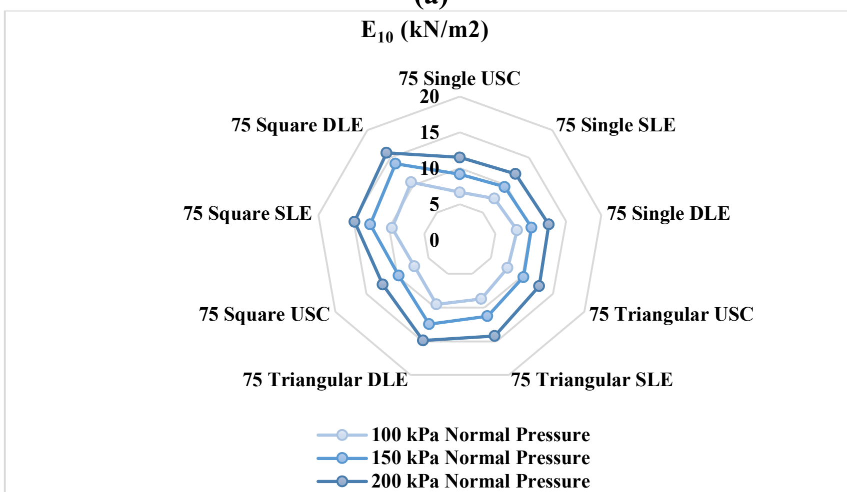

(b)

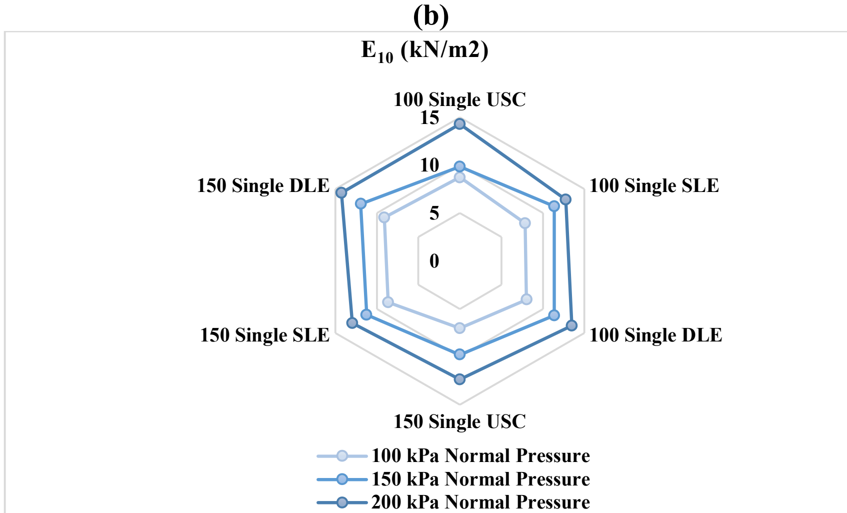

(c)

Fig 5.28: - Comparison of Secant Modulus E_{10} for Various patterns of arrangement with radar Graph
(a) 50 mm diameter (b) 75 mm diameter (c) 100 mm and 150 mm diameter

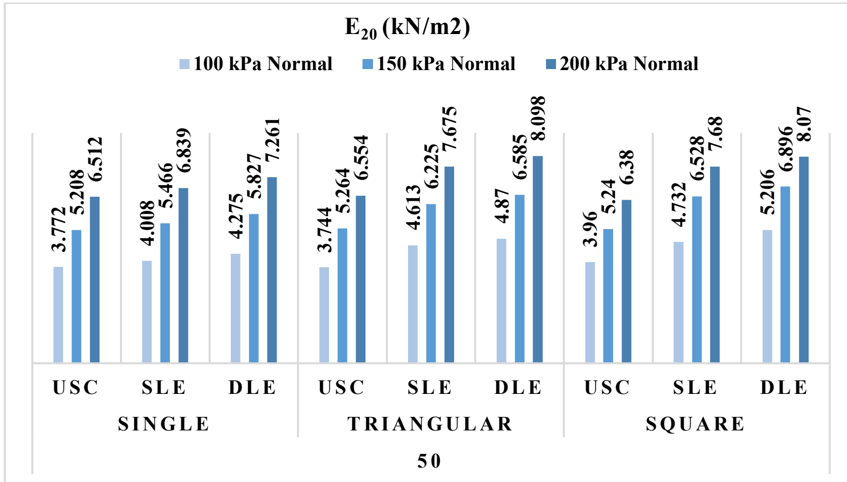

(a)

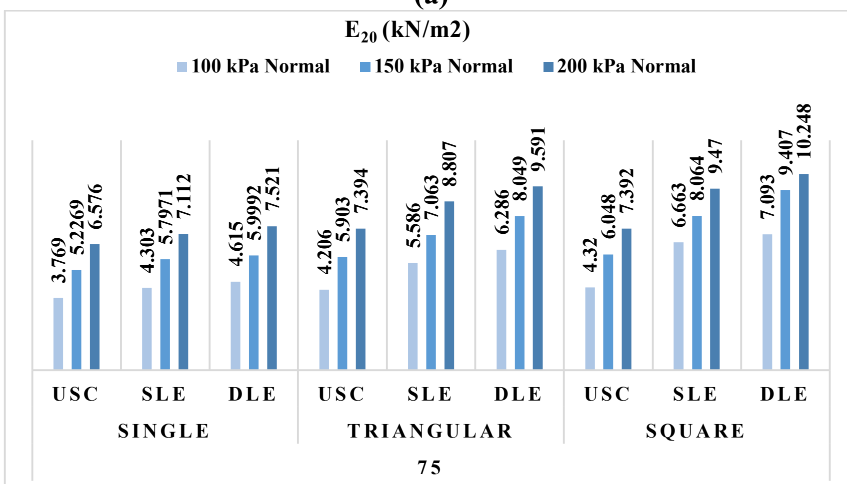

(b)

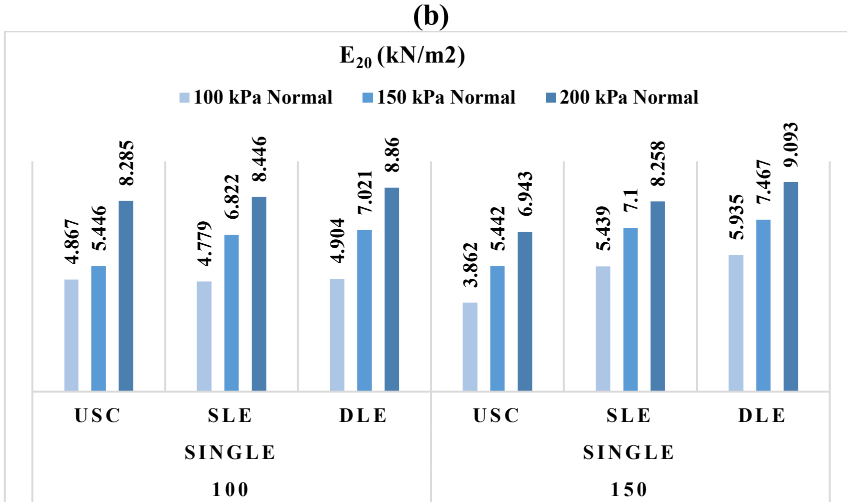

(c)

Fig 5.29: - Comparison of Secant Modulus E_{20} for Various patterns of arrangement
(a) 50 mm diameter (b) 75 mm diameter (c) 100 mm and 150 mm diameter

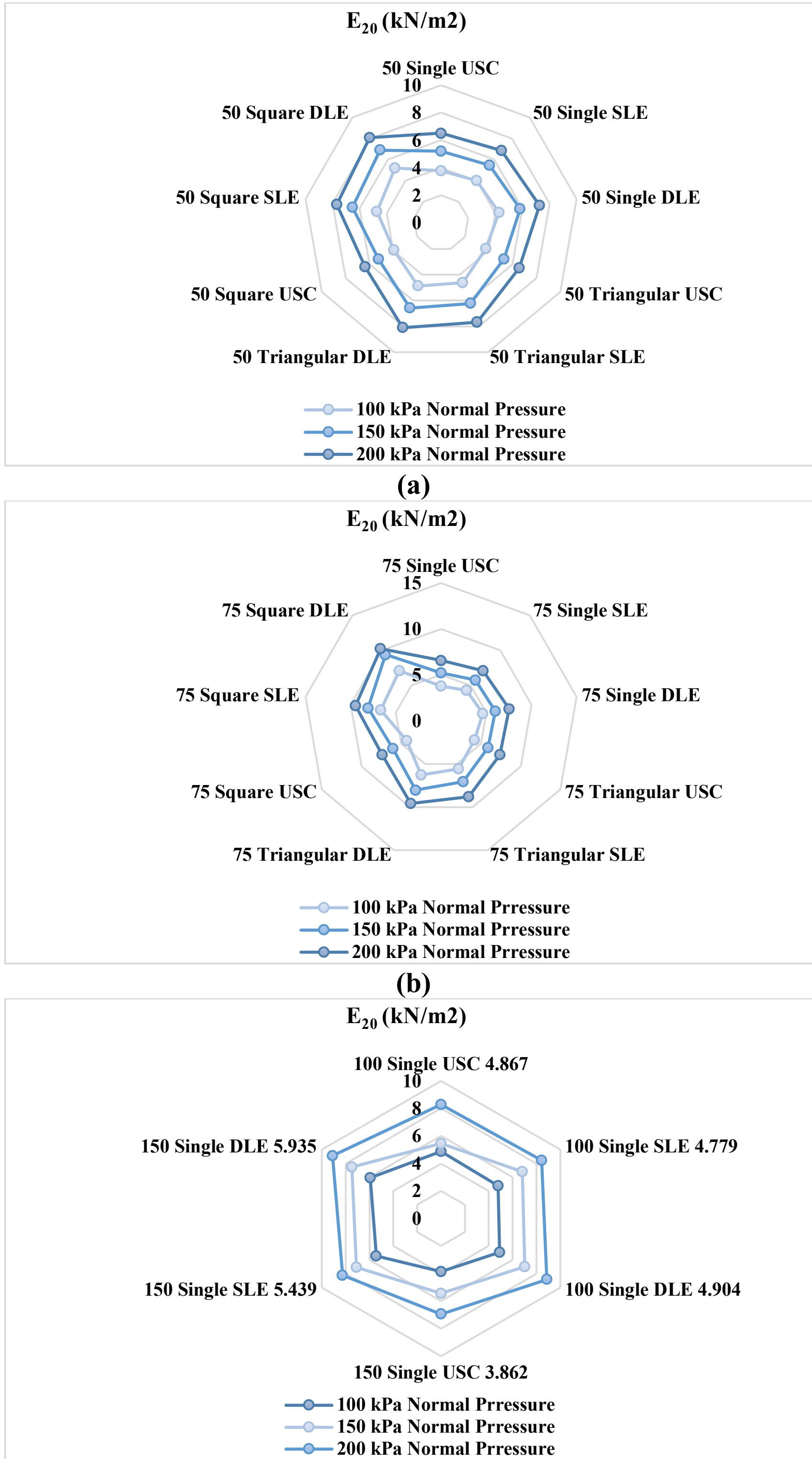

(c)

Fig 5.30: - Comparison of Secant Modulus E_{10} for Various patterns of arrangement with radar Graph
(a) 50 mm diameter (b) 75 mm diameter (c) 100 mm and 150 mm diameter

The findings suggest that the E20 values are higher in both SLE and DLE patterns than in the USC pattern (Fig. 5.29-5.30). The DLE pattern consistently shows the highest E20 values across all normal load conditions compared to the other two patterns. The results highlight the impact of pattern selection on the E20 values of stone columns.

5.2.3 Arrangement of Stone Column

For loose sand under normal pressures of 100, 150, and 200 kPa, the shear resistance at 25% deformation is measured at 76, 106, and 134 kPa, respectively. However, when a group of 50 mm diameter stone columns is arranged in a triangular pattern, the maximum shear resistance increases to 82, 114, and 144 kPa, surpassing the values obtained with a square arrangement by approximately 2-4 kPa. This increase in shear resistance ranges from 6% to 15% higher than that observed in the sand bed alone. When a larger diameter of 75 mm is employed for the grouped stone columns, the maximum shear stress in the loose sand bed case further increases by 25-30% for the square pattern and 16-18% for the triangular pattern under varying normal pressure conditions.

The enhanced shear stress mobilization resulting from the presence of a group of stone columns is attributed to the higher strength exhibited by the aggregate or granular material in the system, which contributes to a predominant area of strength at the shear plane. Mohapatra et al. (2016) also noted that the neighboring columns create a confining effect on each other and the underlying soil, leading to the increased overall resilience of the composite body.

Figures 5.27-5.28 present the plot of the shear modulus for 10% displacement against the normal pressure, illustrating that the shear modulus increases with higher normal pressure. The increased friction between surfaces or particles under a greater vertical load or normal pressure enhances the shear resistance at the shear plane and the overall rigidity of the body. Comparatively, the stiffness of single-column sand bed systems is lower than that of grouped stone column systems. When the sand is tested under a normal pressure of 100 kPa, the secant shear modulus is measured at 6.4 kN/m^2, which increases to 6.77, 6.9, and 7.1 kN/m^2 for single, triangular, and square arrangements, respectively. In the case of un-encased columns, the most significant increase in system stiffness is observed with a 75 mm stone column in a square pattern, where the secant modulus is 8.02 kN/m^2.

5.2.4 Effect of encasement conditions

An encasement is applied to investigate the impact of encasement on the stone column body. The shear resistance of encased stone columns increases across all normal pressure values, indicating that encasing the stone column enhances the confinement phenomenon. The shear stress-strain graphs in Figures 5.2-5.25 demonstrate that the slope of the graphs becomes steeper when the column material is constrained. Furthermore, it is observed that introducing a single layer of encasement leads to a greater change in shear resistance compared to unencased stone columns over a sand bed.

The percentage improvement from un-encased stone columns (USC) to single layer encasement (SLE) is found to be the lowest in single-column testing, ranging from 5% to 12%. This improvement increases from 20% to 22% for the triangular pattern arrangement and reaches a maximum of 23% to 52.5% when employing a square pattern arrangement within the sand sample. The comprehensive results for the composite samples are presented in Table 5.1. These findings suggest that the soil between the stone columns is stronger, making it suitable for supporting structures by providing a stable foundation for load transfer to the surrounding strata.

To investigate the impact of dual-layered encasement on stone columns, experimental studies were conducted using 75 mm diameter stone columns. It has been observed that the dual-layered encased (DLE) stone columns exhibit greater effectiveness in shear resistance compared to single-layer encased (SLE) stone columns. Figures 5.2-5.25 clearly illustrate a significant increase in shear stresses at later stages of displacements when compared to the sand bed. When a single column is subjected to lateral displacement under varying normal pressures, DLE demonstrates a 14-20% enhancement in shear stresses compared to un-encased stone columns. Similar to SLE, the addition of shear strength is more pronounced in the case of grouped stone columns. For a normal pressure of 150 kPa, the shear strength ratio of DLE to the un-encased stone column is 1.45 and 1.58 times higher for triangular and square arrangements, respectively. This improvement is even more significant for a lower normal pressure of 100 kPa, with shear resistance 1.6 and 1.65 times higher in DLE than in USC.

Under a normal pressure of 100 kPa, the E_{10} (secant shear modulus) obtained for DLE in square and triangular patterns is 9.91 kN/m² and 10.98 kN/m², respectively, which are 1.55 and 1.71 times higher than the sand bed. It is evident that the dual encasements greatly enhance the soil-stone column combined system. While the improvement remains considerable under higher overburden pressure, it is 1.48, 1.62, 1.39, and 1.45 times higher in square and triangular patterns for overburden pressures of 150 kPa and 200 kPa, respectively. Square pattern arrangements provide stronger resistance to shear stress, and this resistance reaches its peak in dual-layered encasements. The application of improved shear resistance can be considered in scenarios where embankments require a stronger stone column base and where the edge lines of stone columns are vulnerable to shear forces caused by the soil's potential to form a slip circle.

5.3 Results of the Numerical Programme

"In small-scale laboratory experiments, alterations to the experimental setup can lead to variations in the results. Utilizing Numerical Analysis, this problem is resolved. To investigate the lateral load capacity of stone columns, additional analyses utilizing PLAXIS 3D to generate large direct shear in numerical models are being conducted. All analyses were conducted in a completely dry environment. For shear strength studies, numerical analysis was performed on 50mm, 75 mm, 100mm, and 150mm diameter columns at 50kPa, 75kPa, 100kPa, 150kPa and 200kPa." Results are discussed in following heads:

5.3.1 Failure mechanism

As depicted in Figure 5.31 (a), the results of the numerical analysis indicate that the column without encasement exhibited visible shear alongside the granular column. Fig. 5.31 (b) depicts that there was no shear in any of the encasement scenarios, indicating that the encasement material did not fracture at the sheared location, the encasement only bends ni the direction of the load. This behavior of the encasement is crucial because it prevents ground failure when a section of the ground is subjected to greater lateral stress than the surrounding area. Experimental evidence demonstrates that the modulus and strength of the geosynthetic encasement influence the shear strength of models with encased column material. This is the case for models with encased column material. Mohapatra et al. (2016) conducted experiments that revealed two types of shear failure: Type-1 and Type-2, which the present study also confirms.

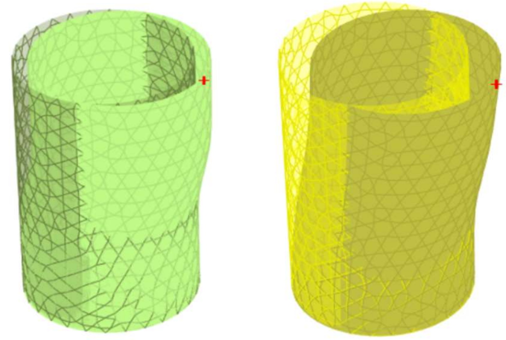

Fig.-5.31 Deformed granular colum body at 50mm horizontal displacment (a)OGC (b) Encased Granular Column

The shear strength of the sand bedwas measured at displacement values of 50mm and under typical pressures of 50, 75,100,150 and 200 kPa. The corresponding shear strength values were 43, 61, 78,110 and 140 kPa, respectively. For granular columns with a diameter of 50mm, the shear strengths were determined to be 46, 66, 84,118 and 150 kPa. A higher overall percentage change was observed when a larger diameter column was used, as shown in Table 5.2. The inclusion of OGCs in the sand reinforcement enhanced the shear resistance of the soil-granular column system. The granular column and the surrounding soil acted as a composite material, leading to improved shear resistance. The behavior was observed as increased shear resistances in columns of various diameters (50, 75, 100 and 200 mm) when the percentage area occupied by the granular column in the shear plane increased.

Table 5.2: Shear Stress value at 50mm displacement

Conditions of Sample			Shear stress (kPa) in different encasement conditions		
Diameter of Stone column	Normal Pressure (kPa)	Arrangement	OGC	SLE	DLE
50		Single	150	159	169
		Triangular	150	181	195
	200	Square	154	183	201
75		Single	150	169	176
		Triangular	167	214	226
		Square	154	243	267
			110		
50		Single	118	127	134
		Triangular	117	147	160
	150	Square	122	150	164
75		Single	118	134	141
		Triangular	130	178	190
		Square	120	207	244
50		Single	84	91	97
		Triangular	82	109	119
	100	Square	88	114	126
75		Single	84	98	104
		Triangular	92	139	150
		Square	82	166	187
50		Single	66	71	77
		Triangular	65	88	98
	75	Square	67	94	103
75		Single	65	80	84
		Triangular	66	109	116
		Square	64	144	162
50		Single	46	52	56
		Triangular	47	67	73
	50	Square	47	72	79
75		Single	46	58	62
		Triangular	46	85	91
		Square	45	118	142

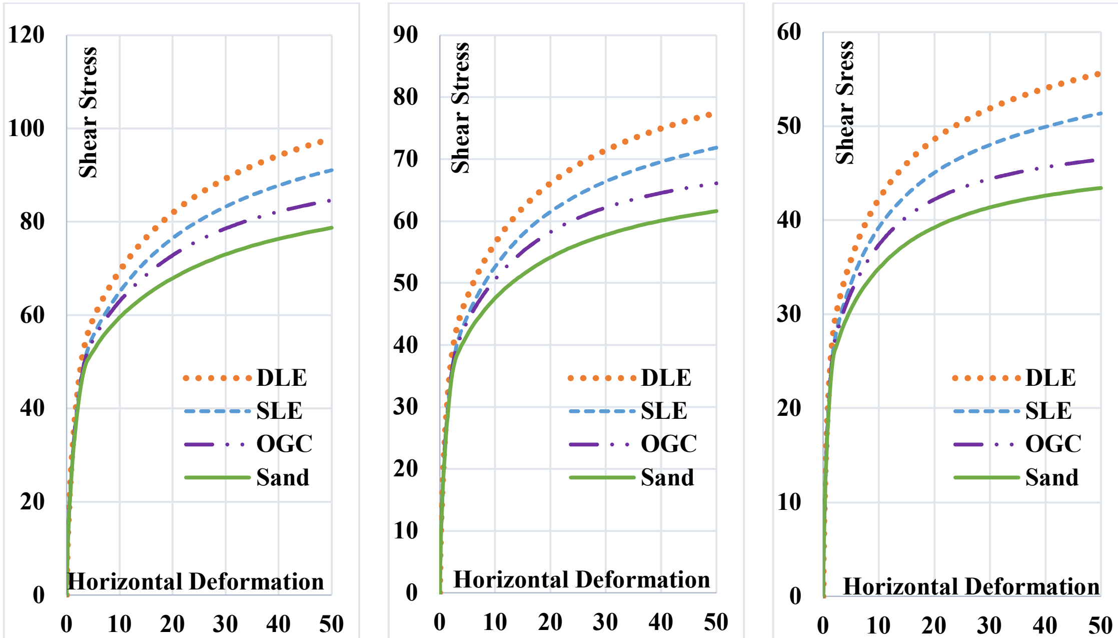

(a) (b) (c)

Figure 5.32: Shear stress vs. horizontal displacement of 50 mm diameter single granular column installed in sand bed at various normal pressure (a)100 (b)75 (c) 50 (kPa)

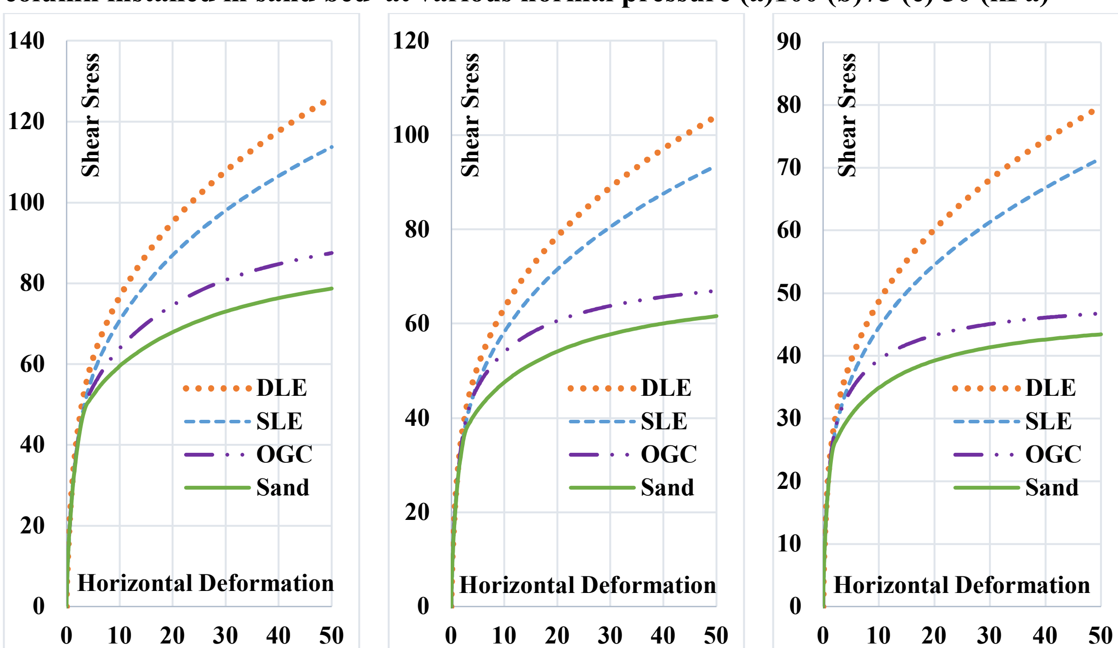

(a) (b) (c)

Figure 5.33: Shear stress vs. horizontal displacement of 50 mm diameter granular column installed in square pattern at various normal pressure (a)100 (b)75 (c) 50 (kPa)

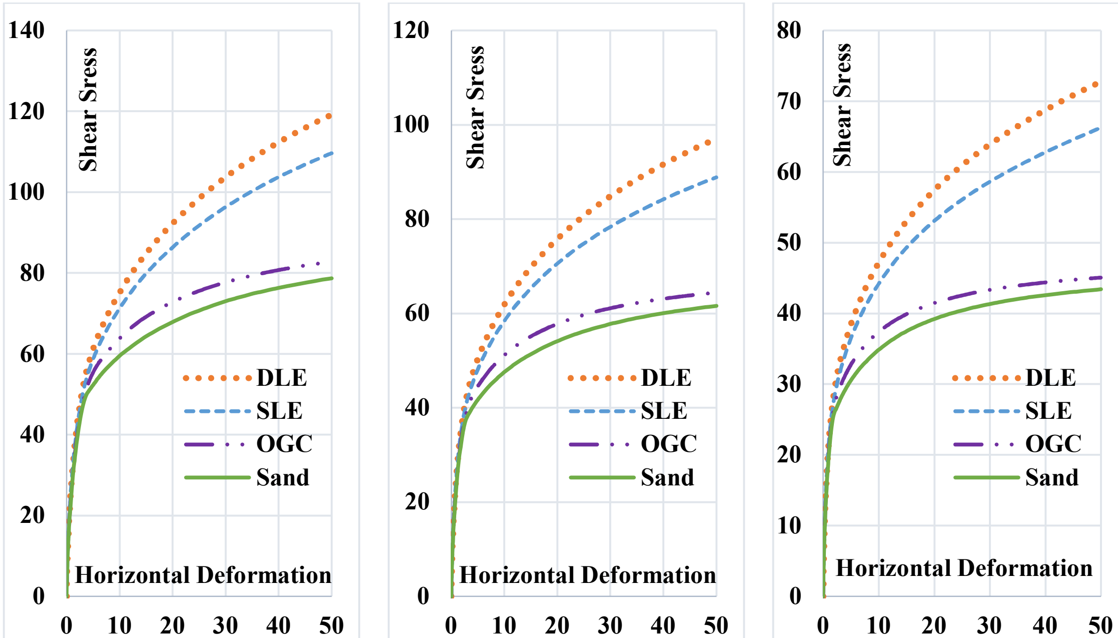

(a) (b) (c)

Figure 5.34: Shear stress vs. horizontal displacement for 50 mm dia granular column installed in triangular pattern at various normal pressure (a)100 (b)75 (c) 50 (kPa)

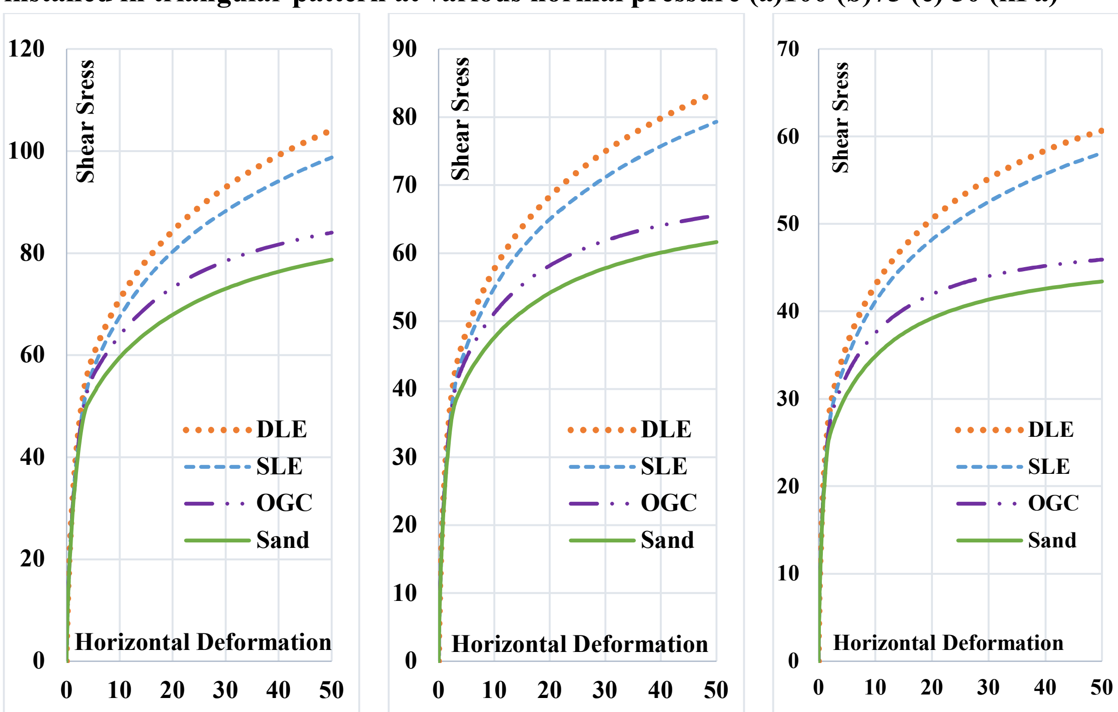

(a) (b) (c)

Figure 5.35: Shear stress vs. horizontal displacement of 75 mm diameter single granular column installed in sand bed at various normal pressure (a)100 (b)75 (c) 50 (kPa)

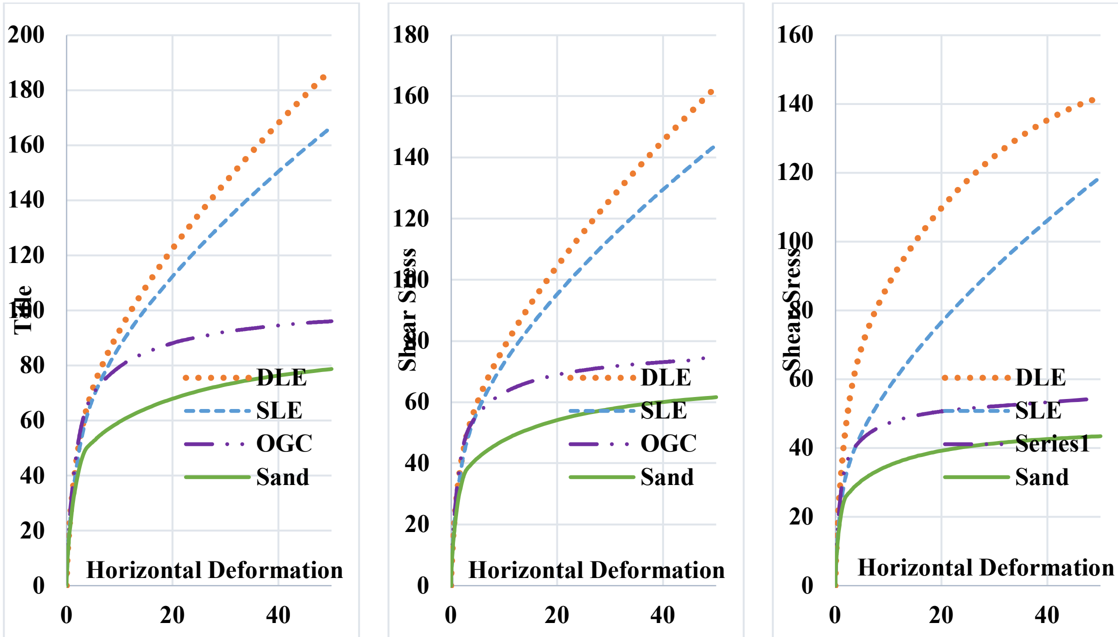

(a) (b) (c)

Figure 5.36: Shear stress vs. horizontal displacement of 75 mm diameter granular column installed in square pattern at various normal pressure (a)100 (b)75 (c) 50 (kPa)

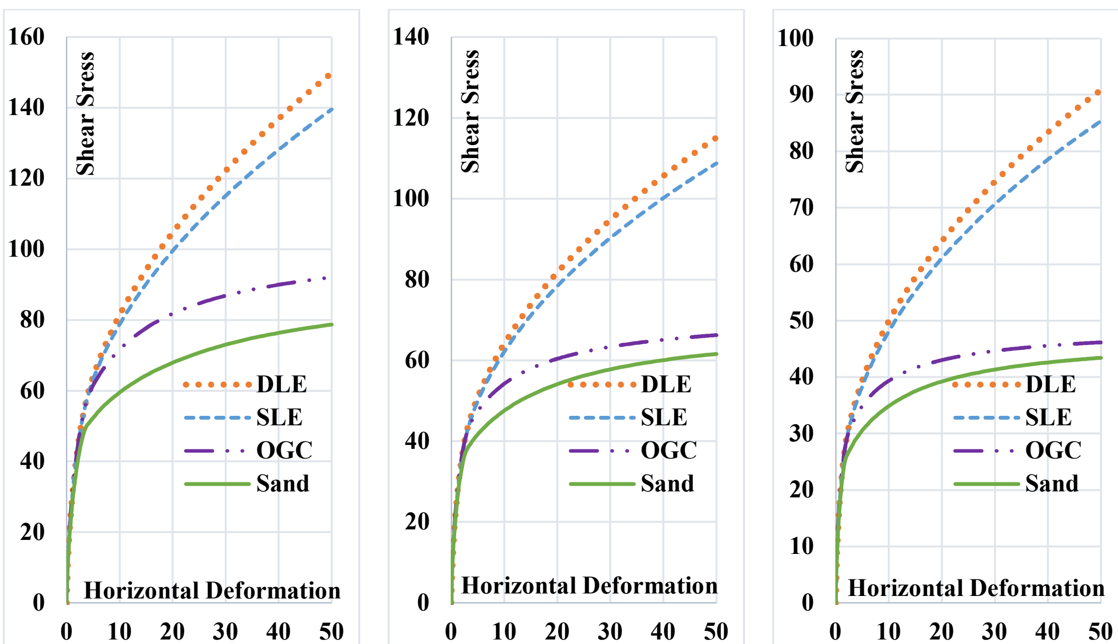

(a) (b) (c)

Figure 5.37: Shear stress vs. horizontal displacement of 75 mm diameter granular column installed in triangular pattern at various normal pressure (a)100 (b)75 (c) 50 (kPa)

5.3.2 Effect of Normal Pressure: -

Various normal pressures were applied in the conducted tests, resulting in distinct outcomes. Depending on the diameter of the granular column used, the addition of OGC in the middle of the soil bed increased shear strength by between 8% and 30% (Figure 5.32-5.37). According to Nazariafshar and Aslani (2020), increasing the normal pressure within a range of area replacement ratios can increase shear strength by between 4 and 46 percent.

Increasing the normal pressure in granular column-treated soil increases its shear strength. In comparison to OGC alone, the addition of an encased granular column in the center increases shear resistance by approximately 50 percent. The rigidity of the granular column contributes to the column's overall ultimate shear strength. The effect of normal pressure on the shear resistance of soil treated with single- and double-layered encased granular columns is depicted in Figure 5.32-5.37. The confinement provided by the encasement enables the mobilization of a greater shear strength during significant stages of displacement.

5.3.3 Parameters of Shear: -

Figure 5.38 depicts the apparent cohesion values for various encasement conditions of a single Granular Column with a 50mm displacement and a 50mm diameter. Utilizing the Mohr-Coulomb failure envelopes, the cohesion values for each case were determined. The apparent cohesion values for the composite configurations of OGC, SLE, and DLE are 18.3, 23.6 and 25.3 kPa, respectively.The confinement provided by the geosynthetic encasing improves the apparent cohesiveness, indicating an increase in shear strength. Notably, significant apparent cohesiveness is mobilized at higher strains because shear displacement generates tensile stresses in the encasement. This enhances the shear strength of the granular columns. The Table 5.3 provides a comprehensive comparison of the apparent cohesion values for different stone column encasement conditions and pattern arrangements.

The arrangement of a single column, the apparent cohesion of OGC was measured to be 18.33 kPa. When an SLE encasement was introduced, the apparent cohesion increased significantly to 23.67 kPa. This represents an approximately 1.29-fold increase in OGC's value. In addition, the DLE encasing exhibited a higher apparent cohesion of 25.33 kPa, which corresponds to a change that is approximately 1.07 times that of the SLE encasing.

Table 5.3: Apparent cohesion for various cases considered

Condition		50 mm Dia		75 mm Dia	
		Apparent Cohesion (kPa)	Change in Multiples	Apparent Cohesion (kPa)	Change in Multiples
Single Column	OGC	18.33		18.33	
	SLE	23.67	1.29	27.17	1.48
	DLE	25.33	1.37	32.33	1.76
Triangular Pattern	OGC	14.33		17.17	
	SLE	37.67	2.63	64.50	3.76
	DLE	44.00	3.7	74.67	4.35
Square Pattern	OGC	22.33		10.67	
	SLE	45.50	2.04	89.83	8.42
	DLE	51.17	2.9	112.67	10.56

Ordinary stone columns (OGC), single-layered stone columns (SLE), and dual-layered stone columns (DLE)

The apparent cohesion for OGC triangular pattern was measured at 14.33 kPa. The addition of an SLE encasement significantly increased the apparent cohesion, which reached 37.67 kPa. This represents a substantial increase from OGC of approximately 2.63 times the previous value. Similarly, the DLE encasing displayed an even higher apparent cohesion of 44 kPa, which corresponds to a change that is approximately 1.17 times that of the SLE encasing. Furthermore, the apparent cohesion for OGC in the square pattern arrangement was measured at 22.33 kPa. The addition of an SLE encasement significantly increased the apparent cohesion, which reached 45,5 kPa. This represents an approximately 2.04-fold increase in the value of OGC. Similarly, the DLE encasing exhibited an even greater apparent cohesion of 51.17 kPa, which corresponds to a change that is approximately 1.12 times that of the SLE encasing. According to Liu (2006) and Bareither et al. (2008), the apparent cohesiveness of dry granular soils is attributable to specific soil deformations that occur in large shear box tests but are absent in small shear box tests.

A comprehensive comparison of the variations in apparent cohesion for various encasing conditions and pattern configurations demonstrates that both SLE and DLE encasements contribute to greater apparent cohesion values than OGC. When combined with encasements, the triangular pattern and square pattern arrangements exhibit particularly significant increases in apparent cohesion compared to OGC. In geotechnical applications, the inclusion of encasement materials and the adoption of particular pattern arrangements can significantly improve the shear strength and overall stability of stone column systems, according to these findings.

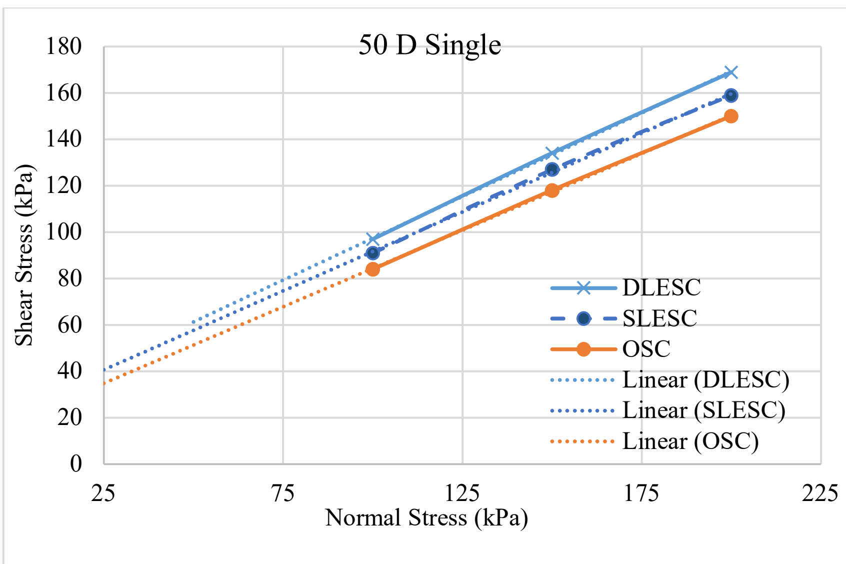

Fig 5.38: - Mohr-Coulomb Envelope for Combined Soil-Column System of 50mm Diameter Single Column

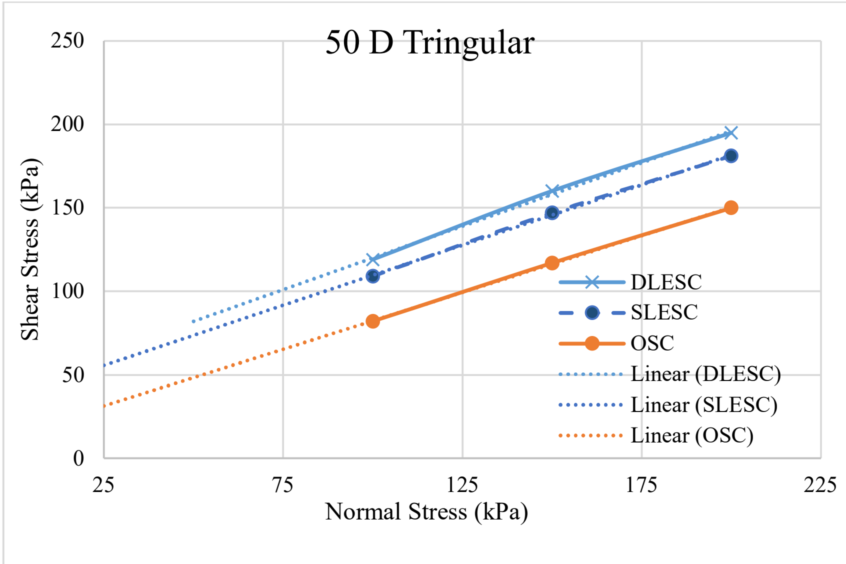

Fig 5.39: - Mohr-Coulomb Envelope for Combined Soil-Column System of 50mm Diameter Triangular Pattern

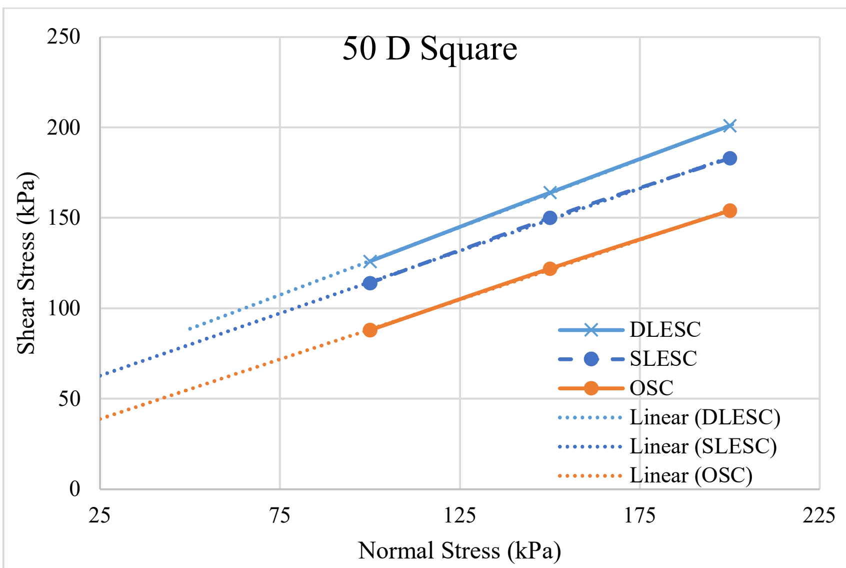

Fig 5.40: - Mohr-Coulomb Envelope for Combined Soil-Column System of 50mm Diameter Square Pattern

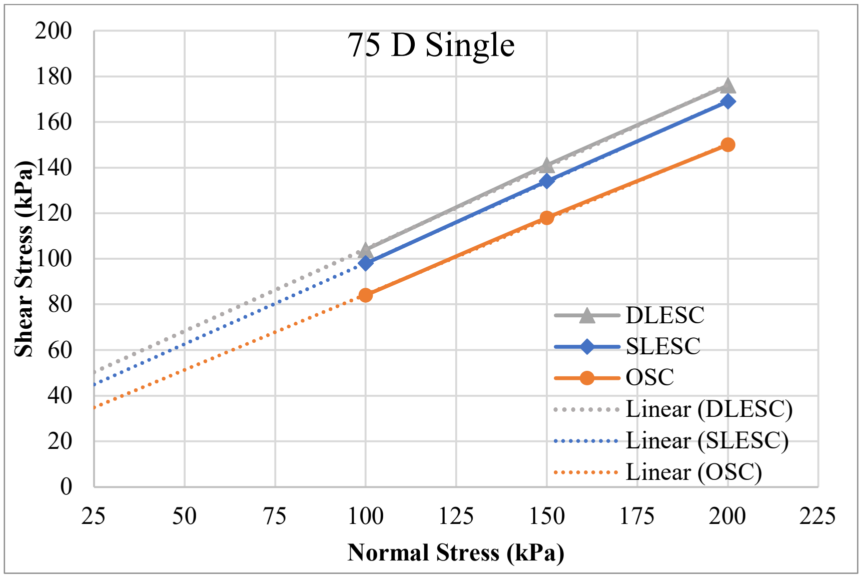

Fig 5.41: - Mohr-Coulomb Envelope for Combined Soil-Column System of 75mm Diameter Single Column

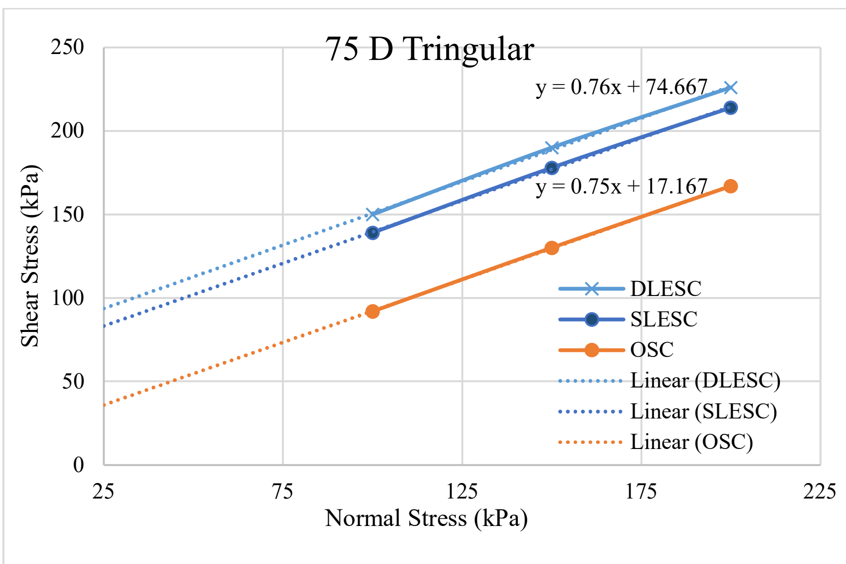

Fig 5.42: - Mohr-Coulomb Envelope for Combined Soil-Column System of 75mm Diameter Triangular Pattern

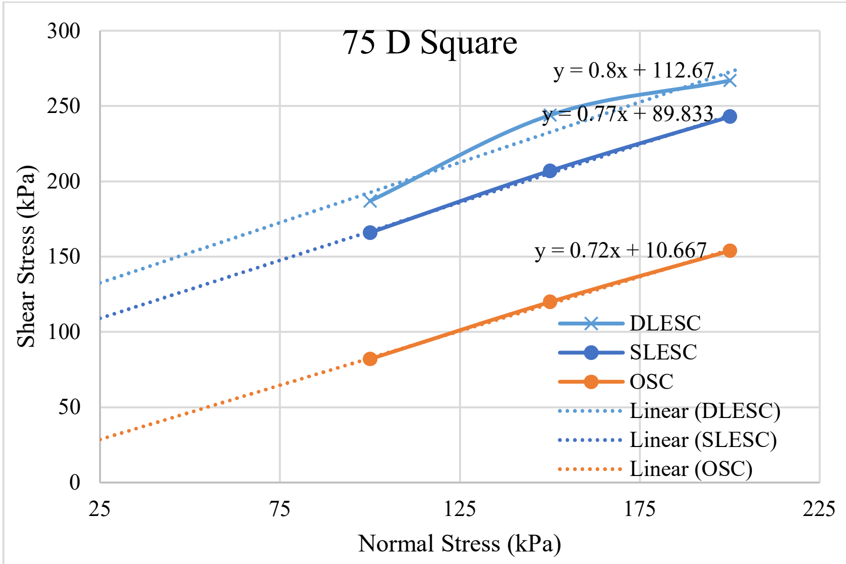

Fig 5.43: - Mohr-Coulomb Envelope for Combined Soil-Column System of 75mm Diameter Square Pattern

5.3.4 Effect of Encasement: -

Large shear tests conducted under various normal loads led to the generation of shear stress versus horizontal displacement curves. Even at a smaller displacement of 5 mm, the mobilized shear stress in sand, OSC, SLE column, and DLE column under the typical load condition of 50 kPa was nearly identical in all cases with the exception of the DLE column. As displacement increased, the increase in mobilized shear stress was observed to be greater in OSC, SLE, and DLE when connected to the sand bed. The DLE system has two layers of encasing, while the SLE system has only one. The shear force mobilized by SLE was less than the shear force mobilized at larger displacements. With a minimum proportion of 68% for 100mm cases and 70% for 50mm cases, the mobilized shear stress was greater for smaller diameter cases with a 10mm displacement.

As shown in Figure 5.32-5.37, the shear strength of installed columns with 50mm, 75mm, and 100mm diameters increased with normal pressures of 50, 75, and 100 kPa. The shear strength increased at a horizontal displacement of 50mm due to the presence of encasement material. For a 50mm diameter column at normal pressures of 50, 75, and 100 kPa, the shear stress of SLE was 1.14, 1.07, and 1.08 times that of OGC. For a 75mm diameter column, the corresponding ratios were 1.26, 1.23, and 1.16. This suggests that the encasement of granular columns increases shear stress, particularly at lower normal stress levels. However, the amplification is diminished at higher levels of normal stress. In addition, the improvement resulting from a greater modulus of elasticity of the encasement is greater for larger diameters (i.e., greater area replacement ratios) of the granular column.

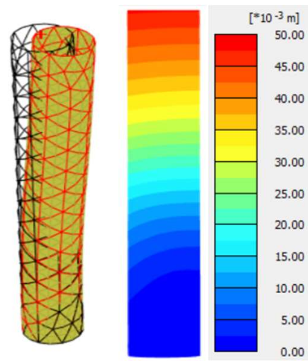

(a)

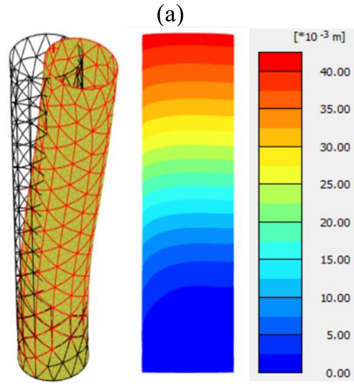

(b)

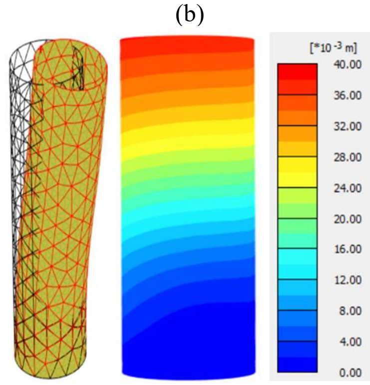

(c)

Fig 5.44: Horizontal displacement for the inner layer of DLE for different diameters of granular column
(a) 50 mm diametere ,(b) 75 mm diameter, (c) 100 mm diameter

In the DLE system, the granular column body is surrounded by two layers of encasement (one around the periphery and one inside the granular column body, i.e., the inner layer of Encasement). For all the diameter cases, both SLE and DLE are superior to OGC.

The horizontal displacement of the inner layer of the DLE encasement varies with the diameter. When a granular column is subjected to 50 kPa of lateral force, Figure 5.44 depicts the horizontal displacement of the inner layer of encasement in DLE. In the large shear box test, the inner layer of encasement of a granular column with a 50mm diameter exhibits a 50mm displacement, while the displacements for 75mm and 100mm diameters are 40mm and 32mm, respectively. This indicates that the combined system of the sand bed and granular column with a larger diameter is more rigid. For columns with diameters of 50mm, 75mm, and 100mm, the outer layer of the casing experiences greater strain than the inner layer. The inner layer of DLE encasing provides the granular column body with later-stage strength.Furthermore, as described previously, the incorporation of OGCs improves shear resistance and stability. In comparison to OGCs, encased stone columns are more resistant to lateral stress. When dealing with weak ground susceptible to shear-pressure-induced failure, installing stone columns on the ground can be an effective solution.

Notably, Chen et al. (2015) note that outer columns located beneath embankments are subject to greater shear loads than columns located at the centreline of the embankment. Because the centreline requires less shear strength, OGCs may be utilized there. For the outer line, however, where greater shear resistance is required, an encased stone column may be used, provided the vertical load resistance remains adequate and settlement within the designed diameter and spacing remains acceptable.

In addition, if additional vertical resistance is required, encased stone columns can be installed along the centreline to provide adequate shear resistance. In situations where corner columns require reinforcement, dual-layered encasing can be used to meet the required shear resistance criteria.

6. CONCLUSIONS

6.1 GENERAL

The purpose of this study was to investigate the effect of conventional stone columns and various encased stone column conditions on soil shear strength. The objective of this study was to investigate the behavior of stone columns subjected to lateral loading by experimental investigation as well as by numerical analysis. A large shear box was utilized to simulate a horizontal displacement of 50 mm on the combined soil bed and soil-stone column system and the PLAXIS 3D software was used to analyze the behavior of both encased and unencased stone columns after the validation of the experimental results. The research involved simulations conducted under various normal pressure for varying diameters of the stone column. In conclusion, based on the findings of this study, the use of soil-stone column combinations, particularly when encased, improves soil shear strength and lateral load-bearing capacity. These findings contribute to a better understanding of the behavior of stone columns under various loading conditions and can be useful in the design and implementation of geotechnical engineering projects. Some of the key findings are listed below.

6.2 CONCLUSIONS

- The granular column and its surrounding soil act as a composite material, increasing shear resistance. This is evidenced by the stone column occupying a larger percentage of the area in the shear plane, resulting in increased shear resistances for both column diameters.
- In cases where compared to the conventional OGC (ordinary granular column), incorporating an encased granular column at the center significantly improves shear resistance. The granular column's increased stiffness contributes to a significantly higher ultimate shear strength. Notably, the shear strength increase ranged from 8% to 30% across various stone column diameter scenarios when the OGC was placed in the center of the soil bed under various normal pressures.
- When shifting from OGC to SLE, the sand sample exhibits varying improvements in shear resistance ranging from 5% to 53%. The single-column configuration

improves shear resistance the least, while the square arrangement improves shear resistance the most.

- When normal pressures are considered, the shear strength ratio of DLE to unencased stone column ranges from 1.4 to 1.8. Notably, the improvement in shear resistance and overall superiority of DLE over USC is more pronounced at lower normal pressures, demonstrating the benefits of the encased arrangement for improving shear performance.
- Encasing stone columns improves shear resistance, resulting in significantly higher shear stresses at all normal pressure levels. When compared to single-layer encased (SLE) columns, dual-layered encasement (DLE) stone columns perform better in terms of shear resistance. DLE improves shear stresses by 14-20% over un-encased stone columns, especially when arranged in square patterns. This increased shear resistance is advantageous for embankments that require a stronger stone column base as well as areas where edge lines are vulnerable to shear forces.
- SLE and DLE encasements demonstrated greater apparent cohesion values than OGC in both triangular and square pattern configurations. The apparent cohesion of the SLE case exhibited a range of 1.3 to 8.42 times greater than that of the OGC case. The DLE cases exhibited an improvement in range ranging from 1.37 to 10.56 times. The results showed that the increase in apparent cohesion was greater in the case with a larger diameter. This suggests that a larger area replacement can significantly enhance the ground.
- According to the findings, encasing stone columns increases their shear modulus compared to unencased columns. The findings demonstrated that the soil-stone column system displayed higher E_{10} and E_{20} values than the sand bed alone under normal pressure conditions. A significant percentage change of up to 23% was observed in encased column cases in comparison to the ordinary stone column. The pattern choice has a significant impact on column performance, especially in columns with larger diameters.

6.3 AUTHORS CONTRIBUTION

The stone column has been encased in a single layer to improve load-bearing conditions, and it has been found in the literature that encasing the column also increases its shear resistance. In the current study, a concept is proposed to introduce dual-layered encasement to enhance the confinement effect, thereby affecting the shear resistance of stone columns. On the large shear box test setup, several experiments have been conducted to examine the behavior of different stone column cases under lateral displacement. The author compared the shear resistance offered by the conventional, single-layer encapsulated stone column and the dual-layer encased stone column. In addition to confirming the experimental work, the numerical analysis using PLAXIS-3D also included cases that were not workable in the experimental analysis. The results of the study are discussed in the "Results and Discussion" section, wherein it was determined that the proposed dual-layer encasement concept outperforms the conventional stone column. In cases where the column provided beneath the foundation has a high propensity to fail under the lateral load, as well as at the corner line of the stone columns beneath any structure (embankment), it is recommended to employ the dual-layered stone column.

PUBLICATION LIST

- Jaiswal, A., & Kumar, R. (2023). Influence of dual layer confinement on lateral load capacity of stone columns: An experimental investigation. Geomechanics and Engineering, 32 (6), 567-581. (https://doi.org/10.12989/gae.2023.32.6.567) ***(SCIE-Q2)***
- Jaiswal, A., & Kumar, R. (2022). Finite element analysis of granular column for various encasement conditions subjected to shear load. Geomechanics and Engineering, 29(6), 645- 655. (https://doi.org/10.12989/gae.2022.29.6.645) ***(SCIE-Q2)***
- Jaiswal, A., & Kumar, R. (2021, July). Study on Response of Dual Layered Reinforced Stone Column Under Shear Loading. In Civil Infrastructures Confronting Severe Weathers and Climate Changes Conference (pp. 107-117). Springer, Cham. (https://doi.org/10.1007/978-3- 030-79798-0_9) ***(SCOPUS)***
- Jaiswal, A., & Kumar, R. (2021, July). Influence of Multiple Layers of Encasement on Bulging Capacity of Granular Column. In Civil Infrastructures Confronting Severe Weathers and Climate Changes Conference (pp. 83-91). Springer, Cham. (https://doi.org/10.1007/978-3- 30-79647-1_6) ***(SCOPUS)***

REFERENCES

- Abusharar, S. W., & Han, J. (2011). Two-dimensional deep-seated slope stability analysis of embankments over stone column-improved soft clay. *Engineering Geology*, *120*(1-4), 103-110. https://doi.org/10.1016/j.enggeo.2011.04.002.
- Aghili, E., Hosseinpour, I., Chenari, R. J., & Ahmadi, H. (2021). Behavior of granular column-improved clay under cyclic shear loading. *Transportation Geotechnics*, *31*, 100654. https://doi.org/10.1016/j.trgeo.2021.100654.
- Ali, K., Shahu, J. T., & Sharma, K. G. (2012). Model tests on geosynthetic-reinforced stone columns: a comparative study. Geosynthetics International, 19(4), 292-305.
- Ali, K., Shahu, J. T., & Sharma, K. G. (2011). An experimental study of stone columns in soft soils. In *Proceedings of Indian Geotechnical Conference* (pp. 1-4).
- Ali, K., Shahu, J.T., Sharma, K.G., (2014) Model tests on single and groups of stone columns with different geosynthetic reinforcement arrangement. Geosynth. Int. 21 (2), 103-118, https://doi.org/10.1680/gein.14.00002.
- Ambily, A. P., & Gandhi, S. R. (2007). Behavior of stone columns based on experimental and FEM analysis. *Journal of geotechnical and geoenvironmental engineering*, *133*(4), 405-415.
- Aslani, M., Nazariafshar, J., & Ganjian, N. (2019). Experimental study on shear strength of cohesive soils reinforced with stone columns. *Geotechnical and Geological Engineering*, *37*, 2165-2188.https://doi.org/10.1007/s10706-018-0752-z.
- Ayadat, T., & Hanna, A. M. (2005). Encapsulated stone columns as a soil improvement technique for collapsible soil. Proceedings of the Institution of Civil Engineers-Ground Improvement, 9(4), 137-147.https://doi.org/10.1680/grim.2005.9.4.137
- Ayadat, T., Hanna, A. M., & Hamitouche, A. (2008). Soil improvement by internally reinforced stone columns. *Proceedings of the Institution of Civil Engineers-Ground Improvement*, *161*(2), 55-63. https://doi.org/10.1680/grim.2008.161.2.55

- Black, J. A., Sivakumar, V., Madhav, M. R., & McCabe, B. (2006). An improved experimental test set-up to study the performance of granular columns. Geotechnical Testing Journal, 29(3), 193-199. https://doi.org/10.1520/GTJ14195
- Bhattacharjee, A., Mittal, S., & Krishna, A. (2011). Bearing capacity improvement of square footing by micropiles. *International Journal of Geotechnical Engineering*, *5*(1), 113-118.
- Bailappanavar, N. I., Kumar, M., Chatterjee, K. (2021). Effect of Stone Columns on Strength and Consolidation Characteristics of Black Cotton Soil. KSCE Journal of Civil Engineering, 25(4), 1214-1228.
- Cengiz, C., Kilic, I. E., and Guler, E. (2019). On the shear failure mode of granular column embedded unit cells subjected to static and cyclic shear loads. *Geotextiles and Geomembranes*, 47(2),193-202. https://doi.org/10.1016/j.geotexmem.2018.12.011
- Chen, J.-F., Li, L.-Y., Xue, J.-F., Feng, S.-Z., (2015) Failure mechanism of geosynthetic encased stone columns in soft soils under embankment. Geotext. Geomembr.43 (5), 424-431, DOI:10.1016/j.geotexmem.2015.04.016
- Das, A. K., & Deb, K. (2017). Modeling of stone column-supported embankment under axi-symmetric condition. *Geotechnical and Geological Engineering*, *35*, 707-730. https://doi.org/10.1007/s10706-016-0136-1
- Dash, S. K., & Bora, M. C. (2013). Influence of geosynthetic encasement on the performance of stone columns floating in soft clay. *Canadian Geotechnical Journal*, *50*(7), 754-765. https://doi.org /10.1139/cgj-2012-0437
- Dash, S. K., Sireesh, S., & Sitharam, T. G. (2003). Model studies on circular footing supported on geocell reinforced sand underlain by soft clay. *Geotextiles and Geomembranes*, *21*(4), 197-219.
- Deb, K., & Dhar, A. (2011). Optimum design of stone column-improved soft soil using multiobjective optimization technique. *Computers and Geotechnics*, *38*(1), 50-57. https://doi.org/10.1016/j.compgeo.2010.10.005
- Fox, Z. P. (2011). *Critical state, dilatancy and particle breakage of mine waste rock*. Colorado State University.

- Gade, V. K., & Dasaka, S. M. (2022). Short-and long-term behavior of EPS geofoam in reduction of lateral earth pressure on rigid retaining wall subjected to surcharge loading. *Geotextiles and Geomembranes*, *50*(5), 868-880.
- Gautam, U. K., Venkatesh, K., & Kumar, V. (2021). Soil stabilization using combined waste material. In *Problematic Soils and Geoenvironmental Concerns: Proceedings of IGC 2018* (pp. 573-582). Springer Singapore.
- Ghazavi, M., and Afshar, J. N. (2013), "Bearing capacity of geosynthetic encased stone columns", *Geotextiles and Geomembranes*, 38,26-36. https://doi.org/10.1016/j.geotexmem.2013.04.003.
- Ghazavi, M., Yamchi, A. E., & Afshar, J. N. (2018). Bearing capacity of horizontally layered geosynthetic reinforced stone columns. *Geotextiles and Geomembranes*, *46*(3), 312-318.
- Gniel, J., & Bouazza, A. (2009). Improvement of soft soils using geogrid encased stone columns. Geotextiles and Geomembranes, 27(3), 167-175. https://doi.org/10.1016/j.geotexmem.2008.11.001
- Gniel, J., and Bouazza, A. (2010). Construction of geogrid encased stone columns: A new proposal based on laboratory testing. *Geotextiles and Geomembranes*, *28*(1), 108-118. https://doi.org/10.1016/j.geotexmem.2009.12.012.
- Guetif, Z., Bouassida, M., & Debats, J. M. (2007). Improved soft clay characteristics due to stone column installation. Computers and Geotechnics, 34(2), 104-111. https://doi.org/10.1016/j.compgeo.2006.09.008
- Han, J., Huang, J., and Porbaha, A. (2005). 2D numerical modeling of a constructed geosynthetic-reinforced embankment over deep mixed columns. *In: ASCE Geotechnical Special Publication (GSP) No.131, Contemporary Issues in Foundation Engineering, ASCE GeoFrontiers, 1-11*, Austin (TX), January. https://doi.org/10.1061/40777(156)13.
- Hasan, M., Samadhiya, N.K., (2016). Influence of combined vertical and horizontal reinforcement on granular piles in soft clays. Indian Geotechnical Conference, IGC2016 15-17 December 2016, IIT Madras, Chennai, India.

- Hasan, M., Samadhiya, N.K., (2017) Performance of geosynthetic-reinforced granular piles in soft clays: Model tests and numerical analysis Computers and Geotechnics 87 ,178–187, https://doi.org/10.1016/j.compgeo.2017.02.016
- Hausmann, M. R. (1990). Engineering principles of ground modification (pp. 321-335). New York: McGraw-Hill. Soil Improvement and Ground Modification Methods By Peter G. Nicholson
- Hong, Y. S., Wu, C. S., & Yu, Y. S. (2016). Model tests on geotextile-encased granular columns under 1-g and undrained conditions. Geotextiles and Geomembranes, 44(1), 13-27. https://doi.org/10.1016/j.geotexmem.2015.06.006
- Hosseinpour, I., Almeida, M. S. S., & Riccio, M. (2015). Full-scale load test and finite-element analysis of soft ground improved by geotextile-encased granular columns. Geosynthetics International, 22(6), 428-438. https://doi.org/10.1680/jgein.15.00023
- Hosseinpour, I., Almeida, M. S., & Riccio, M. (2016). Ground improvement of soft soil by geotextile-encased columns. *Proceedings of the Institution of Civil Engineers-Ground Improvement*, *169*(4), 297-305. https://doi.org/10.1680/jgrim.16.00009
- Hegde, A. (2017). Geocell reinforced foundation beds-past findings, present trends and future prospects: a state-of-the-art review. *Construction and Building Materials*, *154*, 658-674.
- Yadav, J. S., Hussain, S., Garg, A., & Tiwari, S. K. (2019). Geotechnical properties of rubber reinforced cemented clayey soil. *Transportation Infrastructure Geotechnology*, *6*, 337-354.
- Yadav, J. S., Tiwari, S. K., & Shekhwat, P. (2018). Strength behaviour of clayey soil mixed with pond ash, cement and randomly distributed fibres. *Transportation Infrastructure Geotechnology*, *5*, 191-209.
- Khabbazian, M., Kaliakin V.N. and Meehan, C.L., (2010) Numerical study of the effect of geosynthetic encasement on the behaviour of granular columns, Geosynthetics International, 17(3), 132-143, https://doi.org/10.1680/gein.2010.17.3.132
- Khabbazian, M., Kaliakin, V. N., & Meehan, C. L. (2015). Column supported embankments with geosynthetic encased columns: validity of the unit cell

concept. *Geotechnical and Geological Engineering*, *33*, 425-442. https://doi.org/10.1007/s10706-014-9826

- Khajeh, A., Jamshidi Chenari, R., & Payan, M. (2020). A review of the studies on soil-EPS composites: beads and blocks. *Geotechnical and Geological Engineering*, *38*, 3363-3383. https://doi.org/10.1007/s10706-020-01252-2.
- Khajeh, A., Ebrahimi, S. A., Mola Abasi, H., Jamshidi Chenari, R., & Payan, M. (2021). Effect of EPS beads in lightening a typical zeolite and cement-treated sand. *Bulletin of Engineering Geology and the Environment*, 80 (11), 8615-8632. https://doi.org/10.1007/s10064-021-02458-1
- Kitazume, M., & Maruyama, K. (2007). Internal stability of group column type deep mixing improved ground under embankment loading. *Soils and Foundations*, *47*(3), 437-455. https://doi.org/10.3208/sandf.47.437
- Kitazume, M., and Maruyama, K. (2006). External stability of group column type deep mixing improved ground under embankment loading. *Soils and foundations*, 46(3), 323-340. https://doi.org/10.3208/sandf.46.323.
- Kranthikumar, A., Sawant, V. A., & Shukla, S. K. (2016). Numerical modeling of granular anchor pile system in loose sandy soil subjected to uplift loading. *International Journal of Geosynthetics and Ground Engineering*, *2*, 1-7.
- Kranthikumar, A., Sawant, V. A., Kumar, P., & Shukla, S. K. (2017). Numerical and experimental investigations of granular anchor piles in loose sandy soil subjected to uplift loading. *International Journal of Geomechanics*, *17*(2), 04016059.
- Lo, S. R., Zhang, R., & Mak, J. (2010). Geosynthetic-encased stone columns in soft clay: a numerical study. *Geotextiles and Geomembranes*, *28*(3), 292-302. https://doi.org/10.1016/j.geotexmem.2009.09.015
- Meenal, G., Saran, S., & Mittal, S. (2009). Pseudo-static analysis of soil nailed excavations. *Geotechnical and Geological Engineering*, *27*, 571-583.
- Miranda, M., & Da Costa, A. (2016). Laboratory analysis of encased stone columns. *Geotextiles and Geomembranes*, *44*(3), 269-277. https://doi.org/10.1016/j.geotexmem.2015.12.001
- Mittal, S., Singh, K., & Mathur, S. (2008). Behaviour of vertical cuts using soil Nailing techniques in saturated conditions. *Geotechnical Engineering*.

- Mohapatra, S. R., Rajagopal, K., & Sharma, J. (2016). Direct shear tests on geosynthetic-encased granular columns. *Geotextiles and Geomembranes*, *44*(3), 396-405. https://doi.org/10.1016/j.geotexmem.2016.01.002
- Mohapatra, S. R., Rajagopal, K., & Sharma, J. (2017). 3-Dimensional numerical modeling of geosynthetic-encased granular columns. *Geotextiles and Geomembranes*, *45*(3), 131-141. https://doi.org/10.1016/j.geotexmem.2017.01.004
- Murugesan, S., & Rajagopal, K. (2006). Geosynthetic-encased stone columns: numerical evaluation. *Geotextiles and Geomembranes*, *24*(6), 349-358. https://doi.org/10.1016/j.geotexmem.2006.05.001.
- Murugesan, S., & Rajagopal, K. (2007). Model tests on geosynthetic-encased stone columns. *Geosynthetics International*, *14*(6), 346-354. https://doi.org/10.1680/gein.2007.14.6.346.
- Murugesan, S., & Rajagopal, K. (2010). Studies on the behavior of single and group of geosynthetic encased stone columns. *Journal of Geotechnical and Geoenvironmental Engineering*, *136*(1), 129-139. https://doi.org/10.1061/(ASC`E)GT.1943-5606.0000187
- Nayak, N. V. (1983). Recent advances in ground improvements by stone column. *In Proceedings of Indian Geotechnical Conference, Madras*.
- Nazariafshar, J., & Aslani, M. (2021). Effect of stress concentration ratio on shear strength of soft soils improved with stone columns. *Iranian Journal of Science and Technology, Transactions of Civil Engineering*, *45*, 315-334. https://doi.org/10.1007/s40996-020-00391-z
- Ou Yang, F., Zhang, J. J., Liao, W. M., Han, J. W., Tang, Y. L., & Bi, J. B. (2017). Characteristics of the stress and deformation of geosynthetic-encased stone column composite ground based on large-scale model tests. *Geosynthetics International*, *24*(3), 242-254. https://doi.org/10.1680/jgein.16.00028
- Paramkusam, B. R., Prasad, A., & Arya, C. (2013). A study on CBR behavior of waste plastic (PET) on stabilized red mud and fly ash. *International Journal of Structural and Civil Engineering Research, vol*, *2*, 232-240.
- Patil, V., Junagade, M., & Murty, D. S. (2022, January). Development of a Full-Scale Retaining Wall Model to Evaluate Lateral Earth Pressure Reduction Using

EPS Geofoam. In *Dynamics of Soil and Modelling of Geotechnical Problems: Proceedings of Indian Geotechnical Conference 2020 Volume 5* (pp. 41-53). Singapore: Springer Singapore.

- Prasad, S. S. G., & Satyanarayana, P. V. V. (2016). Improvement of soft soil performance using stone columns improved with circular geogrid discs. *Indian Journal of Science and Technology*, *9*(30), 1-6. https://doi.org/10.17485/ijst/2016/v9i30/99186
- Pulko, B., Majes, B., & Logar, J. (2011). Geosynthetic-encased stone columns: analytical calculation model. *Geotextiles and geomembranes*, *29*(1), 29-39. https://doi.org/10.1016/j.geotexmem.2010.06.005.
- Rajesh, S., Jain, P., (2015) Influence of permeability of soft clay on the efficiency of stone columns and geosynthetic encased stone columns - a numerical study. Int. J. Geotech. Eng. 9 (5), 483–493. https://doi.org/10.1179/1939787914Y.0000000088
- Roy, R., Venkateswarlu, H., & Hegde, A. (2019). Numerical Study on Cyclic Shear Behavior of Soil–Geosynthetics Interface. In *Geotechnics for Transportation Infrastructure: Recent Developments, Upcoming Technologies and New Concepts, Volume 2* (pp. 235-245). Springer Singapore.
- Samadhiya, N., Maheshwari, P., Zsaki, A., Basu, P., & Kundu, A. (2009). Strengthening of clay by geogrid reinforced granular pile. International Journal of Geotechnical Engineering, 3(3), 377-386. https://doi.org/10.3328/IJGE.2009.03.03.377-386
- Samanta, M., Sawant, V. A., & Ramasamy, G. (2010, December). Ground improvement using displacement type sand piles. In Proceedings of the Indian geotechnical conference, Mumbai, India (pp. 629-632).
- Satyendra, M. (2006). Soil Nailing Application in erosion control–an experimental study. *Geotechnical and Geological Engineering*, *24*(3), 675-688.
- Saxena, S., & Roy, L. B. (2022). Suitability Analysis of Stone Column Materials with PLAXIS. *Engineering, Technology & Applied Science Research*, *12*(2), 8421-8425.

- Saxena, S., & Roy, L. B. (2022). The Effect of Geometric Parameters on the Strength of Stone Columns. *Engineering, Technology & Applied Science Research*, *12*(4), 9028-9033.
- Shahu, J. T., Madhav, M. R., & Hayashi, S. (2000). Analysis of soft ground-granular pile-granular mat system. *Computers and Geotechnics*, *27*(1), 45-62.
- Shahu, J. T., & Reddy, Y. R. (2011). Clayey soil reinforced with stone column group: model tests and analyses. Journal of Geotechnical and Geoenvironmental Engineering, 137(12), 1265-1274.
- Shahu, J. T., Madhav, M. R., & Hayashi, S. (2000). Analysis of soft ground-granular pile-granular mat system. Computers and Geotechnics, 27(1), 45-62.
- Sitharam, T. G., Sireesh, S., & Dash, S. K. (2005). Model studies of a circular footing supported on geocell-reinforced clay. *Canadian Geotechnical Journal*, *42*(2), 693-703.
- Sivakumar, V., McKelvey, D., Graham, J., & Hughes, D. (2004). Triaxial tests on model sand columns in clay. Canadian Geotechnical Journal, 41(2), 299-312.https://doi.org/10.1139/t03-097
- Stoeber, J.N., (2012) Effects of Maximum Particle Size and Sample Scaling on the Mechanical Behavior of Mine Waste Rock; a Critical State Approach. Master's Thesis. Colorado State University, Fort Collins, USA.
- Tandel, Y. K., Solanki, C. H., & Desai, A. K. (2012). Reinforced granular column for deep soil stabilization: A review. *International Journal of Civil & Structural Engineering*, *2*(3), 720-730.
- Tiwari, S. K., & Sharma, J. P. (2013). Influence of Fiber-Reinforcement on CBR-Value of Sand. Electronic Journal of Geotechnical Engineering, 18, 4303-4311.
- Yoo, C., Kim, S.B., (2009) Numerical modeling of geosynthetic-encased granular column-reinforced ground. Geosynth. Int. 16 (3), 116-126, https://doi.org/10.1680/gein.2009.16.3.116.
- Yoo, C., & Kim, S. B. (2009). Numerical modeling of geosynthetic-encased stone column-reinforced ground. Geosynthetics International, 16(3), 116-126. https://doi.org/10.1680/gein.2009.16.3.116